



**The treatment of biodiesel wastewater using an integrated electrochemical and
adsorption process**

by

Dirk Petrus Myburgh

Thesis submitted in fulfilment of the requirements for the degree Master of

Engineering: Chemical Engineering

in the Faculty of Chemical Engineering

at the Cape Peninsula University of Technology

Cape Town

Supervisor: M Aziz

Co-supervisor: Prof TV Ojumu

CPUT copyright information

The dissertation/thesis may not be published either in part (in scholarly, scientific or technical journals), or as a whole (as a monograph), unless permission has been obtained from the

University

DECLARATION

I, Dirk Petrus Myburgh, declare that the contents of this dissertation/thesis represent my own unaided work, and that the dissertation/thesis has not previously been submitted for academic examination towards any qualification. Furthermore, it represents my own opinions and not necessarily those of the Cape Peninsula University of Technology.

Signed

Date

Acknowledgements

I would like to thank the following, sincerely:

Mr M Aziz, for the countless hours that he has invested in me; Thank you, Sir, for always having a positive attitude, giving insight, motivation and guidance; you have contributed not only to my academic but my personal growth as well;

Professor T.V Ojumu, thank you Prof for your kind and generous assistance and contribution to the success of my studies;

Oom Alwyn, Hannalene en Elizma; Baie dankie vir al julle bystand deur die jare, sonder julle sou my projek nie suksesvol gewees het nie; Julle is werklik die drie steunpilare wat die departement staande hou;

NMT Electrodes South Africa, for generously supplying us with materials, which without the project would not have been possible;

The Chemical Engineering Department – Cape Peninsula University of Technology;

The Environmental Engineering Research Group in Lab 1.11; I wish you all the best for your future endeavours;

Green-biodiesel, for supplying us with wastewater; may your business be ever successful!

My family and friends for their support and motivation;

Dedication

Thank you,

**To my parents, my sisters,
my family and my friends.**

**Thank you for always allowing me,
Allowing me to think,
Allowing me to feel,
Allowing me to be.**

Abstract

The production of biodiesel is an energy and water intensive process. The wastewater that is produced during this process is high in concentrations of COD, BOD, FOG and various other contaminants. Since it contains low levels of nutrients, it is difficult to degrade using natural processes such as conventional activated sludge wastewater treatment. The discharge of untreated biodiesel wastewater also raises serious environmental concern. It interferes when remediated with biological processes and results in additional costs during the production of biodiesel when penalties and fines are applied. Conventional treatment processes are not capable of treating contaminants and pollutants in biodiesel to satisfactory concentrations and hence advanced treatment processes are necessary.

In this research, a lab scale integrated treatment process was used to investigate the successful reduction of contaminants, in particular COD, BOD and FOG. The integrated treatment process used in this study consisted of three consecutive steps; acidification, electrochemical oxidation and adsorption using chitosan as an adsorbent.

The electrochemical oxidation process with $\text{IrO}_2\text{-Ta}_2\text{O}_5/\text{Ti}$ anodes was applied to treat biodiesel wastewater. Different operating conditions were tested to establish favourable conditions. The current density applied as well as the concentration of NaCl as the supporting electrolyte greatly affected the process. A NaCl concentration of 0.08M was deemed sufficient, whereas a current density of 1 mA/cm² showed superior performance compared to lower or higher current densities.

Adsorption of pollutants in biodiesel wastewater was investigated using Chitosan as the adsorbent. Various chitosan concentrations, initial pH of the wastewater and repetitive adsorption stages were investigated. It was discovered that all three operating conditions greatly affect the performance of the process. The three consecutive adsorption stages using a chitosan concentration of 4.5 g/L at a pH of 2 resulted in the highest pollutant removal.

It was observed that the integrated treatment process could reduce COD, BOD and FOG levels by 94%, 86% and 95% respectively. This concludes that the treated effluent complies with local industrial effluent discharge standards, which could be disposed safely without further treatment.

Research outputs

Oral presentations:

- Myburgh D.P. & Aziz, M. 2017. Treatment of biodiesel wastewater using electrochemical oxidation. Proceedings of the WISA-Water sustainability symposium [Somerset West, South Africa, 7 – 9 May 2017]. Paper ID WSS17-060.
- Myburgh D.P. & Aziz, M. 2017. The treatment of biodiesel wastewater using electrochemical and adsorption processes. Water Research Seminar [CPUT, Bellville, South Africa, 02 June 2017].
- Myburgh D.P. & Aziz, M. 2017. An integrated approach to the treatment of biodiesel wastewater. 8th International Young Water Professionals Conference. [CTICC, Cape Town, South Africa, 10 – 13 December 2017. Paper ID: 3749823

Journal Publication

Myburgh D.P., & Aziz, M. 2017. Treatment of biodiesel wastewater using an integrated electrochemical and adsorption process.

Table of contents

DECLARATION	ii
Acknowledgements.....	iii
Abstract v	
Research outputs.....	vi
List of Figures	xii
List of tables.....	xv
List of Photos	xviii
List of symbols	xx
Chapter 1 Introduction.....	2
1. Background.....	2
1.1. Research problem	4
1.2. Research questions.....	4
1.3. Aims and objectives	5
1.4. Significance of this research.....	5
1.5. Delineation of the study	6
1.6. Structure of the thesis	7
Chapter 2 Literature review and theory	9
2. Introduction	9
2.1. Global Fresh water supply	9
2.2. Water in South Africa	10

2.3.	Water usage in South Africa	13
2.4.	City of Cape Town: Wastewater and Industrial Effluent By-Law, 2013.....	15
2.5.	Biodiesel	16
2.5.1.	Biodiesel wastewater.....	18
2.5.2.	Biodiesel wastewater generation	18
2.5.3.	Biodiesel wastewater characteristics	20
2.6.	Conventional wastewater treatment technologies.....	21
2.6.1.	Adsorption.....	21
2.6.2.	Coagulation and Flocculation	22
2.6.3.	Electrocoagulation.....	23
2.6.4.	Biological Treatment.....	24
2.7.	Treatment Technologies used in this study.....	25
2.8.	Acidification	26
2.9.	Electrochemical oxidation.....	27
2.9.1.	Electrochemical oxidation mechanism.....	28
2.9.2.	Instantaneous current efficiency	31
2.9.3.	Mixed metal oxide anodes.....	32
2.9.4.	Addition of NaCl	33
2.10.	Adsorption using Chitosan.....	34
2.10.1.	Structure	35
2.10.2.	Adsorption equilibrium and isotherms.....	36

2.10.3.	Adsorption equilibria	36
2.10.4.	Langmuir Isotherm	36
2.10.5.	Freundlich Isotherm.....	37
2.10.6.	Dubinin-Raduschkevich Isotherm	38
3.	Research Methodology.....	41
3.1.	Introduction	41
3.2.	Research design	41
3.3.	Experimental details	41
3.3.1.	Acidification	42
3.3.2.	Electrochemical oxidation.....	42
3.3.3.	Electrochemical oxidation factorial trial.....	45
3.3.4.	Adsorption with Chitosan.....	47
3.3.5.	Integrated treatment process.....	48
3.4.	Research apparatus	49
3.4.1.	Glass ware	49
3.4.2.	Equipment.....	49
3.4.3.	Materials	52
4.	Results and Discussion	54
4.1.	Biodiesel wastewater characteristics	54
4.2.	Acidification of biodiesel wastewater	55
4.3.	Instantaneous current efficiency	57

4.3.1.	Effect of current density.....	58
4.3.2.	Effect of NaCl concentration.....	59
4.4.	Electrochemical oxidation experiments.....	60
4.4.1.	Additional electrochemical oxidation experiments.....	63
4.4.2.	Effect of current density on pollutant removal.....	66
4.4.3.	Effect of NaCl concentration on pollutant removal.....	68
4.5.	Energy consumption.....	72
4.6.	Development of COD removal model.....	74
4.6.1.	COD removal model validation.....	76
4.6.2.	Effect of process parameters on COD removal.....	78
4.7.	Adsorption using chitosan.....	83
4.7.1.	Effect of adsorption time.....	83
4.7.2.	Effect of initial wastewater pH.....	85
4.7.3.	Effect of Chitosan dosage.....	87
4.8.	Adsorption equilibrium and isotherms.....	90
4.8.1.	Langmuir isotherm.....	91
4.8.2.	Freundlich Isotherm.....	93
4.8.3.	Dubinin-Raduschkevich isotherm.....	95
4.9.	Integrated treatment.....	97
Chapter 5: conclusion and recommendation.....		103
5.1.	Conclusion.....	103

5.2.	Recommendation	104
6.	References.....	106
	Appendix A	124
	Appendix B	126
	Appendix C	134
	Appendix D	173
	Appendix E	198
	Appendix F.....	211

List of Figures

Figure 2. 1: Earth's water supply (WWF-SA, 2016)	10
Figure 2. 2: Projections of water shortages by the year 2030 (Water Resources Group, 2009) .11	
Figure 2. 3: Water use in South Africa by sector (Siebrits & Fundikwa, (2017))......	13
Figure 2. 4: Biodiesel reaction (Ma & Hanna, 1999).	17
Figure 2. 5: Biodiesel production reaction steps.	17
Figure 2. 6: Schematic of anodic oxidation (Comninellis, 1994).	28
Figure 2. 7: Oxidation power of various anode materials. (Comninellis et al., 2008)	31
Figure 2. 8: Chitin and chitosan (Muxika et al., 2017).	35
Figure 4. 1: Oil removed through acidification.	55
Figure 4. 2: Instantaneous current efficiency - Effect of current density.....	58
Figure 4. 3: Instantaneous current efficiency - Effect of NaCl concentration.....	59
Figure 4. 4: COD removal (%) – experiments.....	60
Figure 4. 5: COD, BOD & FOG removal efficiencies - experiments.....	61
Figure 4. 6: COD removal (%) - Additional experiments.	63
Figure 4. 7: COD, BOD & FOG removal efficiencies - Additional experiments.....	64
Figure 4. 8: Effect of current density on COD removal.	66
Figure 4. 9: Final values for COD removal – Current density.....	67
Figure 4. 10: Effect of NaCl concentration on COD removal.....	69
Figure 4. 11: Final values for COD removal - NaCl concentration.	70
Figure 4. 12: Effect of NaCl concentration of pollutant removal efficiencies.....	70
Figure 4.13: Mean energy consumption.	73
Figure 4.14: Normal probability (%) and internally studentised residuals.....	76

Figure 4.15: Predicted COD removal vs actual (experimental) COD removal.....	77
Figure 4.16: Perturbation plot showing the effect of current density and electrochemical oxidation time on COD removal.	79
Figure 4. 17: Interaction effect between current density and electrochemical oxidation on COD removal.....	80
Figure 4. 18: 2D contour plot showing the effect of current density and electrochemical oxidation on COD removal.	81
Figure 4. 19: 3D surface plot showing the effect of current density and electrochemical oxidation on COD removal.	82
Figure 4. 20: Single stage adsorption capacity	83
Figure 4. 21: COD removal at adsorption stages.....	88
Figure 4. 22: Adsorption operational parameters.....	89
Figure 4. 23 :Linearized Freundlich isotherms.....	93
Figure 4. 24: Linearized D-R isotherms.....	95
Figure 4. 25: Integrated treatment COD removal over time	100
Figure C. 1: Average COD removal from experiment 1.1 and 1.2:.....	138
Figure C. 2: Average COD removal from experiment 2.1 and 2.2.....	141
Figure C. 3: Average COD removal from experiment 3.1 and 3.2.....	144
Figure C. 4: Average COD removal from experiment 4.1 and 4.2.....	147
Figure C. 5: Average COD removal from experiment 5.1 and 5.2.....	150
Figure C. 6: Average COD removal from experiment 6.1 and 6.2.....	153
Figure C. 7: Average COD removal from experiment 7.1 and 7.2.....	156
Figure C. 8: Average COD removal from experiment 8.1 and 8.2.....	160
Figure C. 9: Average COD removal from experiment 9.1 and 9.2.....	163

Figure C. 10: Average COD removal from experiment 10.1 and 10.2.....	166
Figure C. 11: Average COD removal from experiment 11.1 and 11.2.....	169
Figure C. 12: Average COD removal from experiment 12.1 and 12.2.....	172
Figure D. 1: Linearized Langmuir Isotherm (2.5 g/L)	187
Figure D. 2: Linearized Langmuir Isotherm (3.5 g/L).	188
Figure D. 3: Linearized Langmuir Isotherm (4.5 g/L).	189
Figure D. 4: Linearized Freundlich Isotherm (2.5 g/L).....	191
Figure D. 5: Linearized Freundlich Isotherm (3.5 g/L).....	192
Figure D. 6: Linearized Freundlich Isotherm (4.5 g/L).....	193
Figure D. 7: Linearize Dubinin-Raduschkevich isotherm (2.5 g/L).	195
Figure D. 8: Linearize Dubinin-Raduschkevich isotherm (3.5 g/L).	196
Figure D. 9: Linearize Dubinin-Raduschkevich isotherm (4.5 g/L).	197

List of tables

Table 2. 1: Maximum limits of permitted discharges.....	15
Table 2. 2: Advantages and disadvantages of wet and dry washing.....	19
Table 2. 3: Typical biodiesel wastewater characteristics.	20
Table 3. 1: Electrochemical oxidation experiments runs.....	43
Table 3. 2: Factors in Central composite design.....	45
Table 3. 3: Central composite design experimental matrix.	46
Table 3. 4: Chitosan adsorption experiments and conditions.....	47
Table 4. 1: Characteristics of the Biodiesel wastewater used in this study.	54
Table 4. 2: Characteristics of biodiesel wastewater after acidification.	56
Table 4. 3: Initial test experiments.....	57
Table 4. 4: Electrochemical oxidation - experiments.....	60
Table 4. 5: Final concentrations for COD, BOD & FOG - experiments	62
Table 4. 6: Electrochemical oxidation: Additional experiments.	63
Table 4. 7: Final concentrations for COD, BOD & FOG - Additional experiments.....	65
Table 4. 8: Electrochemical oxidation: Addition of NaCl experiments.	68
Table 4. 9: Final concentrations for COD, BOD & FOG - NaCl experiments.....	71
Table 4. 10: Mean energy consumption.	72
Table 4. 11: Energy consumption for various wastewater types.	73
Table 4.12: ANOVA for Response surface reduced quadratic model.	74
Table 4. 13: Langmuir isotherm parameters at pH of 2.....	92
Table 4. 14: Freundlich isotherm parameters	94

Table 4. 15: D-R isotherm parameters	96
Table 4. 16: Integrated treatment COD removal.....	97
Table 4. 17: Integrated treatment process: Final pollutant concentrations	98
Table B 1: Results from experiment A.....	128
Table B 2: Results from experiment B.....	128
Table B 3: Results from experiment C.....	129
Table B 4: Results from experiment D.....	131
Table B 5: Results from experiment E.....	131
Table B 6: Results from experiment F.....	132
Table B 7: Results from experiment G.....	132
Table B 8: Results from experiment H.....	133
Table C 1. 1: Results from experiment 1.1.....	136
Table C 1. 2: Results from experiment 1.2.....	137
Table C 1. 3: Results from experiment 2.1.....	139
Table C 1. 4: Results from experiment 2.2.....	140
Table C 1. 5: Results from experiment 3.1.....	142
Table C 1. 6: Results from experiment 3.2.....	143
Table C 1. 7: Results from experiment 4.1.....	145
Table C 1. 8: Results from experiment 4.2.....	146
Table C 1. 9: Results from experiment 5.1.....	148
Table C 1. 10: Results from experiment 5.2.....	148
Table C 1. 11: Results from experiment 6.1.....	151

Table C 1. 12: Results from experiment 6.2.	151
Table C 1. 13: Results from experiment 7.1.	154
Table C 1. 14: Results from experiment 7.2.	155
Table C 1. 15: Results from experiment 8.1.	158
Table C 1. 16: Results from experiment 8.2.	159
Table C 1. 17: Results from experiment 9.1.	161
Table C 1. 18: Results from experiment 9.2.	162
Table C 1. 19: Results from experiment 10.1	164
Table C 1. 20: Results from experiment 10.2	165
Table C 1. 21: Results from experiment 11.1	167
Table C 1. 22: Results from experiment 11.2.	168
Table C 1. 23: Results from experiment 12.1	170
Table C 1. 24: Results from experiment 12.2	171
Table D. 1: Adsorption data from experiment 1.	175
Table D. 2: Adsorption data from experiment 2.	176
Table D. 3: Adsorption data from experiment 3.	177
Table D. 4: Adsorption data from experiment 4.	179
Table D. 5: Adsorption data from experiment 5	180
Table D. 6: Adsorption data from experiment 6	181
Table D. 7: Adsorption data from experiment 7.	183
Table D. 8: Adsorption data from experiment 8	184
Table D. 9: Adsorption data from experiment 9	185
Table D. 10: Langmuir Isotherm Data Experiment 1.....	187

Table D. 11: Langmuir Isotherm Data Experiment 2.....	188
Table D. 12: Langmuir Isotherm Data Experiment 3.....	189
Table D. 13: Freundlich Isotherm Data Experiment 1.....	191
Table D. 14: Freundlich Isotherm Data Experiment 2.....	192
Table D. 15: Freundlich Isotherm Data Experiment 3.....	193
Table D. 16: Dubinin-Raduschkevich Isotherm Data Experiment 1	195
Table D. 17: Dubinin-Raduschkevich Isotherm Data Experiment 2.	196
Table D. 18: Dubinin-Raduschkevich Isotherm Data Experiment 3.	197

List of Photos

Photo 3. 1: Electrochemical Reactor	44
Photo 3. 2: Magnetic heater/stirrer.	49
Photo 3. 3: Thermo-reactor	50
Photo 3. 4: Photometer	50
Photo 3. 5: Multiparameter meter.....	51
Photo 3. 6: pH meter.....	51
Photo 3. 7: Turbidity Meter	52
Photo 4. 1: Wastewater after each respective treatment stage.....	99

List of acronyms

EO:	Electrochemical oxidation
COD:	Chemical Oxygen Demand
BOD:	Biological Oxygen Demand
FOG:	Fats, Oils & Greases
BD:	Biodiesel
BDWW:	Biodiesel Wastewater
FAME:	Fatty Acid Methyl Ester
FFA:	Free Fatty Acid
DD:	Degree of deacetylation
rpm:	Revolutions per minute
TDS:	Total Dissolved solutes
EC:	Electrical conductivity
MMO:	Mixed Metal oxides
DSA:	Dimensionally stable anodes
D-R:	Dubinín-Raduschkevich
ICE:	Instantaneous Current efficiency

List of symbols

Symbol	Definition	Unit
Q_e / q_e	amount of COD adsorbed at equilibrium / amount of COD adsorbed at any given time	mg/g
C_0	initial concentration of COD in solution	mg/L
C_e	concentration of COD in solution at equilibrium	mg/L
V	volume of solution	litre
m	mass of adsorbent used	g
q_m	practical limiting adsorption capacity	mg/g
K_L	Langmuir constant	L/mg
R_L	dimensionless constant separation factor	
K_F	Freundlich constant	
n	heterogeneity factor	
K	constant related to adsorption energy	mol^2/kJ^2
ϵ	Polanyi potential	J/mol
R	universal gas constant	J/mol.K
T	temperature	Kelvin/ Celcius
mA	milli-ampere	mA
M	Molarity (mol/Litre)	
μm	length	micrometer
g	mass	gram
L	volume	Litre
cm^2	area	squared centimeter
m^3	cubic meter	m^3
i	current	ampere
V_m	mean cell voltage	volt
Δt	reaction time	hour
V_R	electrolyte volume	Litre
E	mean energy consumption	kWh/kgCOD
F	faraday constant	C/mol

CHAPTER 1

Introduction

Chapter 1 Introduction

1. Background

Global energy consumption has been increasing significantly due to substantial population growth and changes in lifestyle (Masum et al., 2013). The transportation sector, being particularly energy demanding, relies primarily on diesel engines which are more efficient and cost effective than gasoline engines (Habibullah et al., 2014). The majority of the energy is currently supplied by petroleum-based fossil fuels. This however, has led to a rapid depletion of the worlds reserves of fossil fuel (Masum et al., 2013).

To meet the growing demand of the population, past research efforts were focussed on the development of fossil crude oil, coal and natural gas based refinery. However, from ecological and environmental points of view, fossil fuel resources are not regarded as sustainable. At the moment 90% of the energy carriers originate from fossil fuels which are associated with the emission of carbon dioxide to the atmosphere (Chandra et al., 2012).

Increased emission of unburned hydrocarbons, carbon monoxide and nitrogen oxides due to combustion of fossil fuels contributes to environmental pollution. As a result, environmental effects such as global warming, smog, deforestation, ozone depletion and acidification are on the rise (Sundus et al., 2017). Every year our earth's atmosphere receives roughly 25 billion tons of CO₂ through anthropogenic activities (Abbasi & Abbasi, 2011).

Solutions aimed at reducing the rapid consumption of non-renewable fossil resources such as petroleum, natural gas, coal and minerals, need to be established. Kamm et al., (2012) suggests that larger parts of the global economy be systematically converted to a sustainable bio-based economy with bio-energy, biofuels, and bio-based products as its main pillars.

Alternative fuels, such as biodiesel, should realise a harmonious correlation with sustainable development, energy conversion, efficiency and environmental preservation (Haseeb et al., 2011). Biodiesel is renewable, bio-degradable, non-toxic and possesses properties close to that of diesel fuel, and can be produced from vegetable oil and animal fats (Fazal et al., 2011).

Additionally, biodiesel can be blended with conventional diesel to various degrees that can be used in conventional compression ignition engines with no modification. The usage of these blends can improve fuel quality and could have a positive effect on emissions (Sundus et al., 2017). According to Jaruwat et al. (2010) the demand for biodiesel as an alternative fuel is increasing exponentially and is being met through the conventional production process. The alkali-catalysed transesterification of vegetable oils produces a high conversion of triglycerides (i.e. vegetable oils) to fatty acid methyl esters (biodiesel) (Chavalparit & Ongwandee, 2009).

Estimated global biodiesel production will increase from 30.1 Million m³ in 2015 to 41.1 Million m³ by the year 2025 (Foley et al., 2015). The biodiesel production process is water and energy demanding with additional environmental and economic costs. The amount of highly polluting biodiesel wastewater, produced through the traditional wet washing process, increases when removing excess contaminants (Ngamlerdpokin et al. 2011).

For every 100L of biodiesel produced an estimated 20L to 120L of biodiesel wastewater is discharged, depending on the amount of biodiesel washing steps involved (Jaruwat et al., 2010; Chavalparit & Ongwandee, 2009; Kumjadpai et al., 2011; Rattanapan et al., 2011).

Biodiesel wastewater is characterised by a high pH and low concentrations of nitrogen and phosphorous which renders the wastewater difficult to degrade naturally. Direct discharge of this wastewater may lead to sewer line clogging and disturbances in microbial activity (Daud et al., 2017). It is therefore clear that effective treatment of biodiesel wastewater is needed to meet effluent standards, reduce its environmental hazards, and conserving water resources (Kumjadpai et al., 2011).

Water has a significant role in our daily activities, its overall consumption is growing daily because of our increasing living standards (Gorjian & Ghobadian, 2015). Scarcity of water is a broad issue that is a concern for national governments and policy making bodies across the world, as such, imbalances in water supply has led to increased attention to the utilisation and allocation of water supply in the water-energy section (Thopil & Pouris, 2016).

1.1. Research problem

Biodiesel wastewater is classified as an industrial wastewater. The discharge of industrial wastewater in the City of Cape Town is regulated under the “City of Cape Town: Wastewater and Industrial Effluent By-Law, 2013”. Currently, an industrial biodiesel production company operating in the City of Cape Town discharges wastewater into the sewer that does not comply with the industrial discharge standards. These actions incur additional costs in terms of fines. Therefore, research studies are being conducted to effectively treat biodiesel wastewater to reduce the adverse effects it has on the environment and biological processes in wastewater treatment facilities, abide by more stringent effluent requirements and avoid fines. Effective treatment of the wastewater may result in recycling of the water during the production process.

1.2. Research questions

1. Can electrochemical oxidation followed by adsorption using chitosan be used to treat biodiesel wastewater sufficiently so that it meets the required industrial wastewater discharge standards?
2. What effect does current density and NaCl concentration have on the removal of COD, BOD and FOG during electrochemical oxidation of biodiesel wastewater?
3. How will the adsorption rate change when the pH is adjusted, and chitosan concentration altered?

1.3. Aims and objectives

The aim of this research is to remove COD, BOD and FOG from biodiesel wastewater in an integrated treatment process using electrochemical oxidation followed by adsorption with chitosan, to meet the required industrial effluent discharge standards.

The research objectives are to:

1. Investigate electrochemical cell operating conditions in terms of various current densities and NaCl concentrations on the removal of COD, BOD and FOG.
2. Study the effect of pH and chitosan dosages on the adsorption rate during the removal COD, BOD and FOG.

1.4. Significance of this research

Effective treatment of biodiesel wastewater may result in compliance with industrial wastewater discharge standards, cost savings regarding fines payed as well as reduced fresh water usage through recycling of water in the production process.

1.5. Delineation of the study

During this study the removal of COD from biodiesel wastewater was observed through an integrated treatment process. This process consists of three consecutive steps:

1. Acidification;
 2. electrochemical oxidation and
 3. adsorption using chitosan.
- Acidification of biodiesel wastewater was only evaluated using H_2SO_4 .
 - Electrochemical oxidation occurred at $60^\circ C$ using $IrO_2-Ta_2O_5/Ti$ anodes.
 - Adsorption using chitosan was investigated using pH values ranging from 2 – 6 with a constant stirring rate of 350 rpm at ambient conditions.
 - All other variables are delineated.

1.6. Structure of the thesis

- Chapter 1** gives the introduction and background to this study. The research problem and research questions are highlighted. The aims and objectives of the research are explained, and the significance of the study is outlined.
- Chapter 2** gives an in-detail literature study related to the research.
- Chapter 3** describes the research methodology.
- Chapter 4** gives the results and discussion in terms of each individual process used as well as the factors affecting them.
- Chapter 5** is the conclusion and recommendations made during this study.

CHAPTER 2

Literature Review and Theory

Chapter 2 Literature review and theory

2. Introduction

This chapter presents a general overview of biodiesel production, biodiesel wastewater generation, characteristics of biodiesel wastewater, local industrial effluent standards as well as the state of fresh water supply in South Africa. Included is a review of the literature on conventional and novel biodiesel wastewater treatment methods and technologies. However, the focus is on electrochemical oxidation using IrO₂-Ta₂O₅/Ti anodes followed by adsorption using chitosan as two of the treatment methods. Certain factors affecting electrochemical oxidation and adsorption have been assessed.

2.1. Global Fresh water supply

To understand the natural water cycle and the effect that human activities might have, it is necessary to have reliable estimates of water resources that are stored in various water bodies and in different physical states. Available estimates of the amounts of water on earth are given in Figure 2.1. The total volume of fresh water, 35 million km³, amounts to only 2.5% of the total water in the hydrosphere. 68.7% of this, 24 million km³, comes in the form of ice and permanent snow situated in the Antarctic and arctic regions. The main sources of human water consumption originates from fresh water rivers and lakes which contain approximately 0.26% or 90 000 km³ of the global fresh water reserves (Shiklomanov, 1993).

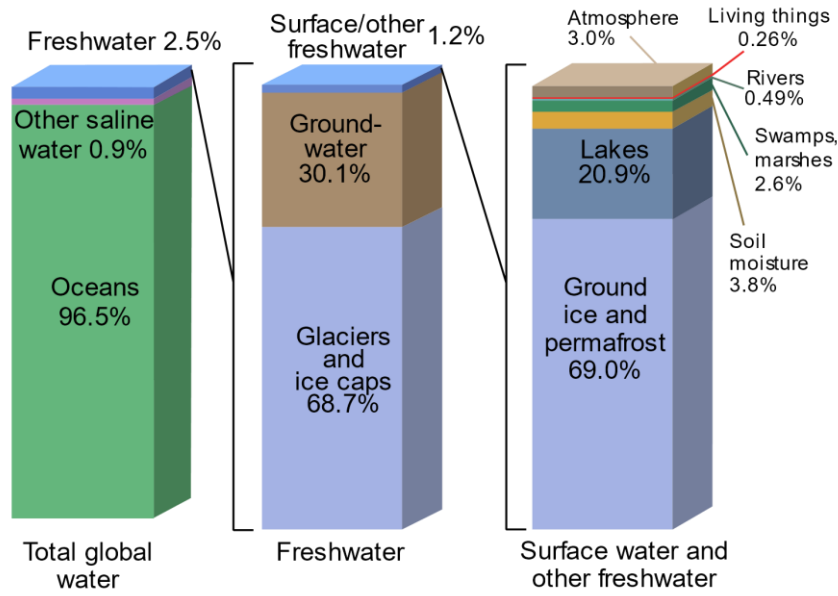


Figure 2. 1: Earth's water supply (WWF-SA, 2016)

2.2. Water in South Africa

Water availability and accessibility in Africa will be subjected to additional stress due to climate change (B.E. et al., 2014). The population at risk of water stress could reach 460 million people by the year 2025 when the availability of water is predicted to be less than 1000 m³/person/year in nine African countries and 1000-1700 m³/person/year in twelve African countries (Nkhonjera, 2017).

South Africa is a semi-arid country subjected to water stress due to low rainfall and high evaporation rates (Ilemobade et al., 2009). It is considered one of the 30 driest countries in the world (Thopil & Pouris, 2016), and recently experienced a severe drought during 2015-16 (Vogel & Zyl, 2016). The country is approaching physical water scarcity and will face higher levels of water stress by the year 2040 (Harding et al., 2017).

Water in South Africa is governed by the Water Services Act of 1997 and the National Water Act (NWA) of 1998. It is founded on the principle that all water forms part of a unitary, independent water cycle, and should therefore be governed under consistent rules.

The NWA contains provisions for the protection, use, development, conservation, management and control of South African water resources. The transformation in the water resource sector includes a shift from central management to decentralised institutions, including the establishment of Water Management Areas which are mainly defined by hydrological catchment borders (WWF-SA, 2016).

The country has been divided into 19 catchment based water management areas (Figure 2.2) to facilitate water management. Nine of these areas encounter moderate shortages and six face severe shortages (Water Resources Group, 2009).

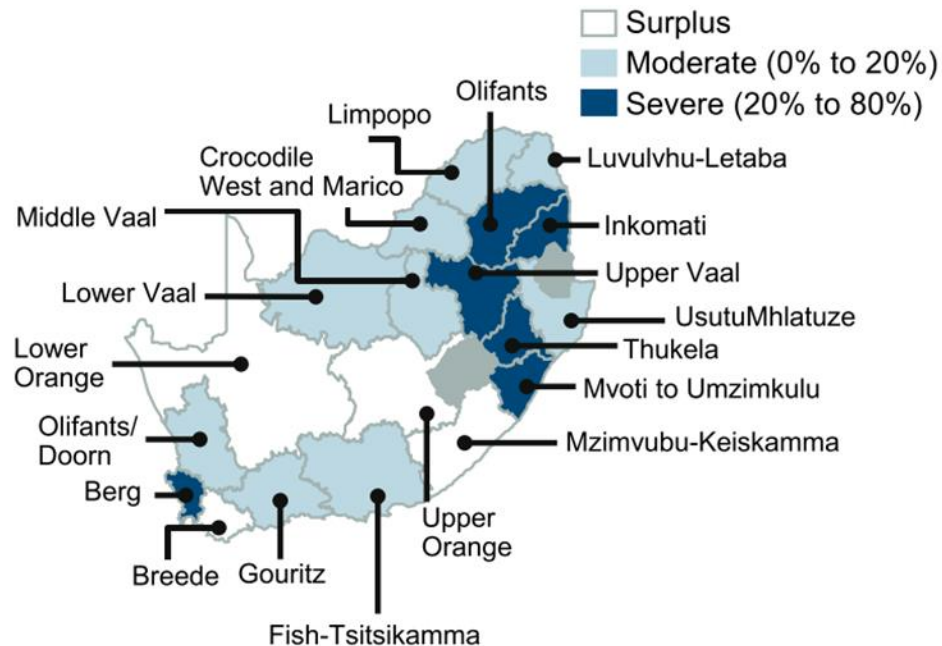


Figure 2. 2: Projections of water shortages by the year 2030 (Water Resources Group, 2009)

The National Water Resource Strategy (Department of Water Affairs, 2004), provided a high-level reconciliation of the requirements for, and availability of water in 2000. The country and each of the 19 water management areas were considered. The total yield of water available from the river systems in South Africa on a reliable basis, was estimated at 13 227 million m³/annum.

Local requirements were estimated at 12 871 million m³/annum whereas 170 million m³/annum was being released or transferred out of South Africa. Even though this implied that a surplus existed for the country, water deficits were observed in more than half of the water management areas. The implication is that South Africa's surface water resources would be fully committed over the medium to long term and that a mix of water sources would be required to reconcile supply and demand (Department of Water Affairs, 2013).

A total renewable water supply of 68 000 million m³ was estimated by Water Resources Group, (2009), including approximately 19 000 million m³ of renewable ground water. Currently only 15 000 million m³ is accessible and reliable. This includes 1 500 million m³ from ground water sources. Ground water amounts to 15% of the total volume available, however over 300 towns and 65% of the rural population depend on this resource for their water supply.

Municipalities are challenged to explore alternative sources and efficient management of water supply, given that water use is approaching water yield. Continuous pollution of surface and ground water resources give rise to additional complications (Adewumi et al., 2010).

Furthermore, Department of Water Affairs, (2013) states that reconciliation strategies have been completed for 8 large systems including the Western Cape and KwaZulu-Natal metropolitan areas. The quality of water is one of the fundamental considerations in water resource management and the Department of Water Affairs lists the main sources of pollution as follows:

- Urban and industrial effluent discharges into the environment
- High concentrations of salinity in irrigation return flows
- Mining operation wash off and leachates
- Inadequate sanitation in some areas of human settlement

The ongoing severe drought has depleted water reserves and resulted in water restrictions being implemented. The economic and socio-economic effects of the drought across the region are evident, extensive and have negatively affected key sectors of the economy, such as agriculture and food security (Baudoin et al., 2017).

2.3. Water usage in South Africa

South Africa has an approximate per capita consumption of 235 litre/capita/day, which is higher than most other countries since the international gross average consumption is only 173 litre/capita/day. The figure was based on the total water supplied which includes losses as well as all commercial and industrial uses (Mckenzie et al., 2012).

A detailed water usage per sector is given by Siebrits & Fundikwa, (2017) in Figure 2.3 where irrigation accounts for 67%, urban 18%, mining 5%, rural 4%, afforestation 3%, power generation 2% and outward transfers 1%.

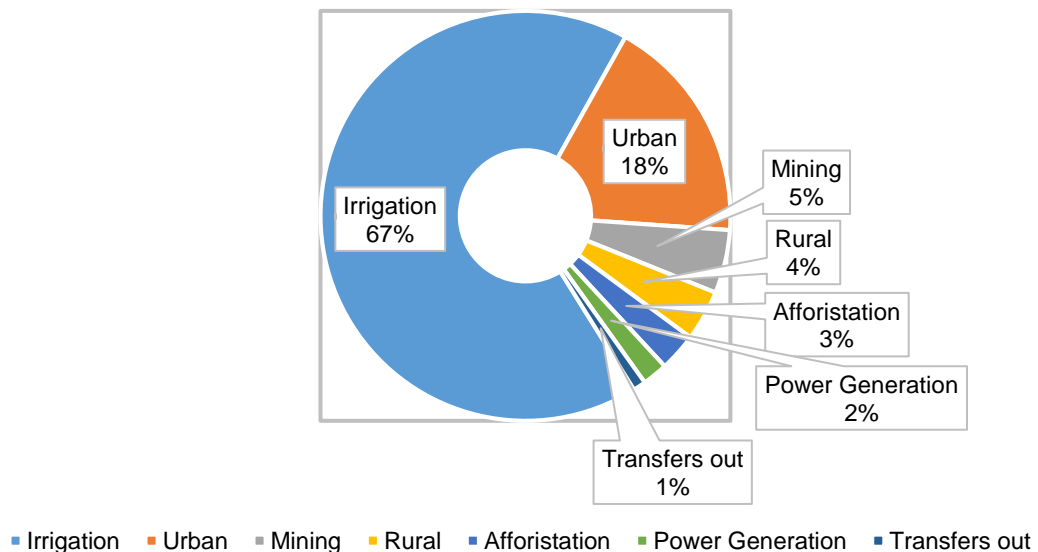


Figure 2. 3: Water use in South Africa by sector (Siebrits & Fundikwa, (2017).

The annual average surface runoff is 49 Billion m³ of which only 30% can be allocated at a high assurance of supply. With the majority (98%) of the usable portion already allocated at a high assurance of supply, only 2% of unallocated usable resources are left. The country faces high levels of water wastage and inefficient use where 37% of the allocated water supply is lost due to leaks in the current urban infrastructure (WWF-SA, 2016).

Certain non-drinking applications such as landscape irrigation, toilet and urinal flushing, and a variety of industrial processes does not need water with the same quality as that of drinking water. However, high quality drinking water is often used for these applications in South Africa which is an unsustainable practice.

Re-use of wastewater as an alternative could form an important component of wastewater management as well as water resource management. This could dramatically reduce environmental impacts associated with the discharge of wastewater to surface waters. It is therefore essential to evaluate the potential of wastewater reuse as a viable alternative in the drive towards overcoming the challenges of current and future water shortages in South Africa (Adewumi et al., 2010).

2.4. City of Cape Town: Wastewater and Industrial Effluent By-Law, 2013

The City of Cape Town: Wastewater and Industrial Effluent By-Law, 2013 was officially published in the Western Cape Provincial Gazette no. 7227 on 7 February 2014 (Government, 2014). The by-law defines “wastewater” as “any liquid waste, whether or not containing matter in solution or suspension, and includes domestic liquid waste and industrial effluent, but excludes storm water”.

It further defines “Industrial effluent” as “any liquid whether or not containing matter in solution or suspension, which is given off in the course of or as a result of any industrial trade, manufacturing, mining or chemical process or any laboratory, research, service, or agricultural activity, and includes matter discharged from a waste grinder” (City of Cape Town, 2013). The discharge of biodiesel wastewater is thus controlled under this By-Law.

The maximum limits of permitted discharges, relevant to this research project, are given in Table 2.1. The full table with all the parameters, as per the By-law, can be found in Appendix A.

Table 2. 1: Maximum limits of permitted discharges (City of Cape Town, 2013).

Parameter	Unit	Not less than	Not to exceed
Temperature at point of entry	°C	0	40
Electrical conductivity at 25°C	mS/m		500
pH Value at 25°C		5.5	12
Chemical Oxygen Demand	mg/L		5000
Total dissolved solids at 105°C	mg/L		4000
Oils, greases, waxes and fat	mg/L		400

The By-law further stipulates that any person who commits an offence, in term of the by-law, is liable to a fine or conviction, to a term of imprisonment not exceeding 12 months, or to both such fine and such imprisonment, to be assessed by the City (City of Cape Town, 2013).

2.5. Biodiesel

Biodiesel is also defined as monoalkyl ester of fatty acid or Fatty Acid Methyl Ester (FAME) (Yaakob et al., 2013). It is biodegradable, non-toxic, almost sulphur free and non-aromatic (Đurišić-Mladenović et al., 2018). Since biodiesel can be used as a blending agent or as a direct replacement for diesel fuel in engines, it has been attracting increasing attention worldwide (Demirbas, 2009). When biodiesel is blended with petroleum based diesel it is referred to as BXX, where XX denotes the percentage of biodiesel in the blend. Blends such as B20 or lower have been utilised by marketers and end users since it can be used in all engines without modification (Silitonga et al., 2013).

Traditionally biodiesel is derived from biomass such as vegetable oils (Simasatitkul et al., 2012) or animal fats (Ito et al., 2012), however, recent studies pursued other sources such as micro-algae (Faried et al., 2017) and scum sludge (Wang et al., 2016) amongst others.

Various methods and processes are used for the production of biodiesel. These include alkali catalysed (Chitra et al., 2005; Meher et al., 2006), acid catalysed (Wang et al., 2006; Jacobson et al., 2008), enzymatic catalysed (Christopher et al., 2014; Adewale et al., 2017), membrane technology (Ferrero et al., 2014; Atadashi, 2015), micro-algae (Faried et al., 2017), microwave assisted (Leadbeater & Stencel, 2006; Xiang et al., 2017), ultrasonic assisted (Stavarache et al., 2003; Mootabadi et al., 2010) and supercritical conditions (CAO et al., 2005; Tan et al., 2010). However, biodiesel is commercially produced through a process known as transesterification (Daud et al., 2014), since it is physically and chemically similar to conventional diesel.

Transesterification is a reaction between vegetable oil (triglycerides) and alcohol that forms esters and glycerol as shown in Figure 2.4. This reaction occurs in the presence of a catalyst in order to improve the reaction rate and yield (Ma & Hanna, 1999). A stoichiometric ratio of 3:1 alcohol to triglyceride is needed for the transesterification reaction, however, practically a higher ratio is used to shift the reaction to the right since this reaction is reversible (Enweremadu & Mbarawa, 2009).

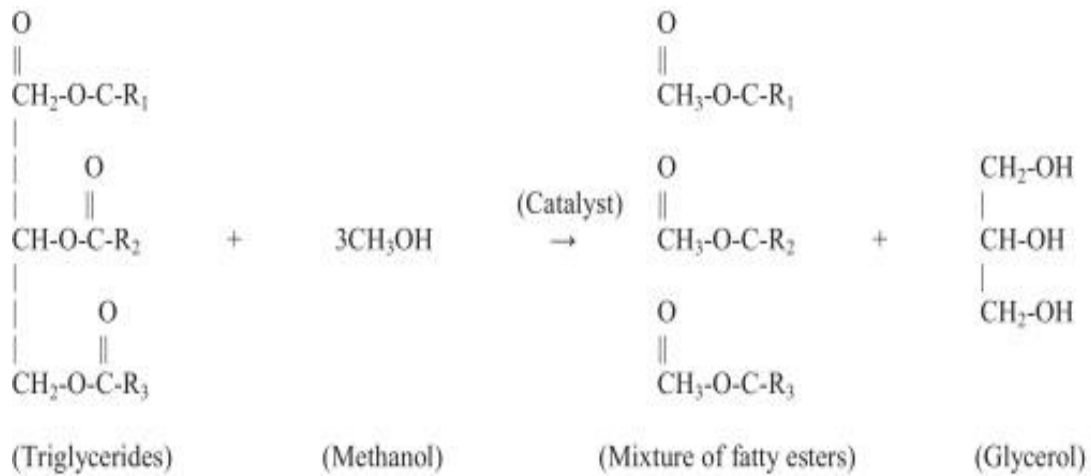


Figure 2. 4: Biodiesel reaction (Ma & Hanna, 1999).

The conversion reaction, transesterification, consists of three consecutive reversible reactions, shown in Figure 2.5. Initially, triglycerides are converted to diglycerides. This is followed by the conversion of diglycerides to monoglycerides. The third step involves the conversion of monoglycerides to glycerol. One ester molecule is produced for each glyceride in each of the three steps.

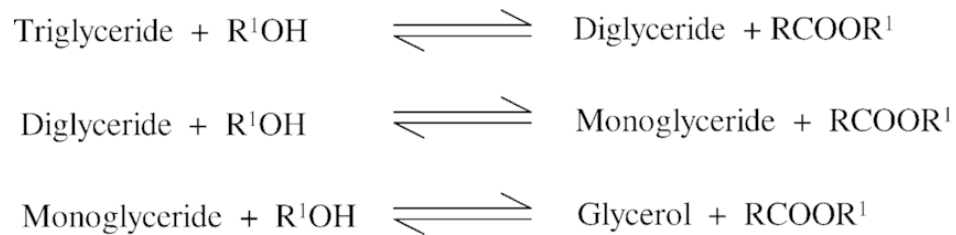


Figure 2. 5: Biodiesel production reaction steps.

2.5.1. Biodiesel wastewater

Biodiesel wastewater is mostly generated through the purification step of biodiesel production. The purification process is necessary to ensure that excess impurities and contaminants are removed to ensure a high quality end product (Daud et al., 2014). Generally, biodiesel purification occurs through the wet washing process (Huaping et al., 2006; Alba-Rubio et al., 2012), as well as the dry washing process (Kouzu & Hidaka, 2013; Shibasaki-Kitakawa et al., 2013). Alternatively, some studies have shown interest in biodiesel purification using membrane technology (Atadashi et al., 2012; Gomes et al., 2010).

2.5.2. Biodiesel wastewater generation

The wastewater used in this study was generated through the wet washing process. The high volumes of wastewater generated through the wet washing process leads to added economic and environmental impacts (Ferrero et al., 2014). Biodiesel wastewater should thus be handled with care and adequately treated before discharge in order to minimize negative effects to the environment (Atadashi et al., 2012; Stojković et al., 2014).

Since the wet washing process is able to produce a purified biodiesel that satisfies stringent quality standards imposed by EN 14214 or ASTM D6751, it is the most used purification method (Atadashi et al., 2012). During the wet washing process water with a temperature between 50 and 60°C, sometimes acidified by the addition of a mineral acid, is used for the washing of crude biodiesel. In doing so, salts and trace amounts of residual glycerol and methanol are effectively removed because of their high solubility in water (Stojković et al., 2014).

Similarly, soaps and catalyst are also removed from crude biodiesel (Gomes et al., 2010; Daud et al., 2014). Depending on the specifics of the production process used to produce biodiesel large amounts of water may be required to effectively purify biodiesel (Stojković et al., 2014; Encinar et al., 2007).

The advantages and disadvantages of wet and dry washing are outlined in Table 2.2.

Table 2. 2: Advantages and disadvantages of wet and dry washing (Stojković et al., 2014)

Method	Advantage	Disadvantage
Wet washing	simple and effective in removing glycerol and methanol	large quantities of water
	removal of soluble compounds and soap	formation of free fatty acids possible
	99% pure biodiesel possible	emulsions may be formed in the presence of soaps
	could use aqueous solutions of acid	time consuming
	lower running cost compared to dry washing	large amounts of wastewater generated
Dry washing	easier than wet washing	standard specification might not be met
	drastic reduction in water usage	glycerol should be removed before dry washing
	decreased production time	methanol not removed
	continuous operation possible	slightly higher running cost
	uses less space	extra equipment needed

2.5.3. Biodiesel wastewater characteristics

Untreated biodiesel wastewater contains various impurities such as glycerol, soap, metals, methanol, Free Fatty Acids (FFA), catalyst and glycerides. It has an opaque white colour and a pH rang of 8 - 11. The wastewater has a low concentration of nitrogen and phosphorous which makes it difficult to degrade naturally and hazardous to the environment as these conditions do not promote bacterial growth (Pitakpoolsil & Hunsom, 2014; Veljković et al., 2014).

Typical biodiesel characteristics can be found in Table 2.3. Furthermore, biodiesel derived wastewater contain long-chain fatty acids which has been shown to be toxic towards anaerobic consortium through adsorption onto the cell wall which interferes with transport and protective functions (Siles et al., 2011).

Table 2. 3: Typical biodiesel wastewater characteristics.

pH	COD (mg/L)	FOG (mg/L)	BOD (mg/L)	Reference
11		15100		(Suehara et al., 2005a)
8.9	30980	6020		(Chavalparit & Ongwandee, 2009)
9 - 10.	312000 - 588800	18000 - 22000	168000 - 300000	(Jaruwat et al., 2010)
8 - 10	60000 - 150000	7000 - 15000	30000 - 60000	(Rattanapan et al., 2011)
	312000 - 588800	18000 - 22000	168000 - 300000	(Ngamlerdpokin et al., 2011)
10	542400	21048	224630	(Kumjadpai et al., 2011)
9 - 10	29595 - 54362	1040 - 1710	1492 - 2286	(Pitakpoolsil & Hunsom, 2013)

2.6. Conventional wastewater treatment technologies

Treatment technologies that are conventionally used for the treatment of wastewater are briefly discussed.

2.6.1. Adsorption

Worch (2012) describes adsorption as an enrichment of chemical species from a fluid phase on the surface of a liquid or solid. Adsorption as a water treatment process has been proved to be efficient. Molecules are adsorbed onto active energy rich sites that can interact with solutes in the adjacent aqueous phase due to specific electronic and spatial properties. Similarly, Gold (2014) states that adsorption is an increase in the concentration of a dissolved substance at the interface of a condensed and liquid phase due to the operation of surface forces. It can also occur at the interface of a condensed and gaseous phase.

Adsorption is a surface phenomenon with a common mechanism for organic and inorganic pollutant removal. When a solution containing a solute comes into contact with a solid having a highly porous surface structure, liquid-solid intermolecular forces of attraction will cause the solute molecules to be concentrated or deposited at the solid surface. The retained solute on the solid surface is called the adsorbate. The solid onto which the adsorbate is deposited is called the adsorbent (Rashed, 2013).

Adsorption is used as a treatment method for its versatility and efficiency in the separation of a wide range of chemical compounds as well as its ease of operation (Zhang et al., 2010). According to Wong (2006) the success of an adsorbent depends on its equilibria and kinetic performance.

A better performing adsorbent is one with a large surface area which requires less time to reach adsorption equilibria (Bhatnagar & Minocha, 2006). Rashed (2013) classify adsorbents as either natural or synthetic. Natural adsorbents include charcoal, clay and clay minerals, zeolites and ores which are relatively cheap, abundant and has the potential for modification to enhance their adsorption capabilities.

Synthetic adsorbents on the other hand are prepared from agricultural wastes, household wastes, industrial wastes, sewage sludge as well as polymeric adsorbents. Each of these adsorbents has their own characteristics in terms of porosity, pore structure and adsorption surfaces. Some wastes used include coconut shell, rice husks, sawdust, chitosan and seafood processing wastes. Physiochemical and microbiological pre-treatment is sometimes required to enhance the adsorption process (Pitakpoolsil & Hunsom, 2014).

2.6.2. Coagulation and Flocculation

Various authors (Li et al., 2016; Daud et al., 2015; Ang et al., 2016) report on the use of coagulation for the treatment of wastewater. A coagulant is added to separate small particles from a solution over time. According to Yang et al. (2016) a coagulant is typically added to rapidly mixed wastewater which destabilises the colloidal particles through electrostatic interactions. This is followed by a slower agitation period where the destabilised particles aggregate/agglomerate and form larger flocs which settle out (Daud et al., 2015). The formation of flocs are responsible for the removal or reduction of COD, BOD, suspended solids and turbidity (Saraswathi & Saseetharan, 2012).

Coagulants can be classified into three groups: inorganic, organic polymers and natural coagulants (Yang et al., 2016). Typical coagulants used include Alum and Poly-Aluminium Chloride (Rodriguez Boluarte et al., 2016), ferric chloride and ferric sulphate (Daud et al., 2015) and chitosan (Renault et al., 2009) amongst others.

The development of natural coagulants is due to several issues that exist around the excessive use of conventional coagulants. Corrosion, production of non-biodegradable sludge and the presence of some neurotoxic and carcinogenic monomers are given as some reasons (Ang et al. 2016). Ngamlerdpokin et al. (2011) states that coagulation provides a low operating cost and that the materials are readily available. However, its principle disadvantages are the need for a large treatment area as well as residual coagulants in the treated wastewater.

2.6.3. Electrocoagulation

According to Emamjomeh & Sivakumar (2009) electrocoagulation (EC) is an efficient method for the treatment of various types of wastewaters. The process is characterised by the destabilisation of emulsified, dissolved and suspended contaminants in a solution. This occurs as a result of electrochemical dissolution of sacrificial electrodes which produce anions. These metal ions neutralise the negatively charged dispersed particles as well as reacting with hydroxyl ions at the anode (Liu et al. 2016).

The hydroxyl ions generate iron and aluminium hydroxides known to be efficient coagulants (Zongo et al., 2009). Khandegar & Saroha (2013) found that the flocs that are formed are large, more stable and contain less water bound to them and therefore can be removed through filtration.

The hydrogen gas formed at the cathode assist in the flotation of the flocs to the surface (Zongo et al., 2009). Lobo et al. (2016) states that EC is an attractive treatment process as it lacks added chemicals, produces less sludge and has simple operational needs.

Other advantages according to Khandegar & Saroha (2013) include removal of species that chemical coagulation does not remove, readily filterable sludge utilised as a soil additive and minimal start-up time; disadvantages of EC include periodic replacement of sacrificial anodes, possible formation of toxic chlorinated compounds and limited use in wastewater with low dissolved solids.

2.6.4. Biological Treatment

von Sperling (2008) describes biological treatment of wastewater as biological mechanisms and processes that take place within a body of water where organic and inorganic matter is converted biologically to inert mineralised materials. Industrial biological treatment aims at utilising these processes under controlled conditions and higher rates. Biological treatment is suitable for all types of wastewater containing biodegradable material if the proper analysis and environmental control is applied (Tchobanoglous et al. 2003). However, biodiesel wastewater is characterised by a high pH, low nutrient concentrations and high free fatty acids. These conditions inhibit microbial growth and therefore biological treatment of biodiesel wastewater should occur under optimum conditions (Veljković et al., 2014).

Tchobanoglous et al. (2003) lists five main types of metabolic functions of biological treatment: Aerobic, which occurs in the presence of oxygen; Anaerobic, which occurs in the absence of oxygen; Anoxic, where nitrate nitrogen is converted to nitrogen gas in the absence of oxygen, also called denitrification; Facultative processes, where the presence or absence of molecular oxygen does not matter and lastly, a combination of all the processes to achieve a specific objective.

In recent years biological treatment in combination with various other technologies has been studied for the treatment of various wastewaters such as: Interior micro-electrolysis/Fenton oxidation-coagulation and biological degradation (Xu et al., 2016); Combined biological and photocatalytic treatment of real coke oven wastewater (Sharma & Philip, 2016); Advanced treatment of biologically treated coking wastewater by membrane distillation coupled with pre-coagulation (J. Li et al., 2016); and Physical–chemical and biomethanization treatment of wastewater from biodiesel manufacturing (Siles et al., 2011).

2.7. Treatment Technologies used in this study

A review conducted by Veljković et al. (2014) shows that the current BDWW treatment technologies focus on physical, chemical, physico-chemical, electrochemical, biological and integrated treatment processes. These processes aim at reducing the COD, BOD and FOG concentrations as a pre-treatment prior to effluent discharge.

This research will focus on the following processes:

1. Acidification
2. Electrochemical oxidation
3. Adsorption with chitosan

2.8. Acidification

Acidification using strong acids such as H_2SO_4 , HNO_3 and HCl are commonly used as a pre-treatment step in the treatment of BDWW (Ngamlerdpokin et al., 2011; Rattanapan et al., 2011; Jaruwat et al., 2010).

Veljković et al. (2014) states that coalescence of fine oil droplets into larger ones occur because the adjustment of pH affects the electrical forces and carboxyl functional groups on the surface of the oil droplets.

According to Rattanapan et al. (2011) acidification is a process that destroys the protective layer of the emulsifying agent and overcomes the repulsive effects of electrical double layers. This allows for the coalescence of fine oil droplets into larger oil droplets. By using HCl and H_2SO_4 at a pH of 3 lead to a 50% reduction in COD and 80% removal of FOG.

Jaruwat et al. (2010) explains that the addition of H_2SO_4 at a pH of 2.5 separates the wastewater mixture into two phases, an oil-rich top phase and an aqueous phase with low turbidity. FTIR spectra of the oil-rich phase was similar to that of the original biodiesel. This indicates that the oil-rich phase could be recovered biodiesel. The extraction of biodiesel from wastewater occurs when a proton substitutes a Na atom in the soap to form fatty acids and substitute H_2O molecules that combines biodiesel to produce free biodiesel.

Similarly Ngamlerdpokin et al. (2011) found that addition of H_2SO_4 , HNO_3 and HCl at a pH of 2.5 automatically separates the wastewater into two phases. The oil-rich top phase consists of FFA and FAME, whereas the bottom phase contains the residual aqueous phase with low turbidity.

2.9. Electrochemical oxidation

The presence of persistent pollutants in water has led to great environmental concern. These pollutants are detected in trace amounts, however, their presence results in environmental risk due to their toxicity (Eljarrat & Barceló, 2003). These pollutants are classified as recalcitrant and therefore difficult to remove through conventional treatment processes (Subedi & Kannan, 2015).

In an effort to treat these recalcitrant pollutants, electrochemical advanced oxidation processes have been receiving increased attention for the treatment of various pollutants such as pharmaceuticals (Domínguez et al., 2012), pesticides (Martínez-Huitle et al., 2008) and carboxylic acids (Scialdone et al., 2011), amongst others.

Besides being able to effectively treat these recalcitrant pollutants electrochemical advanced oxidation processes present other advantages such as the possible operation under ambient conditions, smaller physical footprint requirements, no additional waste being produced and the ability to be integrated with existing conventional treatment technologies. Electrochemical Oxidation falls into the group of electrochemical advanced oxidation processes and has been the subject of many studies given its ease of scalability and versatility (Garcia-Segura et al., 2018). Electrochemical processes mainly rely on the redox reactions that occur at the electrodes. Oxidation of pollutants occur at the anode, whereas reduction of heavy metals occur at the cathode (Garcia-Segura et al., 2018).

The Electrochemical Oxidation (EO) process is based on the in situ generation of the hydroxyl radical ($\bullet\text{OH}$) (Comninellis, 1994). After fluorine, the hydroxyl radical is the strongest oxidizing species with a high standard reduction potential. This allows it to non-selectively react with most organics which ultimately results in their complete or partial mineralization to CO_2 , water and inorganic ions (Comninellis, 1994; Garcia-Segura & Brillas, 2011).

2.9.1. Electrochemical oxidation mechanism

There are two ways in which organics can be oxidised during EO. Direct anodic oxidation and indirect oxidation (Panizza & Cerisola, 2009; Rajkumar & Palanivelu, 2004).

Direct oxidation occurs when pollutants are oxidised directly at the anode surface through the generation of physically adsorbed active oxygen (adsorbed hydroxyl radicals), or chemisorbed oxygen (oxygen in the oxide lattice MO_{x+1}) (Comninellis, 1994). Complete mineralisation or selective conversion into oxidation products are schematically described in Figure 2.6.

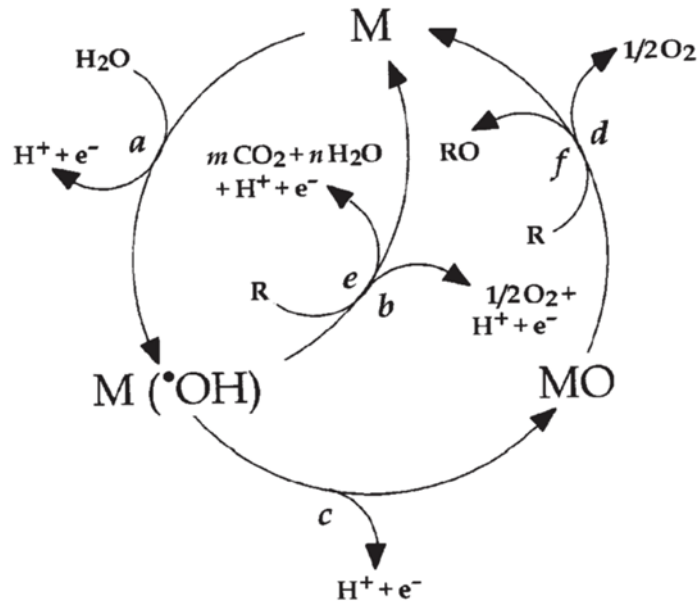


Figure 2. 6: Schematic of anodic oxidation (Comninellis, 1994).

The work done by Comninellis, (1994) describes two limiting cases: “Active anodes” and “non-active anodes”. In both cases the first reaction (a) involves the oxidation of water molecules that lead to the formation of adsorbed hydroxyl radicals shown in Equation a:



With active anodes the interaction between the electrode (M) and the hydroxyl radical ($\cdot OH$); the adsorbed hydroxyl radical may interact with the anode and form a higher oxide (MO) (Equation b).



Consequently, with active anodes the redox couple MO/M acts as a mediator in the oxidation of organics (Equation c), which is in competition with the side reaction of oxygen evolution due to the chemical decomposition of the higher oxide (Equation d):



The oxidative reaction via the surface redox couple MO/M (Equation c) can be much more selective than the reaction involving hydroxyl radicals (Equation e). According to Moreira et al. (2017) active anodes such as Ruthenium dioxide (RuO_2), iridium dioxide (IrO_2), platinum (Pt), graphite and other sp^2 carbon based electrodes are typical examples of active anodes.

When considering non-active anodes, weak interactions exist between the hydroxyl radical and the electrode surface. The oxidation of organics is mediated by the hydroxyl radicals (Equation e) that may result in fully oxidised products such as CO_2 .



In the descriptive schematic (Figure 2.6) R is the fraction of an organic compound containing no heteroatoms, which needs one oxygen atom to be fully transformed into CO₂. This reaction competes with the side reaction of hydroxyl radicals to oxygen (Equation f) without any participation of the anode surface:



A non-active anode does not participate in the anodic reaction and does not provide any catalytic active site for the adsorption of reactants and/or products from the aqueous medium. In this case the anode serves only as an inert substrate which can act as a sink for the removal of electrons (Martínez-Huitle & Ferro, 2006).

Anode materials can be classified in terms of their oxidation power in acidic media as shown in Figure 2.7. The oxidation potential of the anode is directly related to the over-potential for oxygen evolution and to the adsorption enthalpy of hydroxyl radicals on the anode surface. For a given anode material, the higher the O₂ over-potential, the higher is the oxidation power (Comninellis et al., 2008).

Electrode	Oxidation potential (V)	Over-potential of O ₂ evolution (V)	Adsorption enthalpy of M-OH	Oxidation power of anode
RuO ₂ -TiO ₂ (DSA-Cl ₂)	1.4-1.7	0.18	Chemisorption of OH radical	
IrO ₂ -Ta ₂ O ₅ (DSA-O ₂)	1.5-1.8	0.25		
Ti/Pt	1.7-1.9	0.3		
Ti/PbO ₂	1.8-2.0	0.5		
Ti/SnO ₂ -Sb ₂ O ₅	1.9-2.2	0.7		
p-Si/BDD	2.2-2.6	1.3	Physisorption of OH radical	

Figure 2. 7: Oxidation power of various anode materials. (Comninellis et al., 2008)

2.9.2. Instantaneous current efficiency

The Instantaneous Current Efficiency (ICE) is a measure of the amount of current directly used for the oxidation of organics, it is calculated using Equation (1.1), (Almomani & Baranova, 2012; Panizza et al., 2001).

In Equation 1.1, COD at time t is $[COD]_t$; COD at time $t+\Delta t$ is $[COD]_{t+\Delta t}$; electrolysis time is t ; current intensity (A) is ; Faraday constant (96485 C/mol) is ; and the volume of wastewater in the electrochemical reactor (l) is L.

$$ICE (\%) = \frac{[COD]_t - [COD]_{t+\Delta t}}{8I\Delta t} FL \times 100 \quad (\text{Equation 1.1})$$

2.9.3. Mixed metal oxide anodes

Mixed Metal Oxide (MMO) anodes have been studied for a wide range of purposes including semiconductors, sensors, photoconductive thin films and electrode materials. Remarkable progress has been made in the research of MMO's application as the anode material for electrochemical oxidation of recalcitrant pollutants in an aqueous environment (Wu, Huang and Lim, 2014). Several anodic materials have been tested, but most of them presented important drawbacks such as a rapid loss of activity (graphite), release of toxic ions (PbO_2), high cost (Si-boron-doped diamond and limited service life (SnO_2)). IrO_2 -based anodes and in particular the binary system IrO_2 - Ta_2O_5 , are reported to exhibit good performance in anodic stability and electro catalytic activity and are actually one of the most adopted catalyst for oxygen evolution in industrial electroplating processes (Scialdone *et al.*, 2009).

Because of the high electric conductivity, sufficient electrochemical activity, and long performance life, the mixed oxides of IrO_2 - Ta_2O_5 on a Ti substrate, or IrO_2 - $\text{Ta}_2\text{O}_5/\text{Ti}$, are widely used as an anode for electrochemical engineering applications, such as waste water treatment, electroplating and electroforming. The IrO_2 - $\text{Ta}_2\text{O}_5/\text{Ti}$ anode is one type of dimensionally stable anode (DSA) and is an effective electron sink during anodic reactions without dimensional loss (Huang *et al.*, 2017). Ti based IrO_2 - Ta_2O_5 coated anodes were rapidly developed in the past decades for their high stability and extreme durability under aggressive operation conditions. The thermal decomposition method of IrO_2 - Ta_2O_5 coatings is well-accepted for their low cost and uncomplicated preparation (Yan *et al.*, 2015).

2.9.4. Addition of NaCl

Although MMO anodes have low oxygen over-potential and therefore a low organic removal efficiency, they possess a high electro-catalytic activity for chlorine evolution. Indirect oxidation of Cl⁻ forms powerful oxidants of active chlorines (HClO and Cl₂). When the active chlorine species are transferred to the bulk solution they promote reactions and lead to the mediated oxidation of organic contaminants (Zhou et al., 2011)

The addition of chloride ions can increase the performance of organic removal through the interaction of active chlorine in the oxidation process. When chloride anion is oxidised on the anode surface, it releases Chlorine (Equation 2.1). Electro generated chlorine diffuses away from the anode and is hydrolysed yielding HClO and Cl⁻ (Equation 2.2) through disproportionation, with hypochlorous acid in acid-base equilibrium with hypochlorite anion species through Equation 2.3 (Garcia-Segura et al., 2018; Rajkumar et al., 2005; Rajkumar & Palanivelu, 2004).



2.10. Adsorption using Chitosan

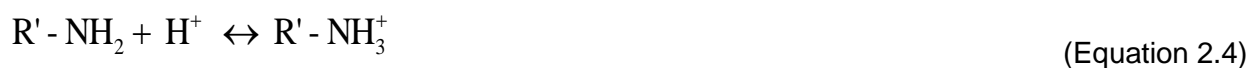
The use of chitosan as a natural adsorbent has been studied for a variety of contaminants such as various dyes (Zhai et al., 2017; Shajahan et al., 2017), heavy metal ions (Gokila et al., 2017; Mohammad et al., 2017), and oily wastewater (Soares et al., 2017; Elanchezhiyan & Meenakshi, 2017).

Some characteristics of Chitosan include hydrophilicity, biocompatibility, biodegradability and antibacterial properties (Riccardo A. A. Muzzarelli, 1983). It has been used commonly because of the abundant amino (-NH₂) and hydroxy (-OH) groups present in chitosan chains which serve as coordination and reaction sites (Wu et al., 2009).

This amino and hydroxyl groups significantly contributes to its high affinity for adsorbates (Kim et al., 2016; Kyzas & Bikiaris, 2015). When the chitosan is used in acidic solutions, the amino groups are even easier to protonate and then adsorb anions and a wide range of molecules through electrostatic forces (Shajahan et al., 2017; Muxika et al., 2017). Chitosan molecules have a strong positive charge at pH < 6.2, this allows it to bind to negatively charged molecules or polyanions through electrostatic interactions (Se-Kwon Kim, 2011).

These properties lead to chitosan being an effective adsorbent for the removal of dyes, odour, organic pollutants and inorganic pollutants from industrial wastewater (Muxika et al., 2017).

The interaction between oil molecules and the adsorption site of chitosan (-NH₂ group) is expected to increase under acidic conditions (Sokker et al., 2011), since the adsorbent surface is completely covered with hydronium ions (Laus et al., 2010), which would promote a high removal efficiency of anionic pollutants. Under acidic conditions, the hydrogen atom (H⁺) in the solution could protonate the amine groups (-NH₂) of chitosan, Equation 2.4.



The anionic charge of FAME or FFA in biodiesel wastewater ($R-COO^-$) can combine with the positive charge of the amine functional group of chitosan, as in Equation 2.5, resulting in the destabilisation of the emulsion by a charge neutralisation mechanism (Pitakpoolsil & Hunsom, 2013).



2.10.1. Structure

Chitosan is obtained from the alkali deacetylation of chitin (Guibal et al., 2006), which is the second most abundant biopolymer in nature (Chang & Juang, 2004). The chitosan molecule is a copolymer comprised of d-glucosamine and N-acetyl-D-glucosamine units that are linked by β -1,4 glycosidic linkages as shown in Figure 2.8 (Soares et al., 2017; Muxika et al., 2017). The ratio between the two units are considered as the Degree of Deacetylation (Verlee et al., 2017).

Chitosan's properties are determined by its molecular weight and degree of deacetylation (DD). At a DD of approximately 50%, chitin becomes soluble in aqueous acidic medium and is then called chitosan (Yang et al. 2016; Muxika et al., 2017).

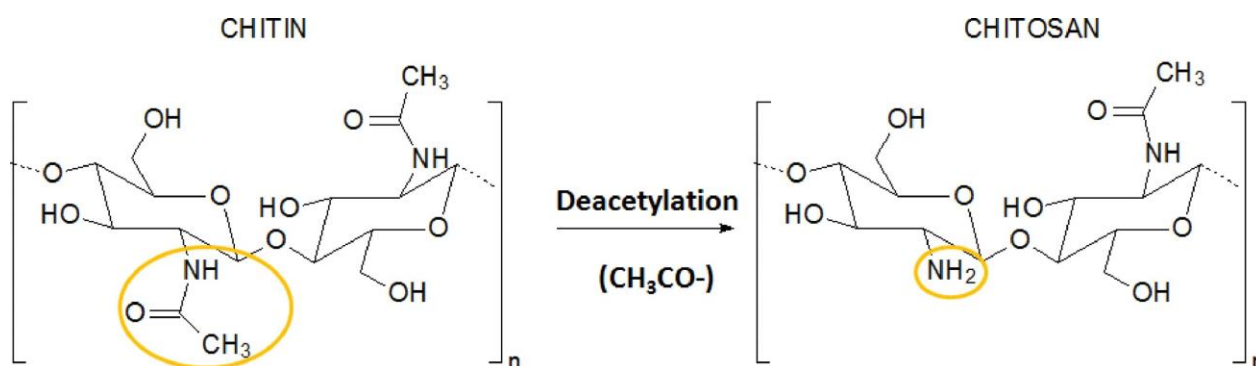


Figure 2. 8: Chitin and chitosan (Muxika et al., 2017).

2.10.2. Adsorption equilibrium and isotherms

The equilibrium adsorption isotherm is fundamental in describing the interactive behaviour between solutes and adsorbents and plays a significant role in the design of adsorption systems (Chiou & Li, 2002).

The Langmuir, Freundlich and Dubinin-Raduschkevich isotherm (D-R) are described on an individual basis below.

2.10.3. Adsorption equilibria

The amount of COD adsorbed at equilibrium can be calculated with Equation 2.6:

$$Q_e = \frac{(C_0 - C_e)V}{m} \quad \text{(Equation 2.6)}$$

Where, Q_e is the amount of COD adsorbed on the adsorbent at equilibrium (mg/g), C_0 is the initial concentration of COD in solution (mg/L), C_e is the concentration of COD in solution at equilibrium (mg/L), m is the mass of adsorbent used (g) and V the volume of COD solution.

2.10.4. Langmuir Isotherm

The Langmuir isotherm has been used extensively to describe the adsorption of adsorbents as well as its equilibrium behaviour (Liu, 2006).

The following Langmuir isotherm, Equation 2.7, was used to describe the equilibrium data (Laus et al., 2010):

$$q_e = \frac{q_m K_L C_e}{1 + K_L C_e} \quad \text{(Equation 2.7)}$$

Where C_e is the equilibrium solution concentration (mg/g), q_e is the amount of COD adsorbed at the equilibrium (mg/g), K_L is the Langmuir constant related to the affinity of binding sites (L/mg) and q_m represents a practical limiting adsorption capacity (mg/g) when the surface is fully covered with contaminant molecules and allows for the comparison of adsorption performance (Chiou & Li, 2002), K_L and q_m can be determined from a linearized form of Equation 2.7. as shown in Equation 2.8.

$$\frac{C_e}{q_e} = \frac{1}{q_m} C_e + \frac{1}{K_L q_m} \quad (\text{Equation 2.8})$$

Therefore, a linearized plot of (C_e/q_e) versus C_e gives a straight line with slope $1/q_m$ and intercept $1/q_m K_L$.

The essential features of the Langmuir isotherm can be expressed in terms of a dimensionless constant separation factor, R_L , expressed by Equation 2.9, where C_0 is the initial concentration of COD (mg/L) (Sokker et al., 2011).

$$R_L = \frac{1}{1 + K_L C_0} \quad (\text{Equation 2.9})$$

The value of R_L indicates the type of adsorption either to be unfavourable ($R_L > 1$), linear ($R_L = 1$), favourable ($0 < R_L < 1$) or irreversible ($R_L = 0$) (Bhatt et al., 2012; Boubarka et al., 2007).

2.10.5. Freundlich Isotherm

Adsorption best described by the Freundlich isotherm is considered occurring through a multi-layer process where the amount of adsorbed solute per unit adsorbent mass increases gradually (Chung et al., 2015).

The Freundlich isotherm is mathematically expressed as shown in Equation 2.10 (Vázquez et al., 2007):

$$Q_e = K_F C_e^{1/n} \quad \text{(Equation 2.10)}$$

This isotherm is usually used in special cases of heterogeneous surface energy which is characterised by the heterogeneity factor $1/n$ and q_e is the solid phase sorbate concentration at equilibrium (mg/g), C_e is the liquid phase sorbate concentration at equilibrium (mg/g), K_f is the Freundlich constant (Sokker et al., 2011). A linear form of the Freundlich isotherm can be obtained by taking logarithms of Equation 2.10, as shown in Equation 2.11:

$$\log q_e = \log K_F + \frac{1}{n} \log C_e \quad \text{(Equation 2.11)}$$

Therefore, a plot of linearized $\log q_e$ versus C_e enables the constant K_f and exponent $1/n$ to be determined.

If n is equal to unity, the adsorption is linear. This means that the adsorption sites are homogeneous (as in the Langmuir model) in energy and no interaction takes place between the adsorbed species. A value of $1/n < 1$ reflects favourable adsorption where the sorption capacity increases, and new adsorption sites occur. However when the value of $1/n$ is larger than 1 the adsorption bond becomes weak and unfavourable adsorption takes place, resulting in decreased adsorption capacity (Özcan et al., 2004).

2.10.6. Dubinin-Raduschkevich Isotherm

Since the Langmuir and Freundlich isotherms do not give information on the adsorption mechanism (Laus et al., 2010), the Dubinin-Raduschkevich isotherm (D-R) can be used.

This isotherm is an analogue of the Langmuir isotherm, but is more general, since it does not assume a homogeneous surface or constant sorption potential (Aksoyoglu, 1989). The D-R isotherm can be used to calculate the mean free energy of adsorption, which is used to identify chemical and physical adsorption.

The Dubinin-Raduschkevich isotherm, Equation 2.12, predicts the nature of the adsorbate sorption onto the adsorbent and it is used to calculate the mean free energy of sorption (Kilislioglu & Bilgin, 2003).

$$q_e = q_m \exp(-k\varepsilon^2) \quad (\text{Equation 2.12})$$

Where C_e is the equilibrium solution concentration (mg/g), q_e is the amount of COD adsorbed at the equilibrium (mg/g), K is a constant related to the adsorption energy (mol^2/kJ^2), q_m is the theoretical saturation capacity (mg/g), ε is the Polanyi potential (J/mol) calculated with Equation 2.13.

$$\varepsilon = RT \ln \left(1 + \frac{1}{C_e} \right) \quad (\text{Equation 2.13})$$

The linear form of Equation 2.12 is shown in Equation 2.14:

$$\ln q_e = \ln q_m - k\varepsilon^2 \quad (\text{Equation 2.14})$$

The values of q_m and K were deduced by plotting $\ln(q_e)$ versus ε^2 . The mean energy of adsorption (E) can be calculated from Equation 2.15.

$$E = (-2K)^{-1/2} \quad (\text{Equation 2.15})$$

This parameter gives information about the adsorption mechanism as either chemical ion-exchange ($8 \text{ kJ/mol} < E < 16 \text{ kJ/mol}$) or physical adsorption ($E < 8 \text{ kJ/mol}$) (OZCAN et al., 2005).

CHAPTER 3

Research Methodology

3. Research Methodology

3.1. Introduction

In this chapter the details are given regarding the use of equipment and materials as well as experimental procedures followed during all experimental runs conducted. Descriptions of instruments used are also included.

3.2. Research design

During this research, a quantitative experimental approach was used. This study consists of three parts. The first entails the investigation of electrochemical oxidation of biodiesel. The second focusses on adsorption using chitosan as the adsorbent whereas the third combines the previous two processes into one integrated treatment process for the evaluation of COD removal.

3.3. Experimental details

Crude biodiesel wastewater was collected from a commercial biodiesel producer operating in the Cape Town area. The name and location of the commercial biodiesel producer is not disclosed as part of an agreement between the company and this research project. The wastewater was collected when available and therefore varied slightly in composition since it was a “real” feed. All experiments were conducted at the Cape Peninsula University of Technology in Chemical Engineering Environmental Research Laboratory 1.11.

3.3.1. Acidification

As a pre-treatment, all wastewater collected for experimental use was acidified using H_2SO_4 at a final pH ranging between 1 to 6. Acidification occurred in a 6L round bottom flask which was magnetically stirred at ambient conditions. The acidified wastewater was mixed for 2 hours and allowed to stand for 12 hours to ensure complete phase separation. The oil rich top phase was removed from the remaining aqueous phase through slow decantation and analysed to quantify pollutant removal. All acidification experiments were duplicated.

3.3.2. Electrochemical oxidation

The biodiesel wastewater was subjected to electrochemical oxidation occurring in a 1L glass reactor. Two commercial $\text{IrO}_2\text{-Ta}_2\text{O}_5$ anodes (NMT electrodes South Africa) was employed with a total surface area of 400 cm^2 . The distance between the anodes were kept at 0.02 m. To ensure good mass transfer and a constant temperature of 60°C , a magnetic heater/stirrer was used. A regulated power supply was employed to supply external electricity to the system. During the treatment process samples were taken in 2-hour intervals and analysed for properties including COD, EC, TDS, Salinity, pH and Turbidity, following standard methods. The experiments are shown in Table 3.1. The experimental setup of the electrochemical reactor is shown in Photo 3.1.

Table 3. 1: Electrochemical oxidation experiments runs.

Experimental Run	Current density (mA/cm²)	NaCl (M)	Time (hrs.)
1	0.5	0.08	100
2	0.75	0.08	100
3	1	0.08	100
4	1.25	0.08	100
5	1.75	0.08	100
6	2	0.08	100
7	4	0.08	100
8	1	0	100
9	1	0.02	100
10	1	0.04	100
11	1	0.06	100
12	1	0.08	100



Photo 3. 1: Electrochemical Reactor

Experiments were conducted in a 1L glass beaker. The electrodes $\text{IrO}_2\text{-Ta}_2\text{O}_5$ had a working surface area of 200 cm^2 . The distance between the anode and cathode was 1cm apart while the electrodes were connected to a power supply. The volume of the solution in the reactor was 1L where the biodiesel wastewater was magnetically stirred and kept at a constant temperature of 60°C . All experiment were conducted with NaCl (>99%, Aldrich) as the electrolyte. The experiments were performed in duplicate and the relative statistical analysis performed to validate the results. Samples were taken initially and thereafter in two-hour intervals to quantify COD, pH, EC, TDS, Salinity and Turbidity.

3.3.3. Electrochemical oxidation factorial trial

Response surface methodology based Central composite design. A central composite design is the most commonly used response surface design experiment. This is a factorial or fractional factorial design with centre points, augmented with a group of axial points which allows for curvature estimation. It can be used to estimate first- and second-order terms as well as model a response variable with curvature by adding centre and axial points.

In this study a two factor 5 level central composite experimental design with an alpha of 1.189 was used to statistically analyse the effect of current density and electrochemical oxidation time. The response surface methodology was based around operating conditions determined during the initial tests to better understand the effects of current density and electrochemical oxidation time on the COD removal. Stat-Ease Design Expert V 10.0.0 was used during this experimental design.

The selected variables, based around the results obtained during the initial test experiments, were current density (mA/cm²) and electrochemical oxidation time (hours). Their ranges are shown in Table 3.2.

Table 3. 2: Factors in Central composite design

Factor	Variable	Levels used				
		+1	-1	+alpha	-alpha	center point
Current density (mA/cm ²)	A	+1 (1.25)	-1 (0.75)	1.35	0.64	1
Electrochemical oxidation time (hours)	B	+1 (96)	-1 (48)	98.7	39	69

Once the operating variables and their ranges were determined, experiments were identified based on the Centre composite design which consisted of 13 experiments with 7 center points. The experiments were designed in a random order through Design Expert software. Randomised experiment runs ensure that the conditions of the previous experiments don't affect the current experiment and ensures that the current experiment can predict the conditions of the following experiment. The 13 experiments were completed in duplication to ensure that statistical analysis may be performed in order to validate the results. Each experiment was allowed to run for 100 hours at the specified conditions after which the needed response values were noted in the modeling software as required. The complete experimental matrix is shown in Table 3.3. The +alpha and -alpha values of 1.35 and 0.64 mA/cm² were taken as the closes tested values, in this case 1.25 and 0.5 mA/cm², respectively.

Table 3. 3: Central composite design experimental matrix.

Standard order	Experimental Run	Factor 1 A: Current density (mA/cm ²)	Factor 2 B: Time (hours)	Response 1 COD Removal (%)
3	1	1	39	40
8	2	1	69	74
13	3	0.64	69	62
4	4	1	69	75
2	5	1.25	90	77
1	6	1	69	76
10	7	1.35	69	50
9	8	0.75	48	35
11	9	1	69	74
6	10	1.25	48	47
7	11	1	98.7	86
5	12	1	69	75
12	13	0.75	90	62

3.3.4. Adsorption with Chitosan

During the adsorption of COD from biodiesel onto chitosan, the concentration of chitosan, initial pH of water and adsorption time were investigated. For the adsorption stage, the pH of the aqueous phase was adjusted to be within the preferred range (2 - 6) by the addition of NaOH (Merck 106498). Approximately 200ml of BDWW was treated by the addition of Chitosan powder (2.5 – 4.5 g/L) as the adsorbent in a glass beaker with a constant stirring rate (350 rpm) for a selected adsorption time of 3hrs (Pitakpoolsil & Hunsom, 2013).

The concentration of COD in the wastewater was measured every hour by taking a sample and filtering it with a 0.45 µm syringe filter and standard analysing methodology followed thereafter. The treated wastewater was then separated from the adsorbent by vacuum filtration through filter paper (No.1 Whatman WHA1001070). Fresh Chitosan was used to repeat the adsorption stages. This was done three times. The experiments were done in duplicates to statistically validate the results. Experiments were followed as shown in Table 3.4.

Table 3. 4: Chitosan adsorption experiments and conditions.

Experimental Run	Dosage g/L	g/200ml	pH
1	2.5	0.5	2
2	3.5	0.7	2
3	4.5	0.9	2
4	2.5	0.5	4
5	3.5	0.7	4
6	4.5	0.9	4
7	2.5	0.5	6
8	3.5	0.7	6
9	4.5	0.9	6

3.3.5. Integrated treatment process

The integrated treatment of biodiesel wastewater consisted of the combinations of acidification, electrochemical oxidation and adsorption stages. Since each of these processes were investigated on a stand-alone basis, the best performing operating conditions of each process were used for the integrated treatment process. Once the operating conditions were determined, a full integrated experiment was performed.

3.4. Research apparatus

The following apparatus and equipment were used during the experiments to collect data and measure the removal of COD from biodiesel wastewater during acidification, electrochemical oxidation and adsorption processes.

3.4.1. Glass ware

- The 5 litres round bottom flask used for acidification
- 2 Litre bottles were used to store the acidified water over night
- 1 litre beakers were used during the electrochemical oxidation and adsorption processes
- 500 ml bottles were used to store the products of electrochemical oxidation and adsorption processes

3.4.2. Equipment

- A Dragonlab MS-H Pro magnetic heater/stirrer was used during electrochemical oxidation for stirring the solution at a constant rpm and keeping the solution at a constant temperature. During the adsorption processes the magnetic stirrer/heater was only used for stirring purposes.



Photo 3. 2: Magnetic heater/stirrer.

- A TR 420 Thermo-reactor from MERCK was used during the COD measurements.



Photo 3. 3: Thermo-reactor

The COD concentration was determined by Chromosulfuric acid oxidation method using Merck reagents. The Analytical procedure and sample preparation followed can be found in Appendix F. The TR 420 Thermo-reactor was used for digestion. The NOVA 60 photometer was used to determine the COD concentration photometrically.

- NOVA 60 Photometer for determination of COD concentrations



Photo 3. 4: Photometer

- Multimeter

The Crison CM 35+ was used to measure the EC, TDS and Salinity.



Photo 3. 5: Multiparameter meter.

- pH meter



Photo 3. 6: pH meter

- Turbidity meter



Photo 3. 7: Turbidity Meter

3.4.3. Materials

The following consumables were utilised during experiments.

- H_2SO_4 (Merck >99%)
- NaOH (Sigma-Aldrich >97%)
- NaCl (Sigma-Aldrich >99.5%)
- Chitosan (Sigma-Aldrich >75% deacetylated, from shrimp shells)
- MMO anodes (NMT Anodes South Africa)
- COD Solution A (Merck 1.14538.0065)
- COD Solution B (Merck 1.14539.0495)

CHAPTER 4

Results and Discussion

4. Results and Discussion

4.1. Biodiesel wastewater characteristics

The industrial biodiesel wastewater used during this study was tested for certain characteristics. The average values are shown in Table 4.1. The COD, BOD and FOG values are much higher than what is required by the City of Cape Town: Wastewater and Industrial Effluent By-Law, 2013.

Table 4. 1: Characteristics of the Biodiesel wastewater used in this study.

Parameter	Unit	Tested value	CCT: Requirements
COD	mg/L	55000 – 65 000	5000
FOG	mg/L	500 – 550	4000
BOD	mg/L	38 000 – 40 000	none
Salinity	g/L	2.03	none
EC	mS/cm	3.5	500 000
TDS	g/L	2.3	4000
pH		9.8	5.5 - 12
Turbidity	NTU	380	none

The COD with an average value of 60000 mg/L was 11-fold higher than the requirements, whereas the FOG (550 mg/L) was in range. The pH, electrical conductivity and total dissolved solids were in range with values of 9.8, 3.5mS/cm and 2.3 g/L respectively.

4.2. Acidification of biodiesel wastewater

Demulsification of BDWW was carried out using H_2SO_4 at various pH values as indicated in Figure 4.1. The addition of acid as a proton donor destabilises the emulsion through the reduction of electric forces or destruction of the electrical double layer which enables the coalescence of fine oil droplets into larger ones, resulting in phase separation.

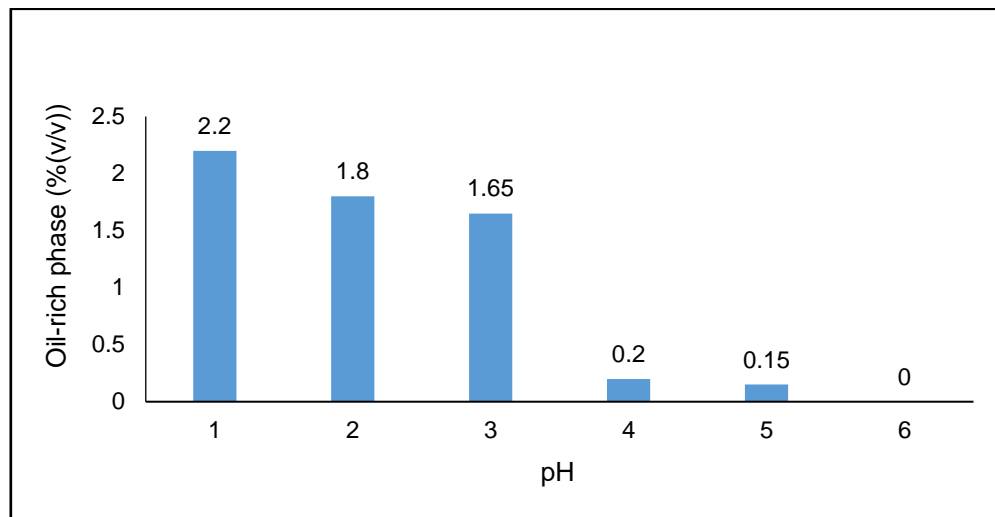


Figure 4. 1: Oil removed through acidification.

The oil rich top layer has a similar colour to that of oil/biodiesel, whereas the residual aqueous phase has a lower turbidity and reduced pollutant concentrations. 1.65 – 2.2% (v/v) vegetable oil was removed in the pH range 1 – 3, however, insufficient amounts of oil 0.2 – 0.15 % (v/v) was removed in the pH range 4 – 5, whereas no oil was recovered under pH conditions ranging from 6 to 9. Therefore, acidic conditions are favourable for oil removal.

Furthermore, acidification was able to remove 11% of COD, 10% of BOD and significant amounts of FOG, 80%, and 70% turbidity as shown in Table 4.2. Other parameters such as TDS, EC and salinity showed slight reductions.

Table 4. 2: Characteristics of biodiesel wastewater after acidification.

Parameter	Unit	Initial Value	Acidified
COD	mg/L	55000 – 60 000	53250
FOG	mg/L	500 – 550	106
BOD	mg/L	38 000 – 40 000	36225
Salinity	g/L	2.03	1.5
EC	mS/cm	3.5	2.6
TDS	g/L	2.3	1.7
pH		9.8	2
Turbidity	NTU	380	100

Rattanapan et al., (2011) adjusted the pH of biodiesel wastewater to a value of 3, and found that it was sufficient for the removal of FOG and COD, reporting removal efficiencies of 80% and 45% respectively. Similarly, Ngamlardpokin et al., (2011) reports that higher levels of oil removal was achieved with a pH value ranging between 1 and 2.5. It is therefore clear that acidification plays a significant role as a pre-treatment step.

4.3. Instantaneous current efficiency

Initial experimental runs were conducted to determine the operational parameters. These initial experimental results gave an indication to parameters that need to be investigated in the electrochemical oxidation of biodiesel wastewater as shown in Table 4.3. The Instantaneous Current Efficiency (ICE) was calculated to quantify the effect that current density and NaCl concentration has on the electrochemical oxidation process.

Table 4. 3: Initial test experiments.

Experimental Run	Current density (mA/cm ²)	Time (hrs.)	NaCl (M)
A	1	24	0
B	2	24	0
C	4	24	0
D	1	24	0.02
E	1	24	0.04
F	1	24	0.06
G	1	24	0.08
H	1	24	0.1

The Instantaneous Current Efficiency (ICE) was calculated by equation (1.1) in Chapter 2, at a constant 2-hour time interval, over a period of 24 hours.

$$\text{ICE (\%)} = \frac{[\text{COD}]_t - [\text{COD}]_{t+\Delta t}}{8I\Delta t} \text{FL} \times 100$$

4.3.1. Effect of current density

The calculated ICE % values for experimental runs A, B and C are shown in Figure 4.2. The data for these experiments can be found in Appendix C. Experimental run A with a current density of 1 mA/cm² achieved the highest ICE value of 3.3% at 2 hours, after which it gradually decreased to 1.1% at 24 hours. Experimental runs B and C achieved significantly lower ICE values of 1.7% and 0.3% respectively. It decreased to values lower than 0.2% at the 24 hour period. Normally, the ICE (%) decreased with an increase in current density. Almomani & Baranova, (2012) and Coledam et al., (2014) found that an increase in current density resulted in a decrease of ICE due to the side reaction of oxygen evolution and/or mass transport limitations. According to Wu et al., (2014b) the oxygen evolution reaction is not favoured at lower current densities, which explains why higher ICE values were obtained at the lower current densities.

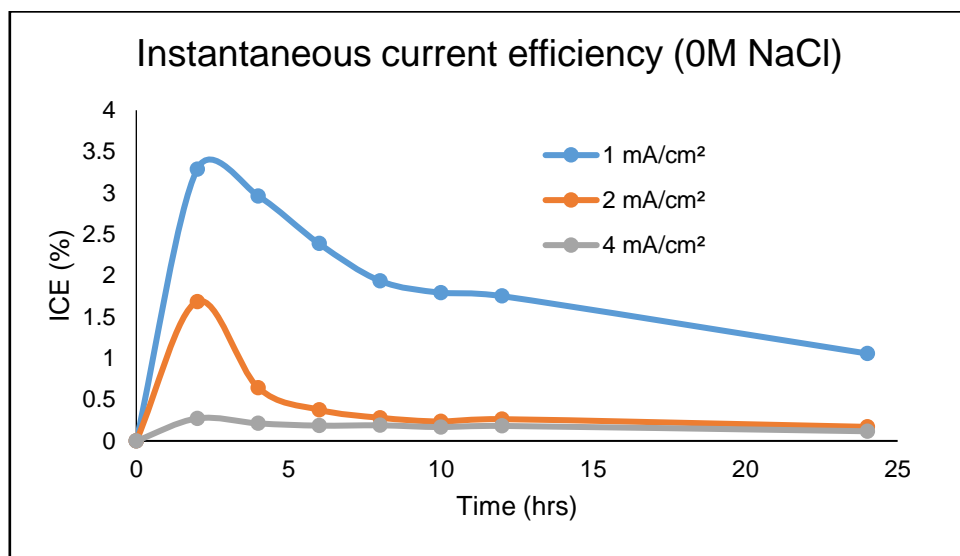


Figure 4. 2: Instantaneous current efficiency - Effect of current density.

Based on the initial experimental runs, a current density of 1 mA/cm² showed favourable results and was chosen for subsequent experimental runs to determine the effect of NaCl as a supporting electrolyte.

4.3.2. Effect of NaCl concentration

The effect of NaCl concentration (M) on the electrochemical oxidation at 1 mA/cm² was investigated by varying the NaCl concentration between 0 and 0.1 M, as shown in Table 4.3. The calculated ICE % values for experimental runs D – G are shown in Figure 4.3. The data for these experiments can be found in Appendix C.

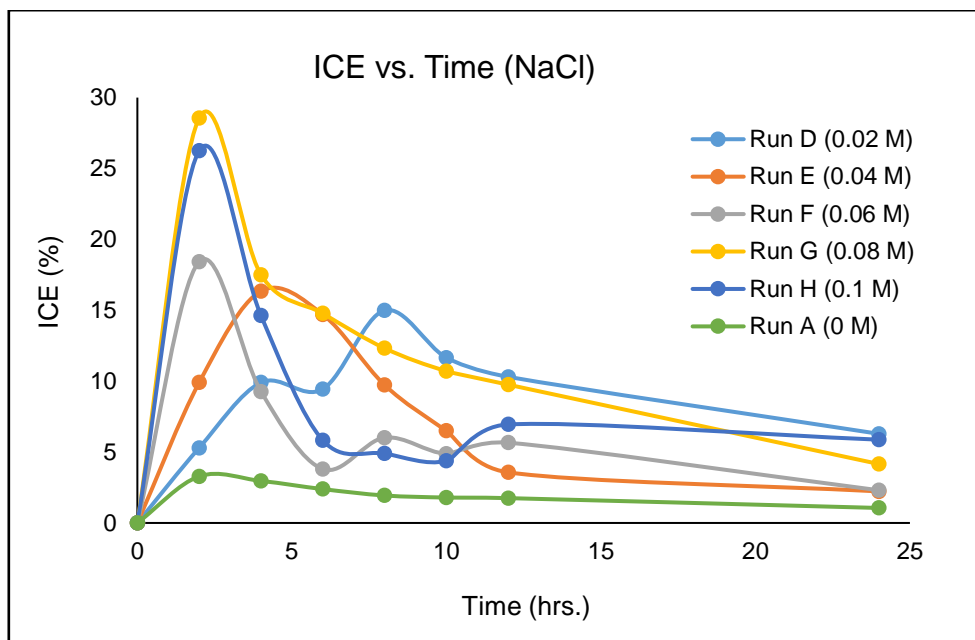


Figure 4. 3: Instantaneous current efficiency - Effect of NaCl concentration.

The ICE increased with an increase in NaCl concentration, thus, confirming the positive effect that NaCl has on the electrochemical oxidation of BDWW. A maximum of 28.5% and 26% efficiency was observed at 0.08M NaCl and 0.1M NaCl, respectively. An efficiency of 3.3% was observed when no NaCl was added. Coledam et al., (2014) reported that higher ICE values are observed in the presence of NaCl compared to that without.

Based on the results obtained a NaCl concentration of 0.08 M was chosen for all subsequent experimental runs.

4.4. Electrochemical oxidation experiments

As mentioned above, the initial experimental results gave an indication to parameters that need to be investigated in the electrochemical oxidation of biodiesel wastewater. Four experimental runs were performed as shown in Table 4.4. Each of these experimental runs operated for 100 hours at 60°C with a constant NaCl concentration of 0.08M.

Table 4. 4: Electrochemical oxidation - experiments

Experimental Run	Current density (mA/cm ²)	NaCl (M)	Time (hrs.)
1	0.5	0.08	100
3	1	0.08	100
6	2	0.08	100
7	4	0.08	100

Samples were taken every two hours to quantify COD, EC, TDS, Salinity, Turbidity, and pH. Detail results can be found in Appendix C. The COD removal % for each of these experimental runs is shown in Figure 4.4. It is observed that the COD removal gradually increases with an increase in time. After 96 hours it stabilises and increases slowly for another 4 hours as shown in Figure 4.4.

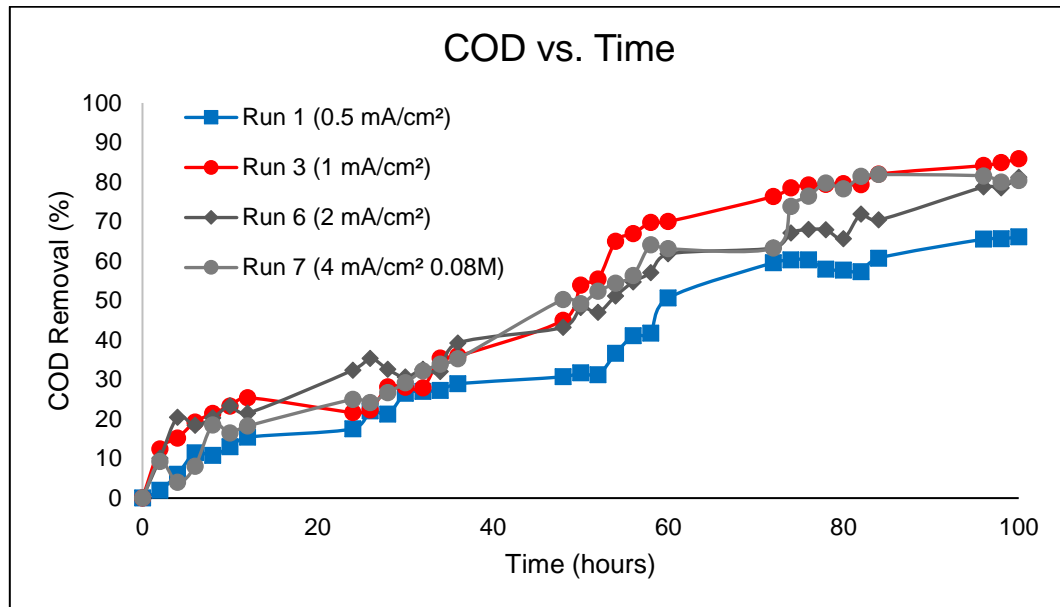


Figure 4. 4: COD removal (%) – experiments

Figure 4.5, shown below, represents the COD, BOD and FOG results of experimental runs 1 (0.5 mA/cm²), 3 (1.0 mA/cm²), 6 (2.0 mA/cm²) and 7 (4.0 mA/cm²), respectively. It can be observed that the experimental run 3 with a current density of 1.0 mA/cm² shows the highest removal of COD (86%), BOD (88%) and FOG (85%) removal, whereas experimental run 1 with a current density of 0.5 mA/cm² shows the least removal. It can also be observed that removal efficiency for current density 2.0 and 4.0 mA/cm² are also quite significant. Wu et al (2014b) states that when high removal efficiencies has been reached, as shown in experimental 3, the increase of current density thereafter will not have a significant effect as observed with experimental run 6 and 7.

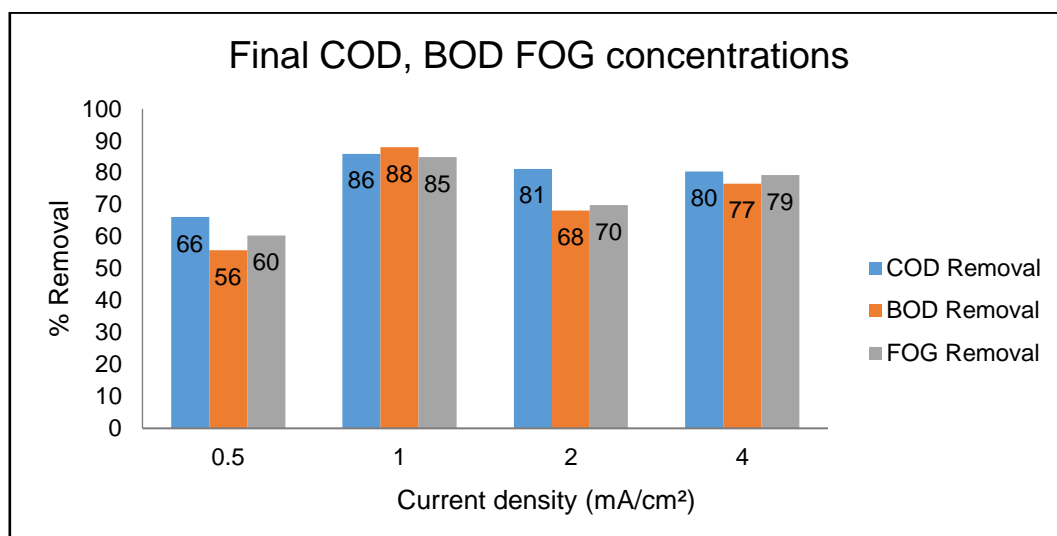


Figure 4. 5: COD, BOD & FOG removal efficiencies - experiments

Comninellis et al., (2008) and Martínez-Huitle & Andrade, (2011) explain these trends by stating that the IrO₂ – Ta₂O₅ anodes are a good catalyst for the oxygen evolution side reaction and therefore only permit for the partial oxidation of organics. However, the effective oxidation of pollutants is possible at lower current densities and longer electrolysis time, as shown with these results.

Table 4. 5: Final concentrations for COD, BOD & FOG - experiments

Current Density (mA/cm²)	Final COD (mg/L)	Final BOD (mg/L)	Final FOG (mg/L)
Experimental run 1 (0.5)	21524	16020	42
Experimental run 3 – (1.0)	7086	4354	16
Experimental run 6 – (2.0)	13629	11531	32
Experimental run 7 – (4.0)	11695	8503	22

The final COD, BOD and FOG values for each experiment are shown in Table 4.5. Significant reductions in these parameters were observed when compared to the CCT effluent standards. Experimental run 3 with a current density of 1 mA/cm² performed particularly well with a final COD value of 7086 mg/L, however this value is about 2000 mg/L above the required industrial discharge standard and needs further treatment.

4.4.1. Additional electrochemical oxidation experiments

Based on the results obtained in experimental runs 1, 3, 6 and 7, additional experiments were completed to better understand the effect of current density on the electrochemical oxidation of BDWW. The current density of these experiments was chosen in small increments where values were chosen below and above 1 mA/cm² to investigate any significant changes, as shown in Table 4.6. In experimental runs 2, 4, and 5, the current density was 0.75, 1.25 and 1.75 mA/cm², respectively.

Table 4.6: Electrochemical oxidation: Additional experiments.

Experimental Run	Current density (mA/cm ²)	NaCl (M)	Time (hrs.)
2	0.75	0.08	100
4	1.25	0.08	100
5	1.75	0.08	100

Samples were taken every two hours to quantify COD, EC, TDS, Salinity, Turbidity, and pH. These results can be found in Appendix C.

The % COD removal for each of these experimental runs is shown in Figure 4.6. These experimental runs follow the same trend as before where COD removal gradually increases with time. It stabilises at 96 hours with small increment increases up to 100-hour mark.

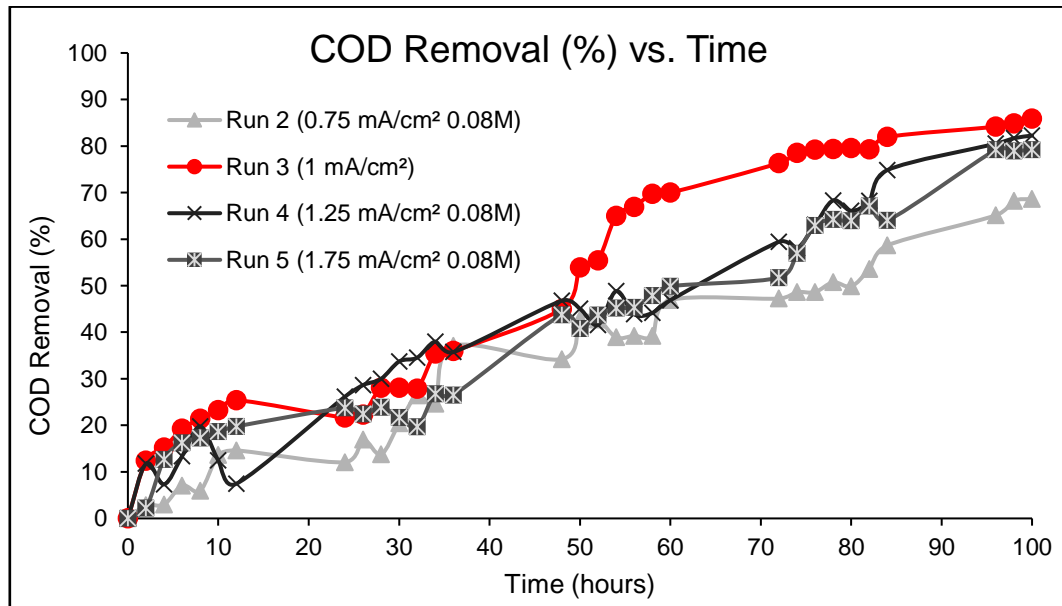


Figure 4. 6: COD removal (%) - Additional experiments.

Figure 4.6, shown above, represents the COD results of experimental runs 2 (0.75 mA/cm²), 3 (1.0 mA/cm²), 4 (1.25 mA/cm²) and 5 (1.75 mA/cm²), respectively. It can be observed that for the first 40 hours, the COD removal rate is almost similar for all experimental runs. After the 50-hour mark, experimental run 3 (1.0 mA/cm²) removal rate increases by almost 20% and decreases as it reaches almost equilibrium at the 100 hour mark. Experimental runs 4 (1.25 mA/cm²) and 5 (1.75 mA/cm²) follow a similar trend, but slower. For experimental runs 2 (0.75 mA/cm²), the % COD removal is the slowest, as expected and confirmed with literature.

In Fig 4.7, the final COD, BOD and FOG % removal for the various current densities is as follows: At 0.75 mA/cm² COD, BOD and FOG removal achieved a maximum 69%, 69% and 62%; 1.25 mA/cm², COD, BOD and FOG removal achieved a maximum of 82%, 79% and 77%; 1.75 mA/cm² removal COD, BOD and FOG removal achieved a maximum 79%, 72% and 72%.

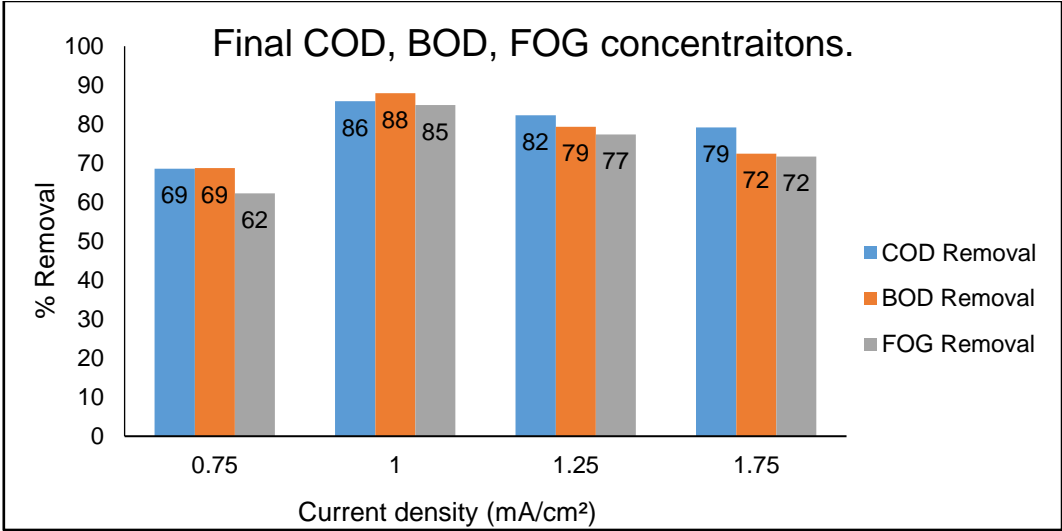


Figure 4. 7: COD, BOD & FOG removal efficiencies - Additional experiments.

When comparing the smaller current density increments, the current density of 1 mA/cm² achieves the highest removal of COD, BOD and FOG at the same operating conditions.

Experimental run 4 with a current density of 1.25 mA/cm² achieved a COD removal efficiency of 82% with a final COD removal concentration of 9903 mg/L as shown in Table 4.7. Similarly, experimental run 3 with a current density of 1.0 mA/cm² achieved a COD removal efficiency of 86% with a final COD removal concentration of 7086 mg/L. Therefore, increasing the current density, with small increments, below or above 1 mA/cm² resulted in lower pollutant removal efficiencies.

Table 4. 7: Final concentrations for COD, BOD & FOG - Additional experiments.

Current Density (mA/cm²)	Final COD (mg/L)	Final BOD (mg/L)	Final FOG (mg/L)
Experimental run 2 (0.75)	14856	11327	40
Experimental run 3 (1)	7086	4354	16
Experimental run 4 (1.25)	9903	7483	24
Experimental run 5 (1.75)	11904	9966	30

Santos et al., (2006) studied the electrochemical oxidation of oily wastewater using a Ru_{0.34}Ti_{0.66}O₂ anode which falls into the same family as IrO₂ – Ta₂O₅ anodes, namely Dimensionally Stable Anodes (DSA).

The operating temperature of 50°C was similar to the temperature used in this research although higher current densities were applied. At a current density of 100 mA/cm² and 70 hours of electrolysis, the system achieved 57% COD removal. These results obtained by Santos et al., (2006) were not significant in terms of COD removal. However, their results strengthen the notion that lower current densities are more favourable for COD removal when using these types of anodes.

4.4.2. Effect of current density on pollutant removal

The effect of current density on the electrochemical oxidation of BDWW using $\text{IrO}_2\text{-Ta}_2\text{O}_5$ anodes were investigated over a range of 0.5 – 4 mA/cm^2 at an initial pH of 2 as shown in Figure 4.8. Lower current densities in the range of 1 – 1.25 mA/cm^2 performed better than higher current densities of 2 – 4 mA/cm^2 .

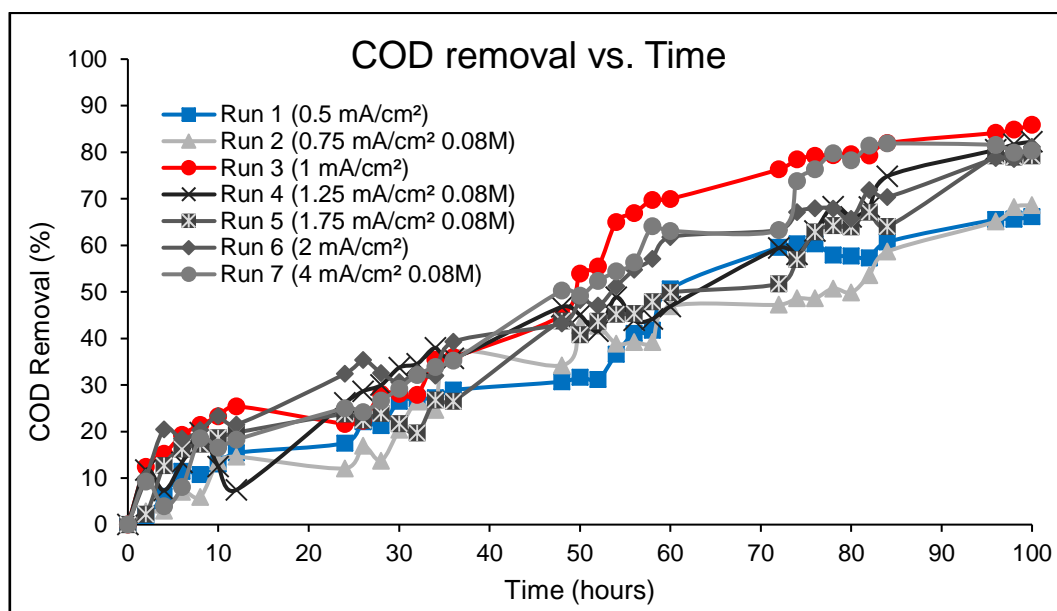


Figure 4. 8: Effect of current density on COD removal.

An increase in the current density from 0.5 to 1 mA/cm^2 followed an increase in COD removal from 66% to 86% respectively within 100 hours of oxidation. The increase of current density above 1.0 mA/cm^2 a slight decrease could be observed, but followed a consistent COD removal in the range of 80%.

In Figure 4.9, the final % COD removal at the 100-hour mark was compared with the different current densities tested at a constant pH of 2. As expected, the current density of 1.0 mA/cm^2 shows the best results.

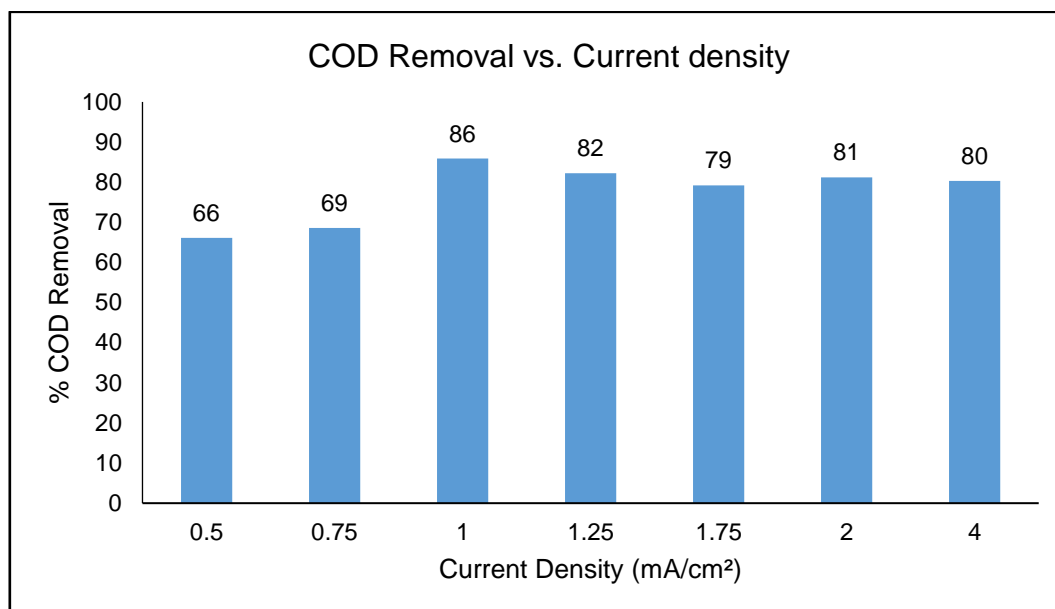


Figure 4. 9: Final values for COD removal – Current density.

The observed COD removal was due to the oxidation of organic pollutants to intermediate species and possible complete mineralization, in the wastewater. Electro-oxidation of organic contaminants using IrO₂– Ta₂O₅ active anodes (M) occurs through mediated oxidation in the bulk solution (Garcia-Segura et al., 2018).

4.4.3. Effect of NaCl concentration on pollutant removal

NaCl at various concentrations, between 0 – 0.1M, was added into the bulk of the electrochemical cell, as a supporting electrolyte. The aim of adding NaCl is to increase the removal of pollutants. The experiments with corresponding operating conditions are shown in Table 4.8. The data for each experiment can be found in Appendix C.

Table 4. 8: Electrochemical oxidation: Addition of NaCl experiments.

Experimental Run	Current density (mA/cm ²)	Time (hrs.)	NaCl (M)
8	1	100	0
9	1	100	0.02
10	1	100	0.04
11	1	100	0.06
3	1	100	0.08
12	1	100	0.1

The influence of NaCl was investigated without any electrolyte added and thereafter changing the NaCl concentration by increasing it by 0.02M until its final experimental run of 0.1M. Samples were taken every two hours to quantify COD, EC, TDS, Salinity, Turbidity, and pH (Appendix C). Below, Figure 4.10 shows the % COD removal over a 100-hour time. It can be observed throughout this period, the influence that NaCl has on the removal rate of pollutants and more specifically, COD. As the NaCl concentration increases, so does the % COD removal.

At a NaCl concentration of 0M, a maximum COD removal of 48.7% was achieved after 100 hours. However, the addition of NaCl at a concentration of 0.06M and 0.08M yielded a 78.5% and 86% COD removal, respectively. When the NaCl concentration further increased to 0.1M similar yet slightly lower COD removal efficiencies of 84% was observed, indicating that a NaCl concentration of 0.08M is sufficient at a maximum 86 % removal.

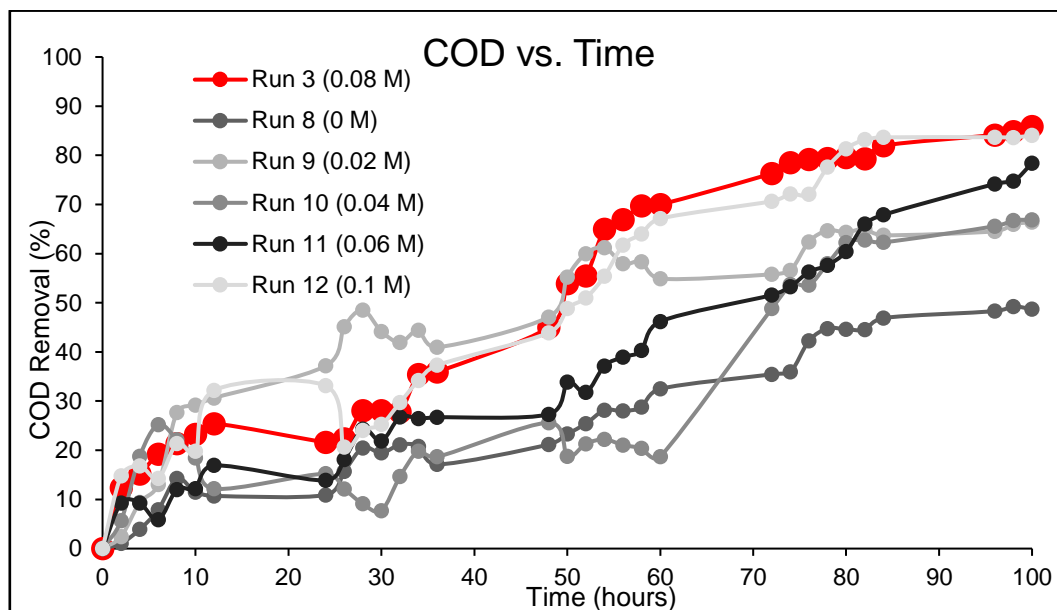


Figure 4. 10: Effect of NaCl concentration on COD removal.

Ltaïef et al., (2017) noted that the indirect oxidation of pollutants in wastewater by active-chlorine species generated by the anodic oxidation of chlorides are widely applied. Although, the addition of NaCl resulted in a decrease of total organic carbon, compared to when an inert supporting electrolyte (Na_2SO_4) was used. This could be attributed to the possible formation of oxidation resistant chlorinated intermediates.

Fajardo et al., (2017) found that the degradation rate of pollutants depends on the supporting electrolyte used. Similar to the results obtained during this study, the authors also found that the addition of NaCl resulted in better degradation values. This behaviour was ascribed to the generation of diverse oxidising species which were able to react directly or indirectly with the organic compounds.

The final % COD, BOD and FOG removal efficiencies are compared at various NaCl concentrations in Figure 4.12, below. When NaCl concentration was at 0M, a final COD, BOD and FOG removal 49%, 55% and 79%, were achieved, respectively.

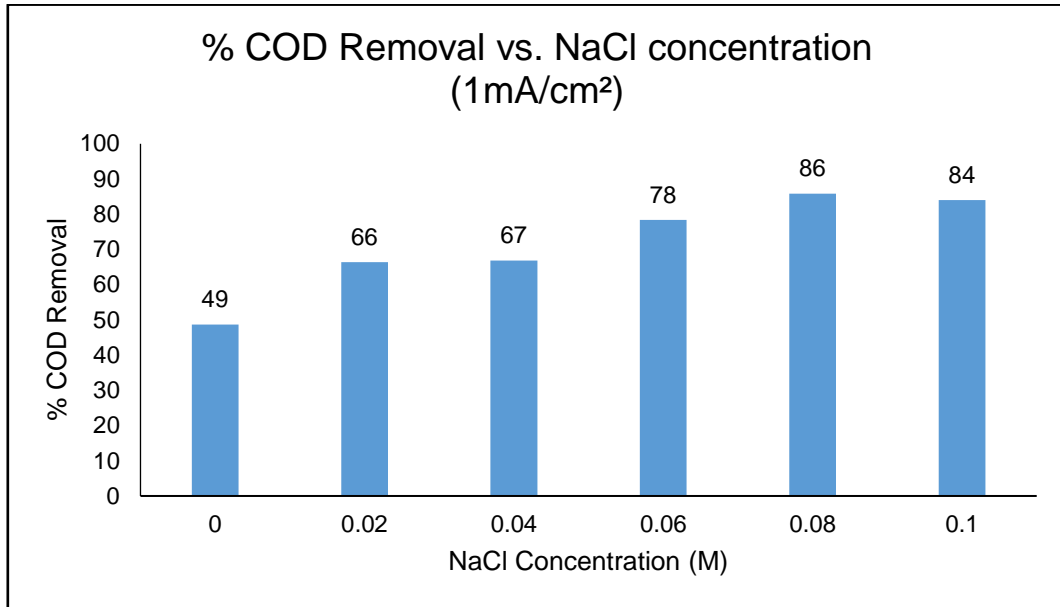


Figure 4. 11: Final values for COD removal - NaCl concentration.

As the NaCl concentration increases to 0.08M, the % COD, BOD and FOG removal reached a maximum of 86%, 88% and 85%, but at NaCl concentration of 0.1M, 84%, 83% and 83% was attained. These results reiterate that a NaCl concentration of 0.08M is sufficient for pollutant removal as stated above.

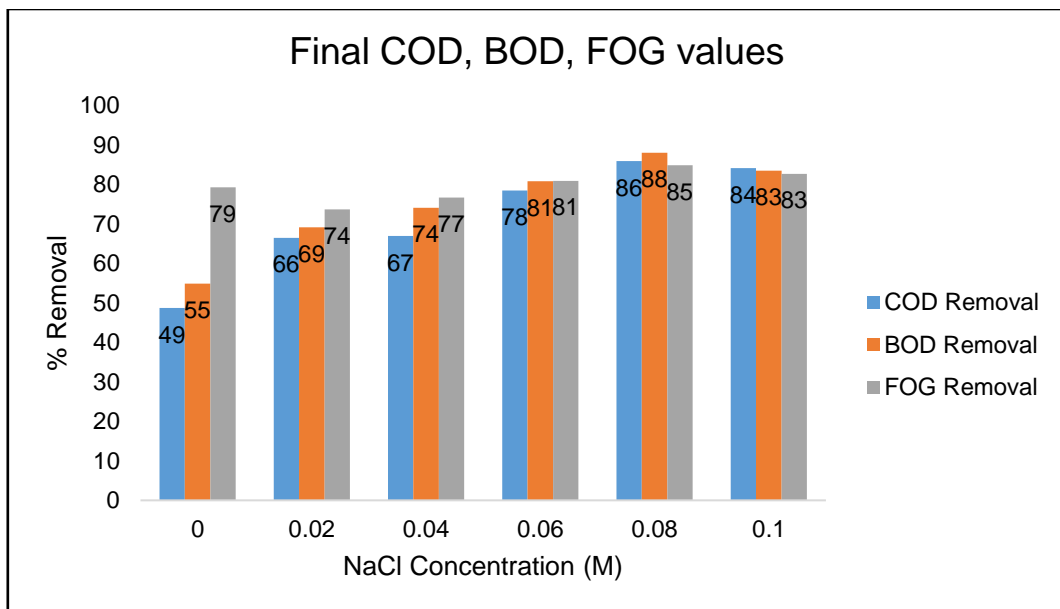


Figure 4. 12: Effect of NaCl concentration of pollutant removal efficiencies.

According to Rajkumar et al., (2005), Zhang et al., (2006) and Jaruwat et al., (2010), the NaCl as a supporting electrolyte has the ability to enhance pollutant removal by oxidizing organic compounds. This happens through the production of active chloro- species (Cl_2/OCl) that are electrochemically generated by the reduction of chloride ions to chlorine. For complete mineralization to occur, the reaction with water, need to produce hypochlorous acid that reacts and oxidises pollutants to intermediate species or CO_2 and H_2O .

Table 4. 9: Final concentrations for COD, BOD & FOG - NaCl experiments

NaCl concentration (M)	Final COD (mg/L)	Final BOD (mg/L)	Final FOG (mg/L)
Experimental Run 8 (0)	25184	16361	22
Experimental Run 9 (0.02)	16445	11188	28
Experimental Run 10 (0.04)	13832	9410	25
Experimental Run 11 (0.06)	10230	6959	20
Experimental Run 3 (0.08)	7086	4354	16
Experimental Run 12 (0.1)	8805	5990	18

The final COD, BOD and FOG concentration values for each experimental run are shown in Table 4.9. Experimental run 3 with a NaCl concentration of 0.08M achieved a final COD concentration of 7086 mg/L, which is better than what was achieved with a NaCl concentration of 0.1M and final COD concentration of 8805 mg/L.

4.5. Energy consumption

The mean energy consumption was calculated for each of the different current densities investigated, using Equation 4.1. where i , V_m , Δt , COD, V_R , and E corresponds to current (ampere), mean cell voltage (volt), reaction time (h), chemical oxygen demand (gO₂/L), electrolyte volume (L), and mean energy consumption (kWh/kg COD removed), respectively.

$$E = \frac{iV_m \Delta t}{(\text{COD}_i - \text{COD}_f) V_R} \quad (\text{Equation 4.1})$$

Calculated values for the mean energy consumption are shown in Table 4.10. As expected, the mean energy consumption increases with an increase in current density. However, this is not only due to a higher current applied, but also an indication of the efficiency of energy usage during COD removal as shown in Fig 4.13.

Table 4. 10: Mean energy consumption.

Current Density (mA/cm²)	Mean Energy Consumption (kWh/kg COD removed)
0.5	6.8
0.75	10.1
1	13.5
1.25	16.9
1.75	23.6
2	27.0
4	54.0

Figure 4.13 shows the mean energy usage at different current densities. The former is than compared to the corresponding % COD removal. It was observed that the lowest mean energy consumption of 6.8 kWh/kg COD removed, occurred at a current density of 0.5mA/cm² and corresponds with a % COD removal of 66%. The current density of 1mA/cm² used twice as much energy, 13.5 kWh/kg COD removed, but resulted in the highest COD removal at 86%.

Further increases in current density only amounted to more energy consumed with lower COD removal efficiencies.

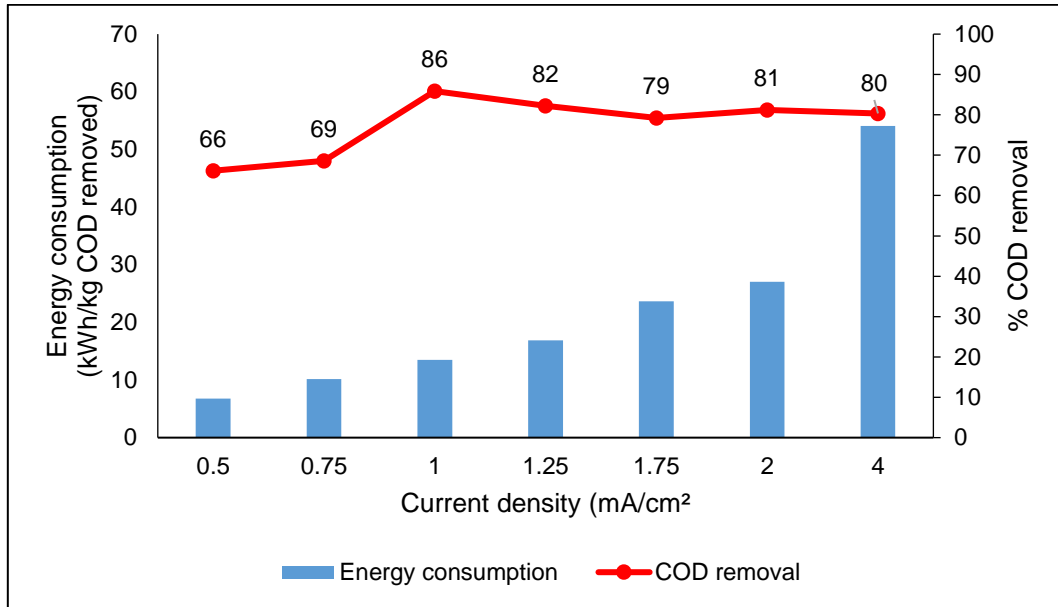


Figure 4.13: Mean energy consumption.

The values for mean energy consumption obtained in this study are reasonable and in line with values obtained in literature for various types of wastewaters as shown in Table 4.11.

Table 4. 11: Energy consumption for various wastewater types.

Wastewater type	Energy consumption (kWh/kg COD removed)	Literature
olive oil	1.237 - 12.3	(Israilides et al., 1997)
tannery	4.8 - 200	(Vlyssides & Israilides, 1997)
textile	11.2	(Zou et al., 2017)
Biodiesel	13.5	This study

According to Zou et al., (2017) as the current density increases so does the energy consumption. The excess energy consumed is due to side reactions. This is similar to what has been observed in Figure 4.13.

4.6. Development of COD removal model

Design-Expert software was used to analyse the measured responses. The significance test for the regression models and the significance test of individual model coefficients were determined by the same statistical software package for all responses. The resulting ANOVA shown in Table 4.12 for the COD removal quadratic model outlines the analysis of variance for this response and shows the significant model terms affecting the COD removal. This table also demonstrates additional adequacy measures, for example, R^2 and adjusted R^2 . The R^2 value indicates the degree of fit and are defined as the ratio of the explained variation to the total variation. It is suggested that a good model fit should be for a R^2 of at least 0.8. In this study these adequacy measures were found to be 0.905 as shown in Table 4.12, suggesting that this quadratic model was a good fit for this data. The model was significant as indicated by the very low probability value of less than 0.05. A p-value that is lower than 0.05 suggests that the model is statistically significant at the 5% level of significance.

Table 4.12: ANOVA for Response surface reduced quadratic model.

Source	Sum of Squares	df	Mean Square	F Value	p-value Prob > F	
Model	2850.74	4	712.68	18.97	0.000382	significant
A-Current Density	13.86	1	13.86	0.37	0.560415	
B-Time	1846.92	1	1846.92	49.17	0.000111	
A ²	766.04	1	766.04	20.39	0.001960	
B ²	340.26	1	340.26	9.06	0.016819	
Residual	300.49	8	37.56			
Lack of Fit	297.69	4	74.42	106.32	0.000259	significant
Pure Error	2.80	4	0.70			
Corrected Total	3151.23	12				
R^2	0.9046		Adjusted R^2	0.857		

A represents the current density, B represents the electrochemical oxidation time, whereas A^2 and B^2 is the quadratic effect of the current density and electrochemical oxidation time respectively. The final model in terms of coded factors is represented in Equation 4.2, and the uncoded actual factors are shown in Equation 4.3.

$$\text{COD Removal} = 74.8 + 1.32*A + 15.19*B - 10.49*A^2 - 6.99*B^2 \quad (\text{Equation 4.2})$$

$$\text{COD Removal} = -223.79 + 341.06*A + 2.91*B - 167.9*A^2 - 0.0158*B^2 \quad (\text{Equation 4.3})$$

These models can be used to predict the yield stress within the range of the factorial trial, by substituting the values of A and B or their -1 to 1 codes as shown in Table 3.2. The actual units for parameter A and B are mA/cm² and hours, respectively.

The coded equation (Equation 4.2) is useful for identifying the relative impact of the factors by comparing the factor coefficients. This equation should not be used to determine the relative impact of each factor because the coefficients are scaled to accommodate the units of each factor and the intercept is not at the centre of the design space.

In Equation 4.3 a positive sign before a term indicates an increasing effect, while a negative sign indicates a decreasing effect on COD removal.

4.6.1. COD removal model validation

Model validation is important to obtain an adequate model. The COD removal model validation was evaluated by plotting a normal probability (%) against the internally studentised residuals as shown in Figure 4.14. The relationship between normal probability and internally studentised residuals fits well linearly as seen in Figure 4.14. The linear fit means that no response transform was necessary, and that there was no specious problem with the normality of the data.

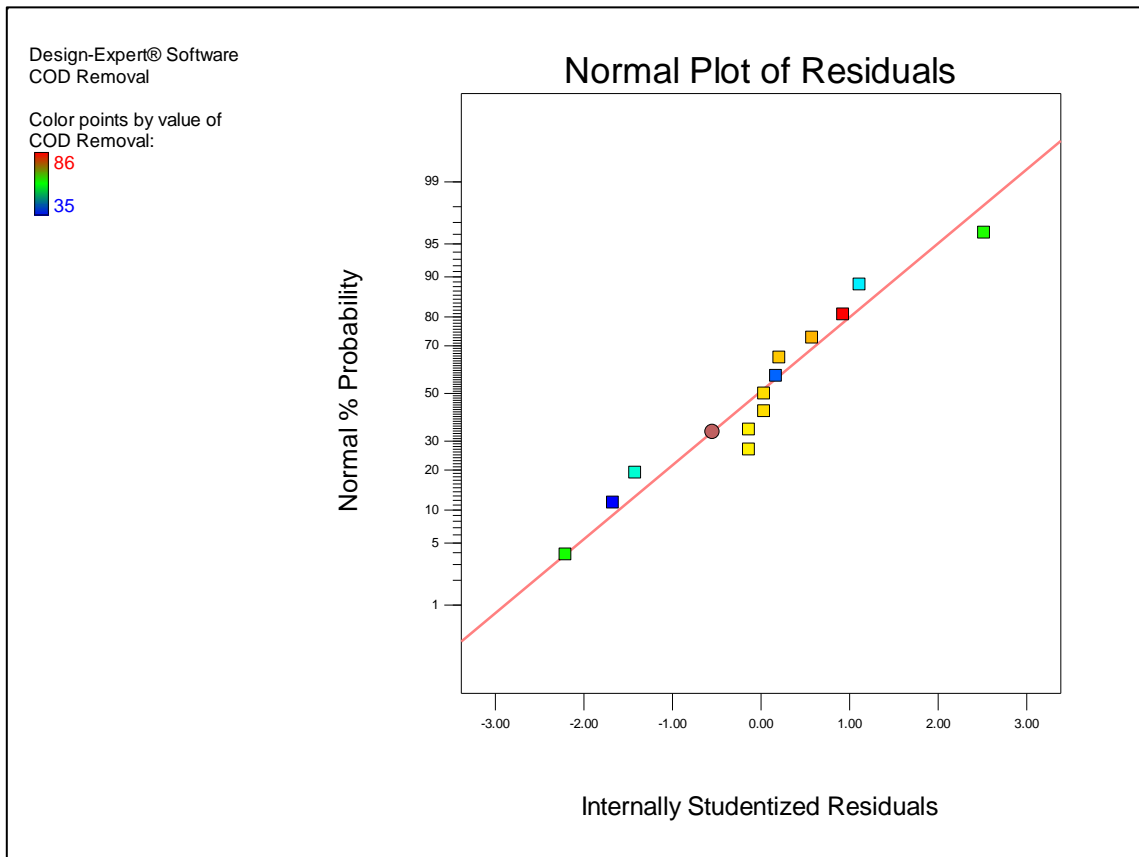


Figure 4.14: Normal probability (%) and internally studentised residuals.

The validation of the COD removal model was assessed by evaluating the relationship between the actual and the predicted values as shown in Figure 4.15. This figure indicates that the developed model was adequate for the prediction of COD removal since the predicted values were relatively close to the observed COD removal values. This was also explained by the R^2 value of 0.9046, indicating that the model explains 90% of the variation.

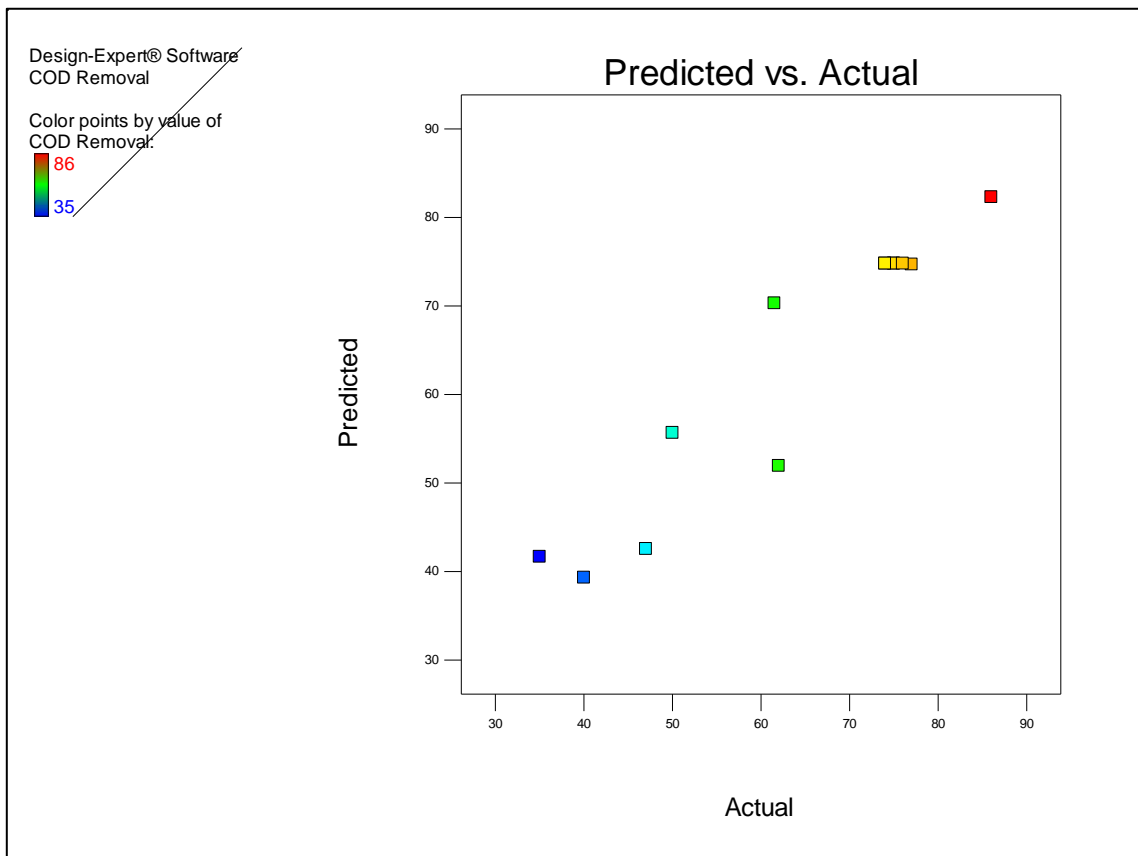


Figure 4.15: Predicted COD removal vs actual (experimental) COD removal.

4.6.2. Effect of process parameters on COD removal

The COD removal during electrochemical oxidation of biodiesel wastewater is directly related to the process parameters investigated, either as a main or as a part of an interaction effect. The reason for predicting the COD removal is to develop a model, to aid in the selection of an appropriate range for process optimisation.

The primary factor most affecting COD removal appears to be electrochemical oxidation time. The model indicates that if the electrochemical oxidation time decreases with 1 coded unit, the COD removal decreases with 23 units, which in this case is % COD removal. This is mainly since COD removal increases with increasing electrochemical oxidation time. Current density also plays a significant role; however, its effect is not as pronounced in the tested range, 0.75 mA/cm² - 1.25 mA/cm². When the current density is changed by 1 coded unit then the % COD removal decreases with approximately 10%. Figure 4.16 shows a perturbation plot highlighting the effect of current density and electrochemical oxidation time on COD removal. Comparisons of the effect of factors can be made at a certain point in the design space using a perturbation plot. It does however not show the effect of interactions of the factors.

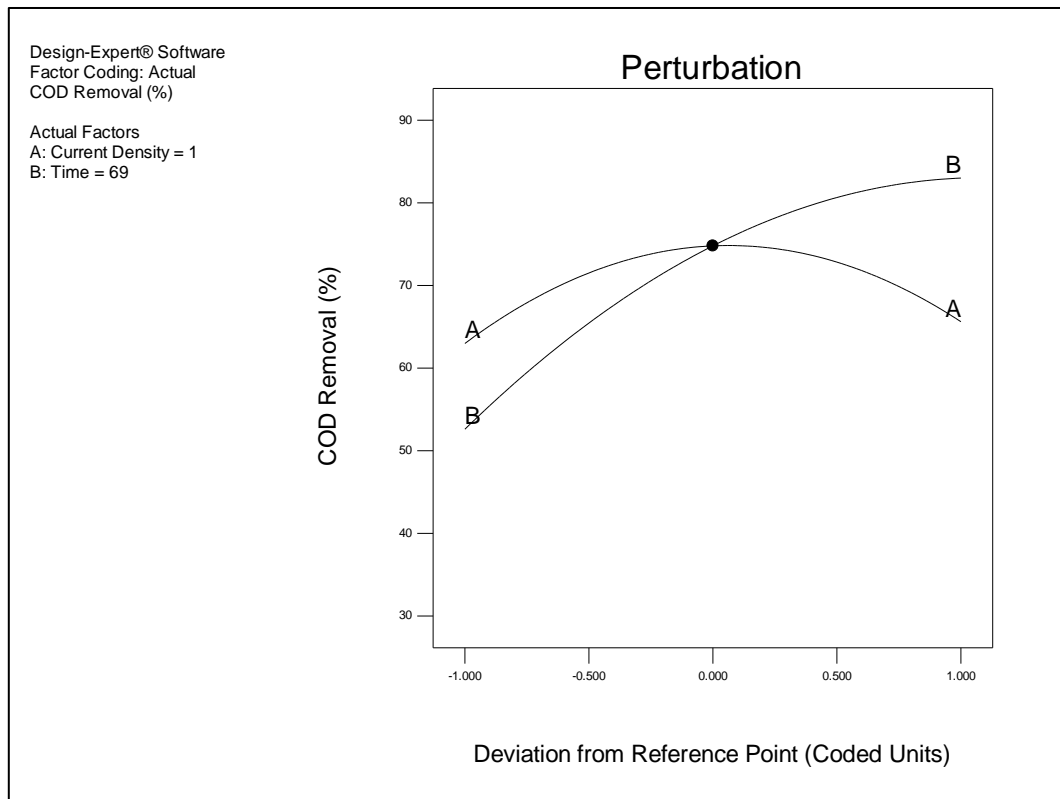


Figure 4.16: Perturbation plot showing the effect of current density and electrochemical oxidation time on COD removal.

Figure 4.17 shows the interaction of current density and electrochemical oxidation time as well as its effects on COD removal, within the design space. A 2-D contour and 3-D surface plot is shown in Figure 4.18 and Figure 4.19, respectively. These plots show the positive influence of increasing electrochemical oxidation time as well as the effects of changes in current density. Figure 4.18 shows that an increase in electrochemical oxidation time beyond 79.5 hours results in 80% COD removal, with a maximum COD removal from 90 hours onwards. Similarly, with a current density ranging between 0.875 – 1.125 mA/cm² a COD removal of 80% can be achieved. The experimental results confirm these indications with the maximum COD removal of 86% reached at a current density of 1 mA/cm² for 100 hours of electrochemical oxidation time. The model thus successfully described the electrochemical oxidation of biodiesel wastewater within the design space of the model.

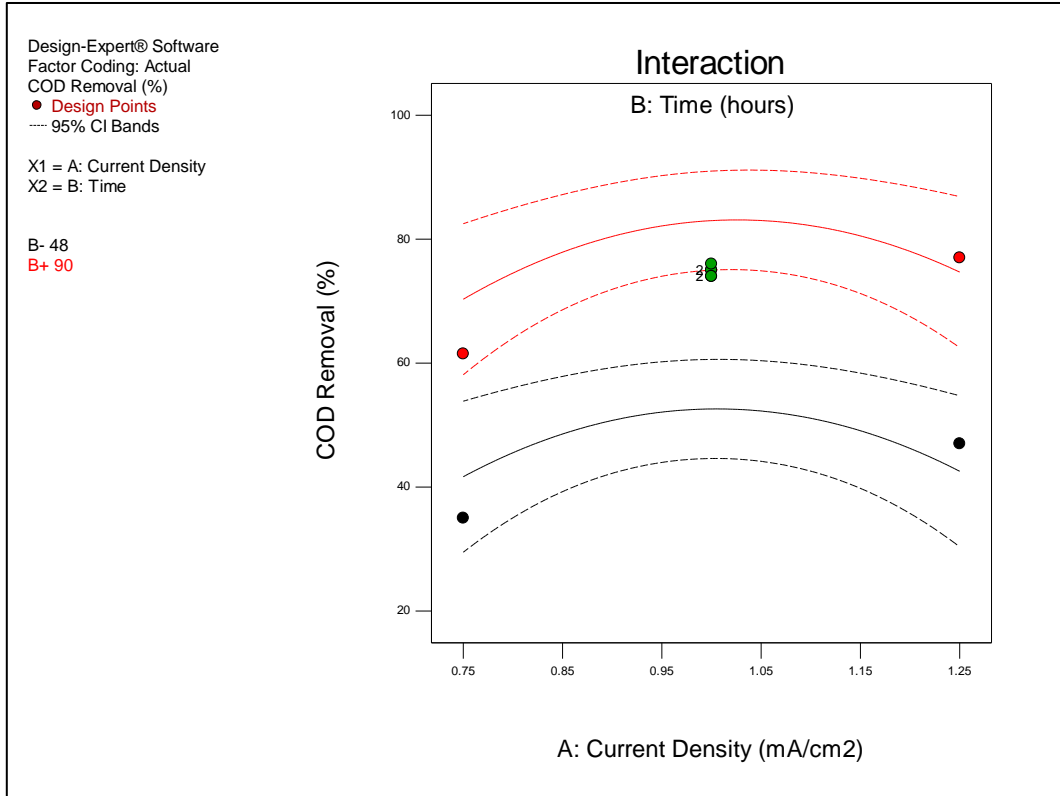


Figure 4. 17: Interaction effect between current density and electrochemical oxidation on COD removal.

Design-Expert® Software
Factor Coding: Actual
COD Removal (%)



X1 = A: Current Density
X2 = B: Time

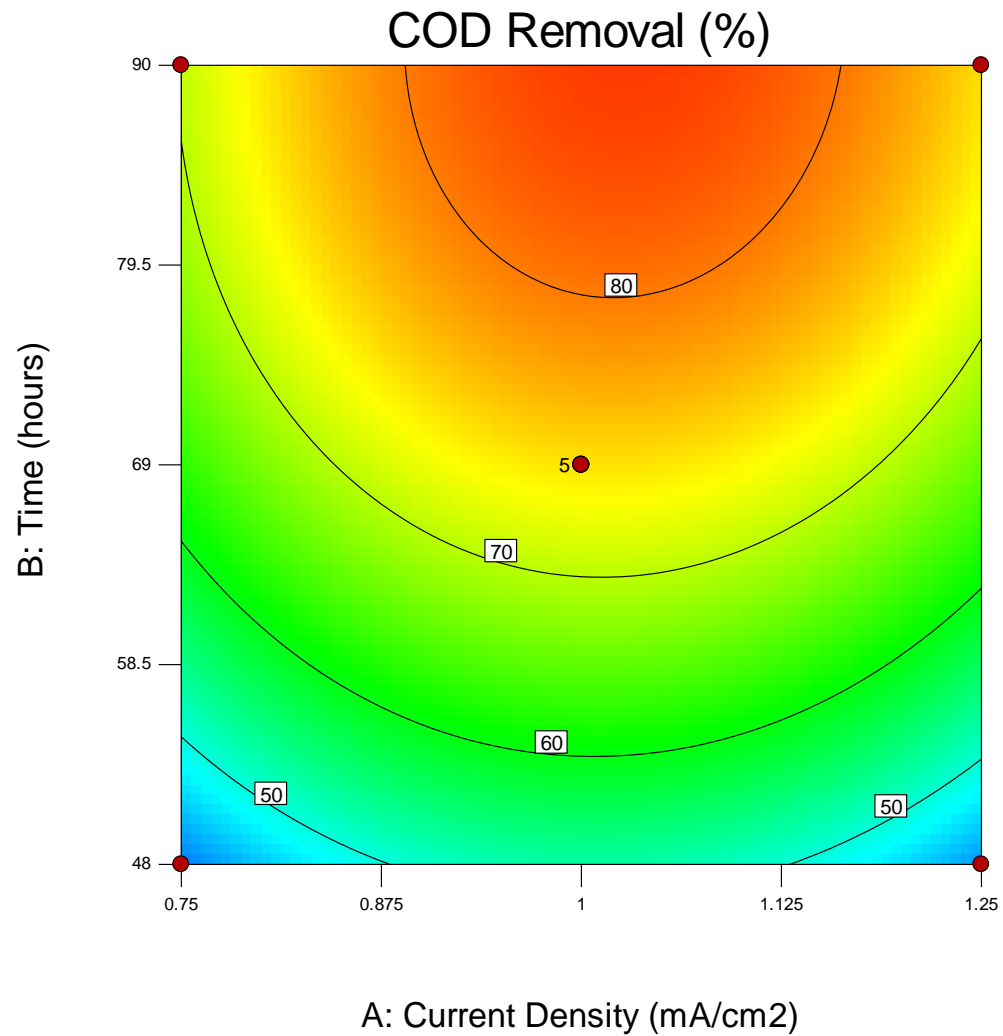


Figure 4. 18: 2D contour plot showing the effect of current density and electrochemical oxidation on COD removal.

Design-Expert® Software

Factor Coding: Actual

COD Removal (%)

● Design points above predicted value

● Design points below predicted value

86

35

X1 = A: Current Density

X2 = B: Time

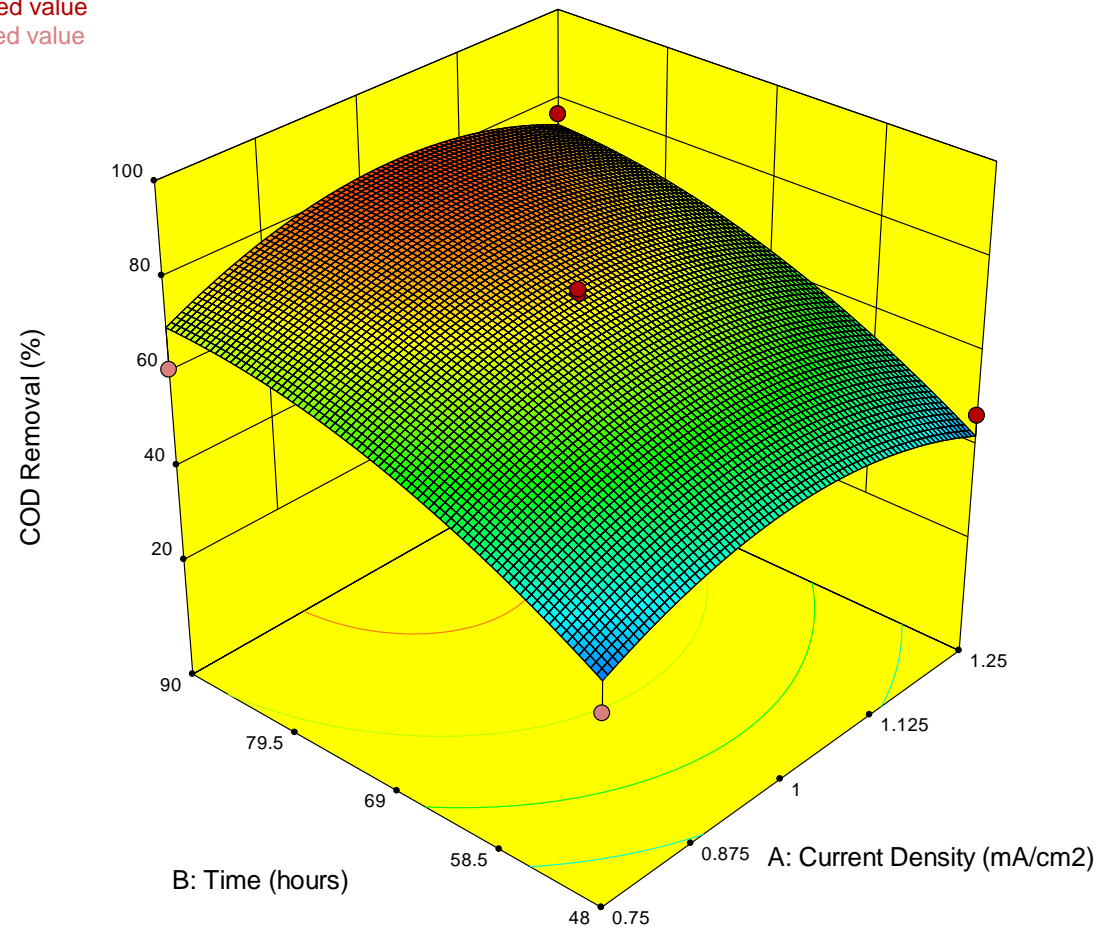


Figure 4. 19: 3D surface plot showing the effect of current density and electrochemical oxidation on COD removal.

4.7. Adsorption using chitosan

The adsorption of COD from biodiesel wastewater onto chitosan was investigated at pH values ranging from 2 to 6, and chitosan concentrations ranging from 2.5 – 4.5 g/L as shown in Table 3.4. The results of these experimental runs can be found in Appendix D.

4.7.1. Effect of adsorption time

The adsorption capacity, using Equation 2.6, was calculated to investigate the effect of adsorption time on the adsorption capacity of COD onto chitosan. Initially it was evaluated over 5 hours using chitosan at 3.5 g/L where samples were taken every hour. A mixing rate of 350 rpm and initial pH of 2 was used.

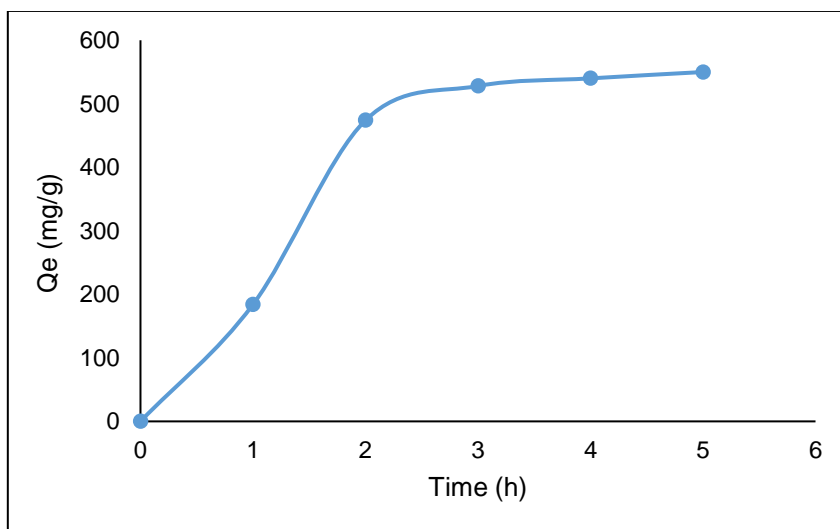


Figure 4. 20: Single stage adsorption capacity

In Figure 4.20, it can be observed that the adsorption rate over the first 2 hours control the rate of the reaction and reach a concentration of 500 mg/g. Thereafter it stabilises, reaching some form of equilibrium. The increase in adsorption rate in the first 2 hours is explained by (Stang et al., 1994), stating that this occurrence is due the increased interaction between pollutant molecules and chitosan particles, as well as an increased adsorption of oil droplets as they broke into smaller sizes leading to greater interfacial contact time.

No further increases in adsorption were noticed beyond 3 hours, possibly since chitosan has reached its saturation point. Consequently, an adsorption time of 3 hours was selected as optimum for the adsorption of COD present in BDWW onto chitosan. At these conditions a single adsorption stage achieved % COD removal of 23%.

4.7.2. Effect of initial wastewater pH

The effect of initial wastewater pH on the pollutant removal was investigated over a pH range 2, 4 and 6. The adsorbent, chitosan powder, was used at the following concentrations: 2.5, 3.5 and 4.5 g/L, respectively. A constant mixing rate of 350 rpm and adsorption time of 3 hours per adsorption stage, at ambient conditions, was witnessed. The initial pH of the wastewater affects the surface chemistry of the adsorbent as well as the chemistry of the pollutants in the BDWW (Pitakpoolsil & Hunsom, 2013)

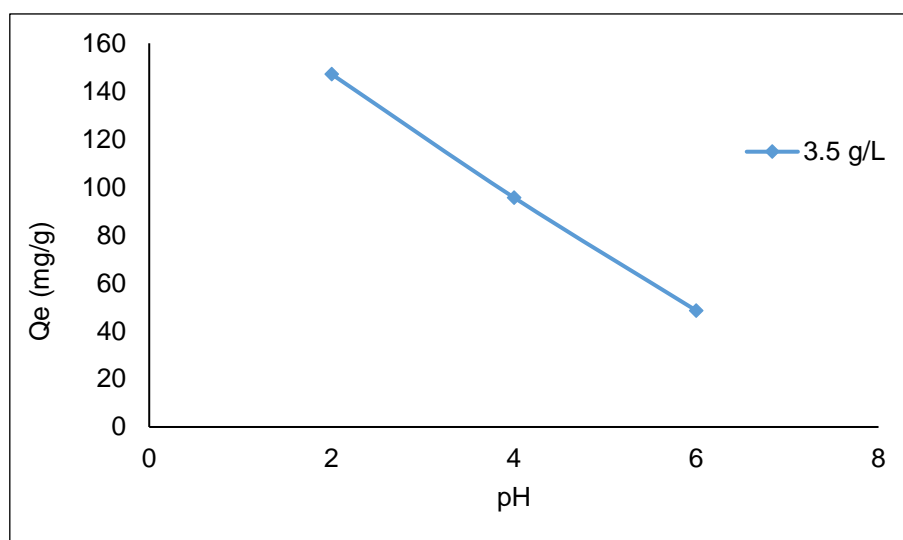


Figure 4. 21: Effect of pH on single stage adsorption capacity

Figure 4.21 demonstrates the comparison of the adsorption capacity over the 3 pH values at a constant chitosan concentration of 3.5g. It can be observed that the adsorption capacity of COD is at its highest of 147 mg/g at a pH of 2 and decreases as the pH increases, indicating that pollutants were better removed in more acidic conditions.

This can be explained by the hydrogen atom (H⁺) in the solution, protonating the amine groups (-NH²) in chitosan, resulting in interaction with anionic molecules (Sokker et al., 2011) the strong acidic conditions destabilise the oil molecules. Chitosan stimulates a physico-chemical effect to

demulsify and increase the droplet size that improves the adsorption of oil (Sakkayawong et al., 2005) and Ruhsing Pan et al., (1999) attribute the increase in chitosan adsorption capacity under acidic conditions to an increase in the number of protonated amine groups in the chitosan polymer. Therefore, the pH of 2 was identified for further experimental runs.

4.7.3. Effect of Chitosan dosage

The effect of the chitosan powder concentration on the adsorption capacity of COD was evaluated over a concentration range of 2.5, 3.5 and 4.5 g/L at a pH of 2. The adsorption capacity of COD increased significantly with corresponding adsorbent dosages as shown in Figure 4.22.

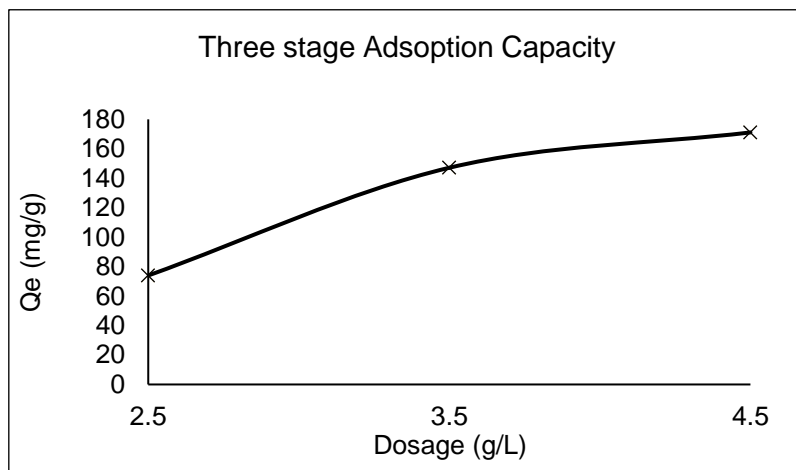


Figure 4. 22: Multi-stage adsorption capacity.

Figure 4.22 shows the results of adsorption capacity over adsorbent dosages. These experimental runs were over a 9-hour period. Fresh chitosan powder was added after every 3 hours at the same dosage concentration as mentioned before. In Figure 4.20, it was observed that equilibrium was reached after 3 hours, indicating that the adsorbent reached its saturation point. Based on this observation, previously, fresh Chitosan was added every 3 hours. According to Pitakpoolsil & Hunsom, (2013) the addition of fresh chitosan concentration assist with the increase of adsorption capacity at constant concentrations, however the adsorption capacity of the chitosan decreases with each additional stage since the process becomes inefficient in the presence of low concentrations of pollutants. The maximum adsorption capacity of 171 mg/g was observed at a dosage of 4,5 g/L after three consecutive adsorption stages using fresh chitosan. Lower adsorption capacities of 137 mg/g and 71 mg/g were obtained at chitosan dosages of 3.5 g/L and 2.5 g/L.

In Figure 4.23, below, the three dosage concentration stages of a 9-hour period are shown with % COD removal. At a dosage concentration of 4.5g after 9 hours, a maximum % COD removal of 55% was achieved. At lower dosages of 3.5g and 2.5g, lower % COD removal efficiencies of 40% and 35% were achieved, respectively. Thus, an increase in concentration dosage enhanced the adsorption capacity. Ahmad et al., (2005) found that an increase in chitosan dosage lead to an increase in oil removal, however this is only true at low dosages, since chitosan possesses a high charge density and therefore only low amounts are needed. Similarly, Thirugnanasambandham et al., (2014) found that an increase in chitosan dosage results into increased pollutant removal efficiencies since higher concentrations lead to higher reaction sites.

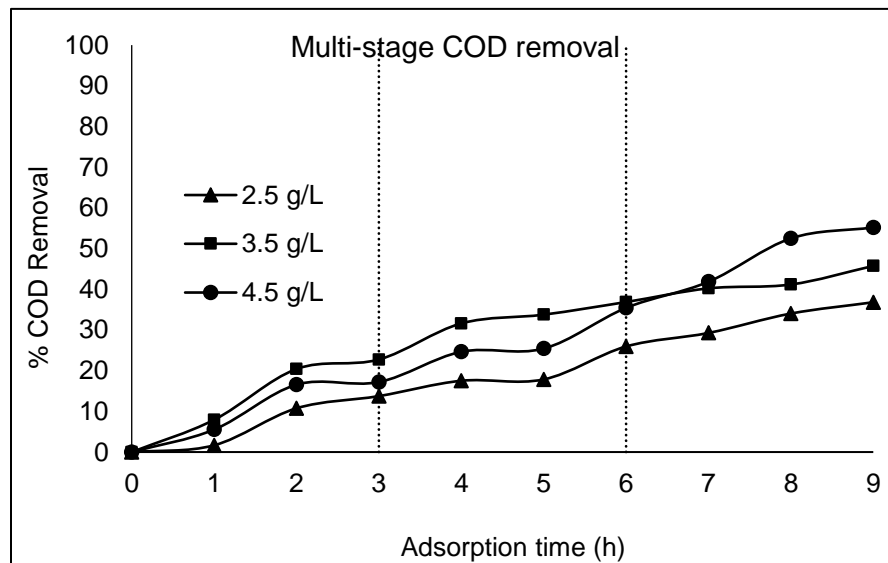


Figure 4. 21: COD removal at adsorption stages

Figure 4.24 represent the effect of various chitosan concentrations and three different pH values on the % COD removal over 9 hours. A maximum COD removal of 55% was achieved at a pH of 2 and a chitosan dosage of 4.5 g/L. The % COD removal decreased as the pH increased from 2 to 6 and the % COD removal increased as the chitosan concentration increased from 2.5 g/L to 4.5 g/L.

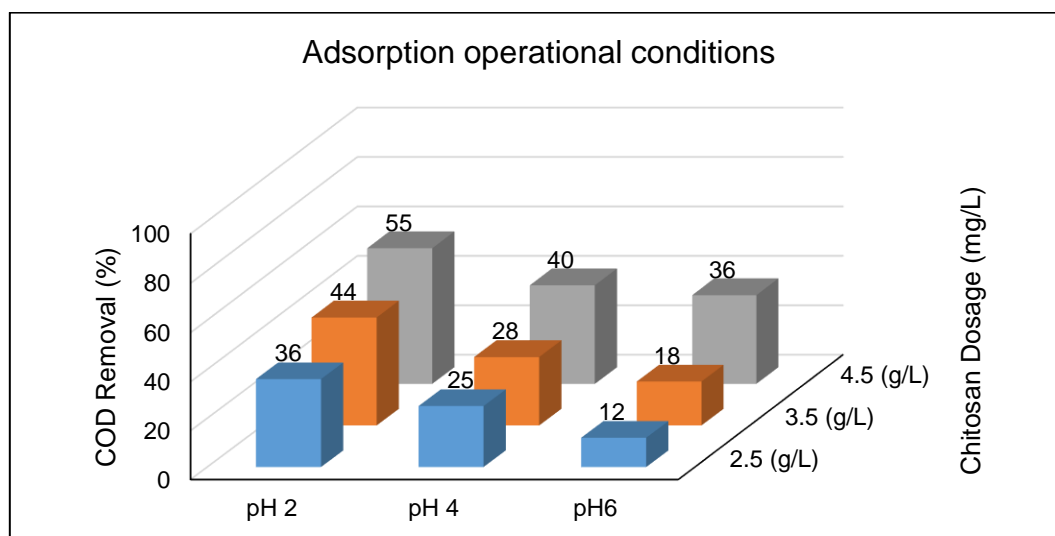


Figure 4. 22: Adsorption operational parameters

The increased removal capacities at lower pH values are explained by the destabilization of oil molecules at strong acidic conditions. Due to the structure of chitosan, the amine groups ($-NH_2$) are protonated that leads to interaction with anionic molecules in the water (Sokker et al., 2011). Similarly an increase in protonated amine groups in the chitosan polymer induces a physical-chemical effect (Ruhasing Pan et al., 1999) which increases the droplet size of oil. This improves the adsorption of oil onto chitosan (Sakkayawong et al., 2005). The increase in adsorption capacity with an increase in chitosan concentration are due to more reaction sites available for pollutant removal (Thirugnanasambandham et al., 2014). However, according to Ahmad et al., (2005), this is only true for low concentrations since chitosan possesses a high charge density and therefore only low amounts are needed.

4.8. Adsorption equilibrium and isotherms

The data obtained from the adsorption experiments where COD concentrations between 65 000 mg/L and 40 000 mg/L were fitted with the Langmuir, Freundlich and Dubinin-Raduschkevich isotherms.

According to Chiou & Li, (2002), the equilibrium adsorption isotherm is essential in describing the interactive behaviour between solutes and adsorbents. These isotherms are central when designing adsorption systems (Chiou & Li, 2002).

The Langmuir and Freundlich models were applied at the start. However, since these models do not give information on the adsorption mechanism (Laus et al., 2010), the Dubinin-Raduschkevich isotherm (D-R) was applied.

Aksoyoglu, (1989) states that the Dubinin-Raduschkevich isotherm (D-R) is an equivalent of the Langmuir isotherm, but is more general, since it does not assume a standardized surface or constant sorption potential. The D-R isotherm can be used to calculate the mean free energy of adsorption, which is used to identify chemical and physical adsorption.

4.8.1. Langmuir isotherm

The equilibrium data of each experiment at a pH of 2, outlined in Table 3.4, were fitted to the Langmuir Isotherm given in Equation 2.7. The results can be found in Appendix D.

$$q_e = \frac{q_m K_L C_e}{1 + K_L C_e}$$

K_L and q_m was determined from a linearized form of Equation 2.7. as shown in Equation 2.8.

$$\frac{C_e}{q_e} = \frac{1}{q_m} C_e + \frac{1}{K_L q_m}$$

Therefore, a linearized plot of (C_e/q_e) versus C_e gives a straight line, with slope $1/q_m$ and intercept $1/q_m K_L$. The linearized plots of chitosan dosages 2.5, 3.5, and 4.5 g/L are shown in Figure 4.25. The calculated values are in Table 4.13.

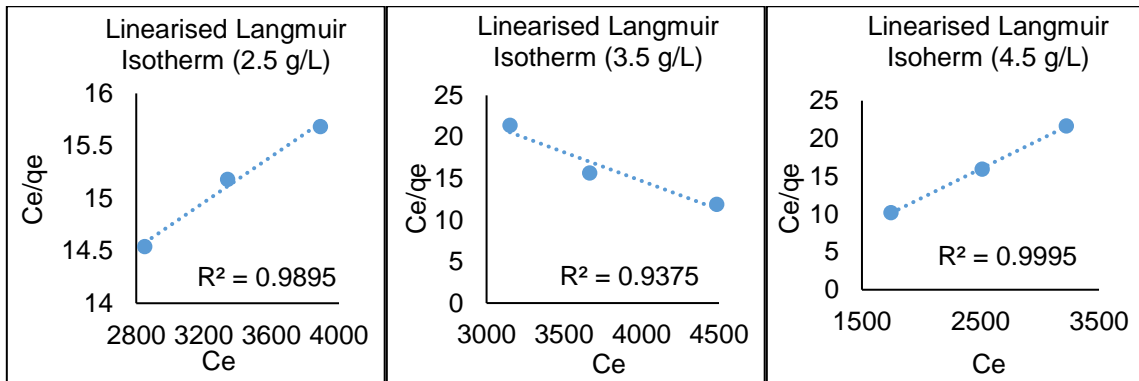


Figure 4. 25: linearized Langmuir isotherms

The essential features of the Langmuir isotherm R_L was calculated using Equation 2.9. The calculated values are shown in Table 4.13.

$$R_L = \frac{1}{1 + K_L C_0}$$

Table 4. 13: Langmuir isotherm parameters at a pH of 2

Langmuir Isotherm parameters at a pH of 2			
Langmuir	2.5 g/L	3.5 g/L	4.5 g/L
R ²	0.9895	0.9375	0.9995
Q _m	909.1	144.9	129.9
K _L	0.000096	0.000163	0.00228
R_L	0.698	0.514	0.101

As the chitosan concentration dosage increased from 2.5, 3.5 and 4.5 g/L the corresponding R_L values decreased from 0.698, 0.514 and 0.101 respectively. Thus, indicating a favorable adsorption. The value of R_L gives an indication of the favorability of the adsorption (Stromer et al., 2018), since these values fall within the favorable range, 0 < R_L < 1. These results show that COD adsorption onto Chitosan is favorable at these conditions.

4.8.2. Freundlich Isotherm

The equilibrium data of each experiment at a pH of 2, outlined in Table 3.4, were fitted to the Freundlich Isotherm given in Equation 2.10. The results can be found in Appendix D.

Equation 2.10 was used to fit the equilibrium data:

$$Q_e = K_F C_e^{1/n}$$

The linear form of the Freundlich isotherm, Equation 2.11, was used to plot $\log q_e$ versus C_e . See Figure 4.26. This allowed for the determination of the constant K_f and exponent $1/n$. The calculated values are given in Table 4.14.

$$\log q_e = \log K_F + \frac{1}{n} \log C_e$$

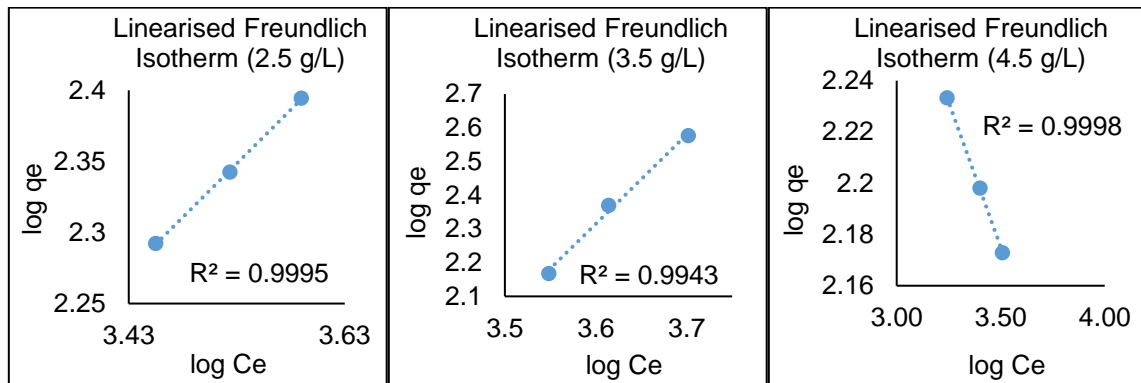


Figure 4. 23 :Linearized Freundlich isotherms

Table 4. 14: Freundlich isotherm parameters

Parameters			
Freundlich	2.5 g/L	3.5 g/L	4.5 g/L
R^2	0.9982	0.9943	0.9998
n_f	0.7562	2.647	0.2262
K_f	1.379	1191.7	19.43

Values of n were found to be 1.3224, 0.3777 and 4.4209 for dosages of 2.5, 3.5 and 4.5 g/L respectively as shown in Table 4.14. Therefore, adsorption was favourable at dosages of 2.5 and 4.5 g/L and unfavourable at 3.5 g/L, since the values of n was more than 1, as stated in Chapter 2. The Freundlich isotherm adequately describes the adsorption kinetics of COD onto chitosan. These results are consistent with those observed by Ahmad et al., (2005), who found that the Freundlich isotherm fitted the adsorption of palm oil mill effluent onto chitosan.

4.8.3. Dubinin-Raduschkevich isotherm

The equilibrium data of each experiment at pH of 2, outlined in Table 3.4, were fitted to the Dubinin-Raduschkevich isotherm given in Equation 2.12. The results can be found in Appendix D.

$$q_e = q_m \exp(-k\varepsilon^2)$$

The Polanyi potential (ε) (J/mol) was calculated with Equation 2.13.

$$\varepsilon = RT \ln \left(1 + \frac{1}{C_e} \right)$$

The linear form of Equation 2.12 allows for the values of q_m and K to be deduced by plotting $\ln(q_e)$ versus ε^2 as shown in Figure 4.27, these calculated values are presented in Table 4.15.

$$\ln q_e = \ln q_m - k\varepsilon^2$$

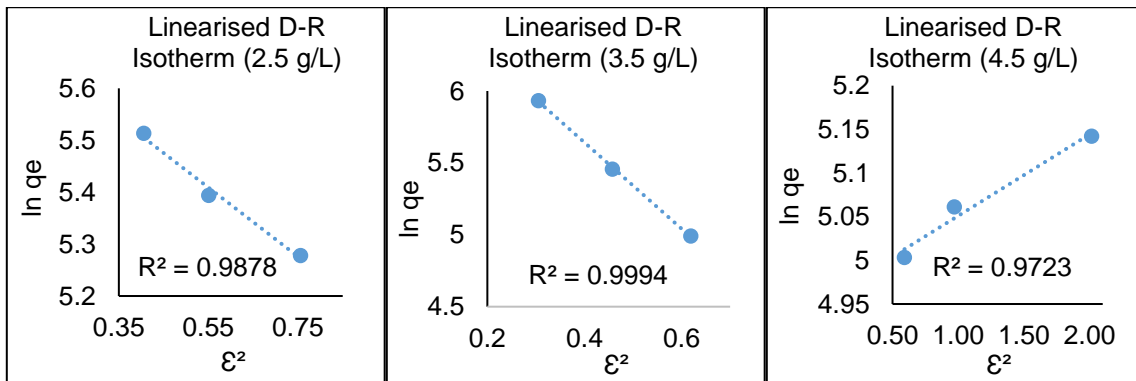


Figure 4. 24: Linearized D-R isotherms

The mean energy of adsorption (E) can be calculated from Equation 2.15.

$$E = (-2K)^{-1/2}$$

Table 4. 15: D-R isotherm parameters

Parameters			
D-R	2.5 g/L	3.5 g/L	4.5 g/L
R ²	0.9878	0.9994	0.9723
Q _m	1.94	20.07	1.10
K	14.224	22.402	11.584
E (kJ/mol)	0.187	0.149	0.208

This parameter gives information about the adsorption mechanism as either chemical ion-exchange or physical adsorption. Calculated values are shown in Table 4.15. Values of 0.187, 0.149 and 0.208 kJ/mol were observed at dosages of 2.5, 3.5 and 4.5 g/L respectively, indicating that physical adsorption occurred at all chitosan dosages, since these values are all below 8 kJ/mol as stated by Laus et al., (2010) and OZCAN et al., (2005).

4.9. Integrated treatment

The integrated treatment of biodiesel wastewater consisted of three consecutive treatment steps: (1) acidification, (2) electrochemical oxidation using $\text{IrO}_2\text{-Ta}_2\text{O}_5$ anodes and (3) adsorption using chitosan as adsorbent. The electrochemical oxidation of biodiesel wastewater was investigated at the start in order to determine the operating conditions that would result in the maximum COD removal. The same methodology were applied with the adsorption process. The operating parameters of these two individual processes were established and pollutant removal confirmed. Thereafter they were combined as consecutive steps in order to remove COD, FOG and BOD from industrial biodiesel wastewater in an integrated process.

During the acidification step at a constant pH of 2, a % COD removal of 11% was achieved. The second step with the electrochemical oxidation process taking place over a 100-hour time period at a current density of 1mA/cm^2 and a NaCl concentration of 0.08M removed the % COD to 86%. During the third treatment step, adsorption with chitosan powder, at a pH of 2 and a chitosan dosage of 4.5 g/L , a 55% COD removal was achieved after three repetitive adsorption stages. These individual processes and their respective COD removal efficiencies are shown in Table 4.16.

Table 4. 16: Integrated treatment COD removal

Process	COD (mg/L)	COD removal (%)
Initial	65000	-
Acidification	55000	11
Electrochemical oxidation	7800	86
Adsorption	3850	55

The biodiesel wastewater effluent obtained after electrochemical oxidation in Experimental Run 3 was used as a feed for the third treatment step, adsorption using chitosan, at a pH of 2 and a chitosan dosage of 4.5 g/L for three consecutive steps. The results of this integrated treatment process are shown in Figure 4.28.

Table 4. 17: Integrated treatment process: Final pollutant concentrations

Parameter	Initial (mg/L)	Final (mg/L)	Removal (%)	CCT:2013
COD	65000	3850	94	5000
BOD	19405	2620	86	-
FOG	265	12	95	4000

The initial COD concentration of the raw biodiesel wastewater was 65000 mg/L. After the first acidification step, the COD was reduced to 55000 mg/L (11 % COD removal). In the second step, during a 100 hours' time period with an electrochemical oxidation cell at a current density of 1 mA/cm² and a NaCl concentration of 0.08 M the COD was further reduced to 7800 mg/L (86 % COD removal). The final step of adsorption with chitosan where three consecutive adsorption stages at a pH of 2 and chitosan dosage of 4.5g/L was followed, reduced the COD further to 3850 mg/L (51% COD removal). The reduction of the initial COD concentration of 65000 mg/L to a final COD concentration of 3850 mg/L resulted to an overall % COD removal of 94%. Table 4.17 shows the final % BOD and FOG removal using this integrated process to 86% and 95% respectively.

A study completed by Siles et al., (2010) treated biodiesel wastewater with an integrated treatment process that consisted of acidification-electrocoagulation and anaerobic co-digestion. During this treatment process the COD was reduced by 80% - 90%.

Rattanapan et al., (2011) studied the treatment of biodiesel wastewater using an integrated treatment process consisting of acidification, coagulation and dissolved air flotation. This process was able to reduce FOG by 85% - 95% and COD by 40% - 50%.

A combined electro-flotation and electro-oxidation process used in a study by Palomino Romero et al., (2013) showed that the system could successfully treat biodiesel wastewater using Ti/RuO₂ anodes. The COD was reduced by 95%, whereas FOG was completely removed.

This study confirms that an integrated process using acidification, electrochemical oxidation and adsorption using chitosan can reduce the COD, BOD and FOG according to the City of Cape Town: Wastewater and Industrial Effluent By-Law, 2013, discharge standards.

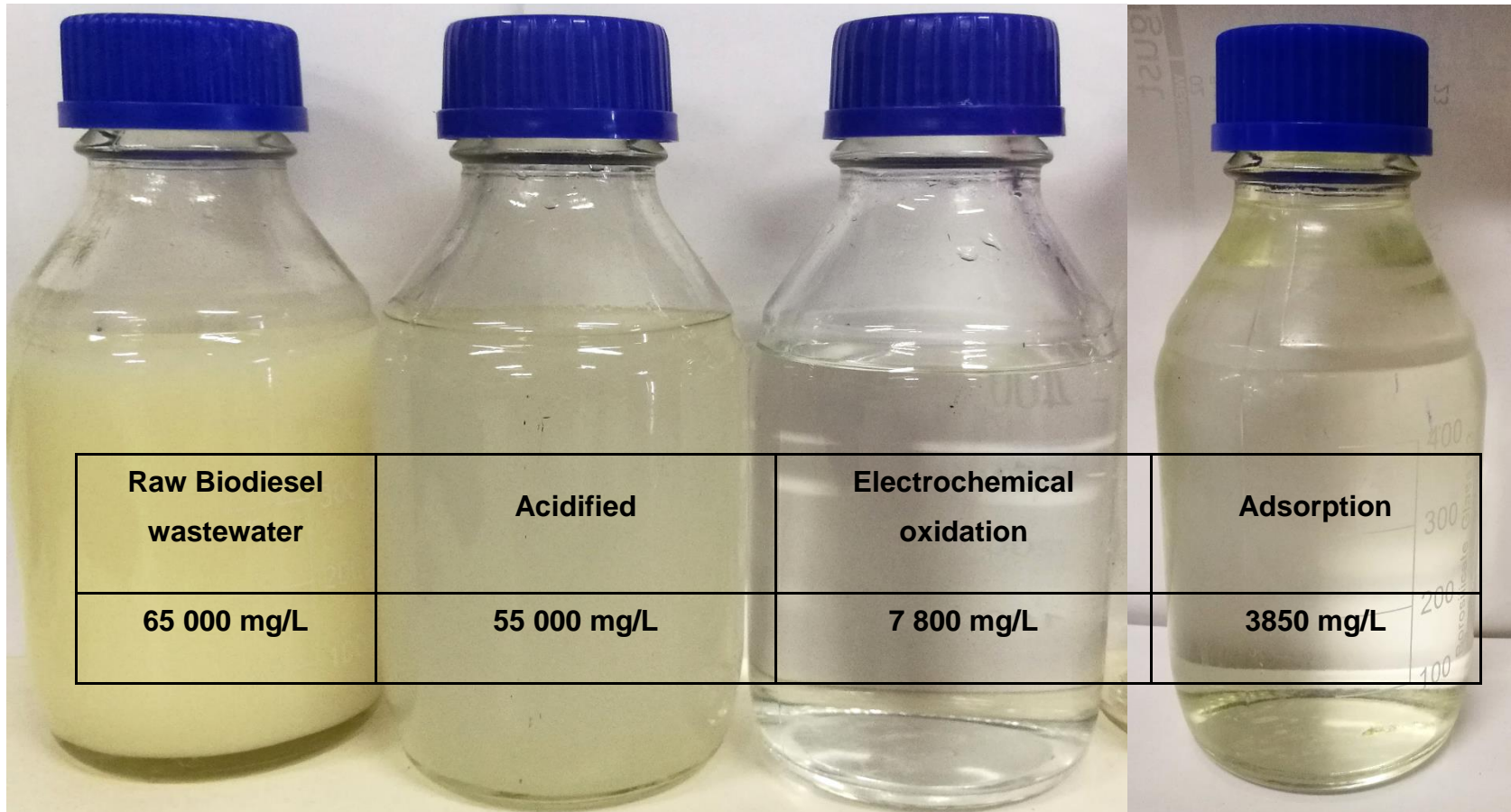


Photo 4. 1: Wastewater after each respective treatment stage.

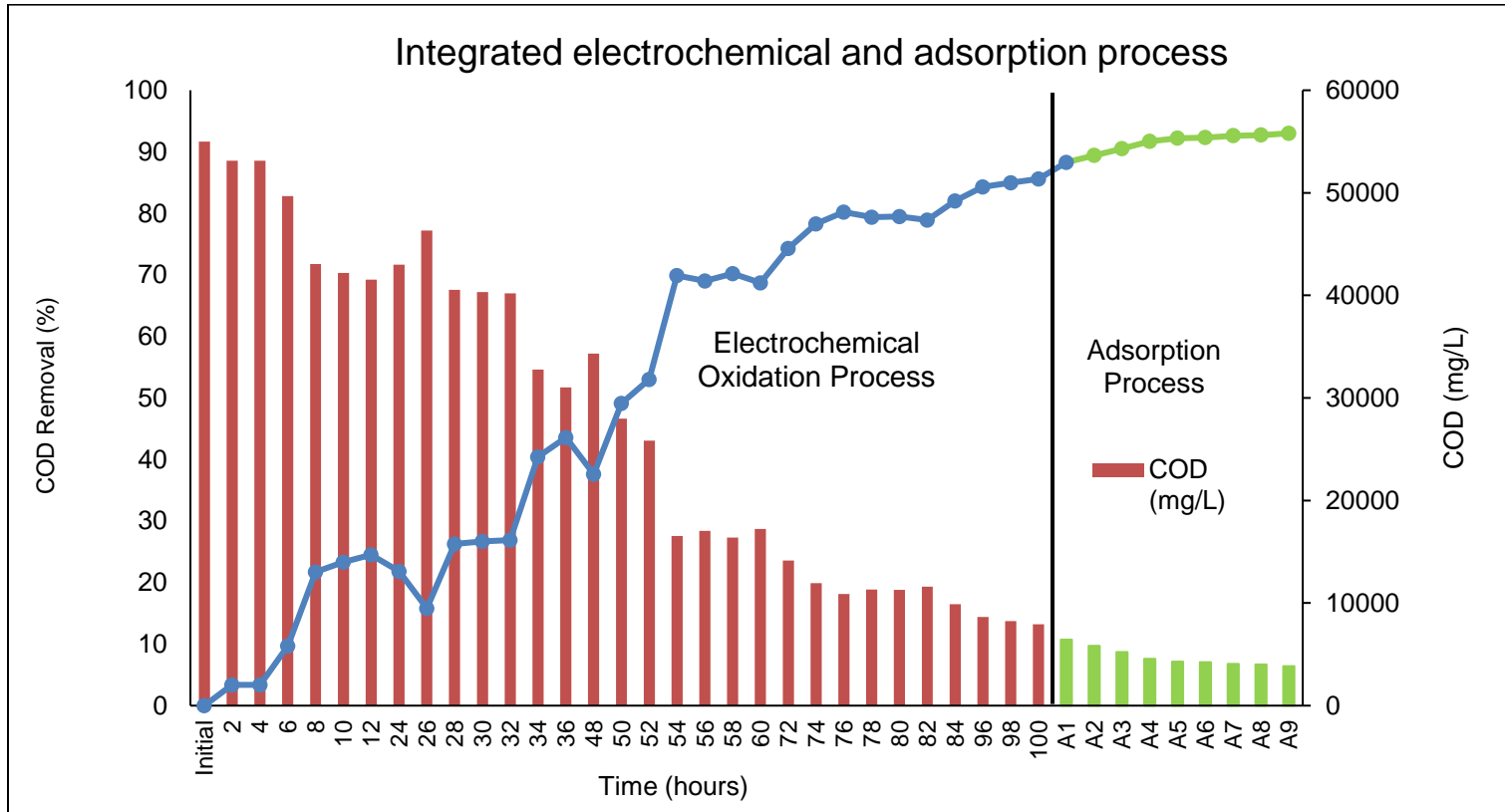


Figure 4. 25: Integrated treatment COD removal over time

Photo 4.1 shows the COD concentration after each integrated step. A clear distinction can be seen between the untreated and treated wastewater when looking at the colour and the clarity. There was no significant change in colour and clarity visible to the naked eye between the electrochemical and adsorption effluents.

Figure 4.28 shows the integrated system where COD concentration and % removal over the time intervals for each of the treatment processes. COD was reduced from 65 000 mg/L to 3850 mg/L after acidification, 100 hours of electrochemical oxidation and three consecutive adsorption stages, indicating successful treatment of industrial biodiesel wastewater using the integrated treatment process.

CHAPTER 5

Conclusion and Recommendation

Chapter 5: conclusion and recommendation

5.1. Conclusion

The integrated treatment process utilised in this study consisted of three consecutive steps, Acidification, electrochemical oxidation and adsorption. The treatment processes were investigated on a separate basis after which favourable conditions were combined into an integrated treatment process.

The first step, acidification at a final pH of 2 removed the COD, BOD and FOG by 11%, 10%, and 80% respectively.

The second step, electrochemical oxidation, using a current density of 1 mA/cm², with a NaCl concentration of 0.08 M, showed excellent removal efficiencies. These conditions could reduce COD, BOD and FOG by 86%, 88% and 85% respectively. The current density and NaCl concentrations had significant effects on the performance of the electrochemical oxidation process. This process was modelled using a central composite design. The proposed model could describe the process with a 90% accuracy level.

The third and final step, adsorption using chitosan, showed favourable results when a chitosan concentration of 4.5g/L at a pH of 2 was used. Three consecutive adsorption stages using fresh chitosan at these conditions resulted in a maximum of 55% COD, 54% BOD and 55% FOG removal. The pH had a major impact on the performance of the process. Under acidic conditions, the COD % removal increased with an increase in chitosan concentration.

The integrated treatment process was able to reduce COD, BOD and FOG levels by 94%, 86% and 95% respectively. This resulted in a treated effluent that complies with local industrial effluent discharge standards. Using this integrated process, the treated biodiesel wastewater effluent could be disposed of safely without further treatment and saving cost.

5.2. Recommendation

1. In the production of biodiesel, different processes and techniques are applied in industry. This results in wastewater quality of various standards and characteristics that need to be investigated as feed into the current integrated treatment process.
2. $\text{IrO}_2\text{-Ta}_2\text{O}_5$ anodes are classified as active anodes that operate through mediated oxidation of organics. More recent Boron Doped Diamond (BDD) anodes that operate through direct oxidation should be investigated.
3. Membrane technology should be used as a polishing step to lower contaminant levels for recycling application during the biodiesel production process.

CHAPTER 6

References

6. References

- Abbasi, T. & Abbasi, S.A. 2011. Decarbonization of fossil fuels as a strategy to control global warming. *Renewable and Sustainable Energy Reviews*, 15(4): 1828–1834. <http://dx.doi.org/10.1016/j.rser.2010.11.049>.
- Adewale, P., Vithanage, L.N. & Christopher, L. 2017. Optimization of enzyme-catalyzed biodiesel production from crude tall oil using Taguchi method. *Energy Conversion and Management*, 154(October): 81–91. <http://linkinghub.elsevier.com/retrieve/pii/S0196890417309792>.
- Adewumi, J.R., Ilemobade, A.A. & Van Zyl, J.E. 2010. Treated wastewater reuse in South Africa: Overview, potential and challenges. *Resources, Conservation and Recycling*, 55(2): 221–231. <http://dx.doi.org/10.1016/j.resconrec.2010.09.012>.
- Ahmad, A.L., Sumathi, S. & Hameed, B.H. 2005. Adsorption of residue oil from palm oil mill effluent using powder and flake chitosan: Equilibrium and kinetic studies. *Water Research*, 39(12): 2483–2494.
- Aksoyoglu, S. 1989. Sorption of U(VI) on granite. *Journal of Radioanalytical and Nuclear Chemistry Articles*, 134(2): 393–403.
- Alba-Rubio, A.C., Alonso Castillo, M.L., Albuquerque, M.C.G., Mariscal, R., Cavalcante, C.L. & Granados, M.L. 2012. A new and efficient procedure for removing calcium soaps in biodiesel obtained using CaO as a heterogeneous catalyst. *Fuel*, 95: 464–470. <http://dx.doi.org/10.1016/j.fuel.2011.12.024>.
- Almomani, F. & Baranova, E.A. 2012. Electro-oxidation of two reactive azo dyes on boron-doped diamond electrode. *Water Science and Technology*, 66(3): 465–471.
- Ang, W.L., Mohammad, A.W., Benamor, A. & Hilal, N. 2016. Chitosan As Natural Coagulant in Hybrid Coagulation-Nanofiltration Membrane Process for Water Treatment. *Journal of Environmental Chemical Engineering*, (2015). <http://linkinghub.elsevier.com/retrieve/pii/S2213343716301087>.
- Atadashi, I.M. 2015. Purification of crude biodiesel using dry washing and membrane technologies. *Alexandria Engineering Journal*, 54(4): 1265–1272. <http://dx.doi.org/10.1016/j.aej.2015.08.005>.

- Atadashi, I.M., Aroua, M.K., Abdul Aziz, A.R. & Sulaiman, N.M.N. 2012. High quality biodiesel obtained through membrane technology. *Journal of Membrane Science*, 421–422: 154–164. <http://dx.doi.org/10.1016/j.memsci.2012.07.006>.
- B.E., T. Oki, Arnell, N.W., Benito, G., Cogley, J.G., Döll, P., T. Jiang & Mwakalila, S.S. 2014. 2014: Freshwater resources. In *Climate Change 2014: Impacts, Adaptation, and Vulnerability. Part A: Global and Sectoral Aspects. Contribution of Working Group II to the Fifth Assessment Report of the Intergovernmental Panel on Climate Change*. New York: Cambridge University Press: 229–269. http://www.ncbi.nlm.nih.gov/entrez/query.fcgi?cmd=Retrieve&db=PubMed&dopt=Citation&list_uids=15236969.
- Baudoin, M.A., Vogel, C., Nortje, K. & Naik, M. 2017. Living with drought in South Africa: lessons learnt from the recent El Niño drought period. *International Journal of Disaster Risk Reduction*, 23(February): 128–137. <http://dx.doi.org/10.1016/j.ijdr.2017.05.005>.
- Bhatnagar, A. & Minocha, A.K. 2006. Conventional and non-conventional adsorbents for removal of pollutants from water - A review. *Indian Journal of Chemical Technology*, 13(3): 203–217.
- Bhatt, A.S., Sakaria, P.L., Vasudevan, M., Pawar, R.R., Sudheesh, N., Bajaj, H.C. & Mody, H.M. 2012. Adsorption of an anionic dye from aqueous medium by organoclays: equilibrium modeling, kinetic and thermodynamic exploration. *RSC Advances*, 2(23): 8663. <http://xlink.rsc.org/?DOI=c2ra20347b>.
- Bouberka, A.K.Z., Kameche, F.S.M. & Derriche, Z. 2007. Adsorption study of an industrial dye by an organic clay. : 149–158.
- CAO, W., HAN, H. & ZHANG, J. 2005. Preparation of biodiesel from soybean oil using supercritical methanol and co-solvent. *Fuel*, 84(4): 347–351. <http://linkinghub.elsevier.com/retrieve/pii/S0016236104002893>.
- Chandra, R., Takeuchi, H. & Hasegawa, T. 2012. Methane production from lignocellulosic agricultural crop wastes: A review in context to second generation of biofuel production. *Renewable and Sustainable Energy Reviews*, 16(3): 1462–1476. <http://dx.doi.org/10.1016/j.rser.2011.11.035>.
- Chang, M.Y. & Juang, R.S. 2004. Adsorption of tannic acid, humic acid, and dyes from water

- using the composite of chitosan and activated clay. *Journal of Colloid and Interface Science*, 278(1): 18–25.
- Chavalparit, O. & Ongwandee, M. 2009. Optimizing electrocoagulation process for the treatment of biodiesel wastewater using response surface methodology. *Journal of Environmental Sciences*, 21(11): 1491–1496. [http://dx.doi.org/10.1016/S1001-0742\(08\)62445-6](http://dx.doi.org/10.1016/S1001-0742(08)62445-6).
- Chiou, M.S. & Li, H.Y. 2002. Equilibrium and kinetic modeling of adsorption of reactive dye on cross-linked chitosan beads. *Journal of Hazardous Materials*, 93(2): 233–248.
- Chitra, P., Venkatachalam, P. & Sampathrajan, A. 2005. Optimisation of experimental conditions for biodiesel production from alkali-catalysed transesterification of *Jatropha curcus* oil. *Energy for Sustainable Development*, 9(3): 13–18. [http://dx.doi.org/10.1016/S0973-0826\(08\)60518-9](http://dx.doi.org/10.1016/S0973-0826(08)60518-9).
- Christopher, L.P., Hemanathan Kumar & Zambare, V.P. 2014. Enzymatic biodiesel: Challenges and opportunities. *Applied Energy*, 119: 497–520. <http://dx.doi.org/10.1016/j.apenergy.2014.01.017>.
- Chung, H.K., Kim, W.H., Park, J., Cho, J., Jeong, T.Y. & Park, P.K. 2015. Application of Langmuir and Freundlich isotherms to predict adsorbate removal efficiency or required amount of adsorbent. *Journal of Industrial and Engineering Chemistry*, 28: 241–246. <http://dx.doi.org/10.1016/j.jiec.2015.02.021>.
- City of Cape Town. 2013. *City of Cape Town: Wastewater and Industrial Effluent By law, 203*. <https://indigo.openbylaws.org.za/api/za-cpt/act/by-law/2013/wastewater-industrial-effluent/eng.pdf>.
- Coledam, D.A.C., Aquino, J.M., Rocha-Filho, R.C., Bocchi, N. & Biaggio, S.R. 2014. Influence of chloride-mediated oxidation on the electrochemical degradation of the direct black 22 dye using boron-doped diamond and β -PbO₂ anodes. *Quimica Nova*, 37(8): 1312–1317. <http://www.gnresearch.org/doi/10.5935/0100-4042.20140219>.
- Comninellis, C. 1994. Electrocatalysis in the Electrochemical Conversion/Combustion of Organic Pollutants. *Electrochimica Acta*, 39(1): 1857–1862.
- Comninellis, C., Kapalka, A., Malato, S., Parsons, S.A., Poulios, I. & Mantzavinos, D. 2008. Advanced oxidation processes for water treatment: Advances and trends for R&D. *Journal of Chemical Technology and Biotechnology*, 83(6): 769–776.

- Daud, N.M., Rozaimah, S., Abdullah, S. & Hasan, H.A. 2017. Response surface methodological analysis for the optimization of acid-catalyzed transesterification biodiesel wastewater pre-treatment using coagulation-flocculation process. *Process Safety and Environmental Protection*. <http://dx.doi.org/10.1016/j.psep.2017.10.006>.
- Daud, N.M., Sheikh Abdullah, S.R., Abu Hasan, H. & Yaakob, Z. 2014. Production of biodiesel and its wastewater treatment technologies: A review. *Process Safety and Environmental Protection*, 94(October): 487–508. <http://linkinghub.elsevier.com/retrieve/pii/S0957582014001712>.
- Daud, Z., Awang, H., Latif, A.A.A., Nasir, N., Ridzuan, M.B. & Ahmad, Z. 2015. Suspended Solid, Color, COD and Oil and Grease Removal from Biodiesel Wastewater by Coagulation and Flocculation Processes. *Procedia - Social and Behavioral Sciences*, 195: 2407–2411. <http://linkinghub.elsevier.com/retrieve/pii/S1877042815037131>.
- Demirbas, A. 2009. Progress and recent trends in biodiesel fuels. *Energy Conversion and Management*, 50(1): 14–34. <http://dx.doi.org/10.1016/j.enconman.2008.09.001>.
- Department of Water Affairs. 2004. National Water Resource Strategy, First Edition, September 2004. *Water Resources*, (September): 55–135.
- Department of Water Affairs. 2013. National water resource strategy: Water for an equitable and sustainable future. , 53(9): 1689–1699.
- Domínguez, J.R., González, T., Palo, P., Sánchez-Martín, J., Rodrigo, M.A. & Sáez, C. 2012. Electrochemical Degradation of a Real Pharmaceutical Effluent. *Water, Air, & Soil Pollution*, 223(5): 2685–2694. <http://link.springer.com/10.1007/s11270-011-1059-3>.
- Đurišić-Mladenović, N., Kiss, F., Škrbić, B., Tomić, M., Mičić, R. & Predojević, Z. 2018. Current state of the biodiesel production and the indigenous feedstock potential in Serbia. *Renewable and Sustainable Energy Reviews*, 81(July 2017): 280–291.
- Elanchezhyan, S.S. & Meenakshi, S. 2017. Synthesis and characterization of chitosan/Mg-Al layered double hydroxide composite for the removal of oil particles from oil-in-water emulsion. *International Journal of Biological Macromolecules*, 104: 1586–1595. <http://dx.doi.org/10.1016/j.ijbiomac.2017.01.095>.
- Eljarrat, E. & Barceló, D. 2003. Priority lists for persistent organic pollutants and emerging contaminants based on their relative toxic potency in environmental samples. *TrAC -*

Trends in Analytical Chemistry, 22(10): 655–665.

- Emamjomeh, M.M. & Sivakumar, M. 2009. Review of pollutants removed by electrocoagulation and electrocoagulation/flotation processes. *Journal of Environmental Management*, 90(5): 1663–1679. <http://dx.doi.org/10.1016/j.jenvman.2008.12.011>.
- Encinar, J.M., González, J.F. & Rodríguez-Reinares, A. 2007. Ethanolysis of used frying oil. Biodiesel preparation and characterization. *Fuel Processing Technology*, 88(5): 513–522.
- Enweremadu, C.C. & Mbarawa, M.M. 2009. Technical aspects of production and analysis of biodiesel from used cooking oil-A review. *Renewable and Sustainable Energy Reviews*, 13(9): 2205–2224.
- Fajardo, A.S., Seca, H.F., Martins, R.C., Corceiro, V.N., Freitas, I.F., Quinta-Ferreira, M.E. & Quinta-Ferreira, R.M. 2017. Electrochemical oxidation of phenolic wastewaters using a batch-stirred reactor with NaCl electrolyte and Ti/RuO₂anodes. *Journal of Electroanalytical Chemistry*, 785: 180–189. <http://dx.doi.org/10.1016/j.jelechem.2016.12.033>.
- Faried, M., Samer, M., Abdelsalam, E., Yousef, R.S., Attia, Y.A. & Ali, A.S. 2017. Biodiesel production from microalgae: Processes, technologies and recent advancements. *Renewable and Sustainable Energy Reviews*, 79(May): 893–913. <http://dx.doi.org/10.1016/j.rser.2017.05.199>.
- Fazal, M.A., Haseeb, A.S.M.A. & Masjuki, H.H. 2011. Biodiesel feasibility study: An evaluation of material compatibility; Performance; emission and engine durability. *Renewable and Sustainable Energy Reviews*, 15(2): 1314–1324. <http://dx.doi.org/10.1016/j.rser.2010.10.004>.
- Ferrero, G.O., Almeida, M.F., Alvim-Ferraz, M.C.M. & Dias, J.M. 2014. Water-free process for eco-friendly purification of biodiesel obtained using a heterogeneous Ca-based catalyst. *Fuel Processing Technology*, 121: 114–118. <http://dx.doi.org/10.1016/j.fuproc.2014.01.020>.
- Foley, T., Thornton, K., Hinrichs-rahlfes, R., Sawyer, S., Sander, M., Taylor, R., Teske, S., Lehmann, H., Alers, M. & Hales, D. 2015. *REN21. 2015. Renewables 2015 Global Status Report*.
- Garcia-Segura, S. & Brillas, E. 2011. Mineralization of the recalcitrant oxalic and oxamic acids by electrochemical advanced oxidation processes using a boron-doped diamond anode. *Water Research*, 45(9): 2975–2984. <http://dx.doi.org/10.1016/j.watres.2011.03.017>.

- Garcia-Segura, S., Ocon, J.D. & Chong, M.N. 2018. Electrochemical oxidation remediation of real wastewater effluents — A review. *Process Safety and Environmental Protection*, 113: 48–67. <https://doi.org/10.1016/j.psep.2017.09.014>.
- Gokila, S., Gomathi, T., Sudha, P.N. & Anil, S. 2017. Removal of the heavy metal ion chromium(VI) using Chitosan and Alginate nanocomposites. *International Journal of Biological Macromolecules*, 104: 1459–1468. <http://dx.doi.org/10.1016/j.ijbiomac.2017.05.117>.
- Gold, V. 2014. Isotopomer. *IUPAC Compendium of Chemical Terminology*: 1670. <http://goldbook.iupac.org/PDF/goldbook.pdf%5Cnhttp://goldbook.iupac.org/I03352.html>.
- Gomes, M.C.S., Pereira, N.C. & Barros, S.T.D. de. 2010. Separation of biodiesel and glycerol using ceramic membranes. *Journal of Membrane Science*, 352(1–2): 271–276.
- Gorjian, S. & Ghobadian, B. 2015. Solar desalination: A sustainable solution to water crisis in Iran. *Renewable and Sustainable Energy Reviews*, 48: 571–584. <http://dx.doi.org/10.1016/j.rser.2015.04.009>.
- Government, W.C. 2014. Province of Western Cape Provincial Gazette. , 7227(February).
- Guibal, E., Van Vooren, M., Dempsey, B.A. & Roussy, J. 2006. A review of the use of chitosan for the removal of particulate and dissolved contaminants. *Separation Science and Technology*, 41(11): 2487–2514.
- Habibullah, M., Masjuki, H.H., Kalam, M.A., Rizwanul Fattah, I.M., Ashraful, A.M. & Mobarak, H.M. 2014. Biodiesel production and performance evaluation of coconut, palm and their combined blend with diesel in a single-cylinder diesel engine. *Energy Conversion and Management*, 87: 250–257. <http://dx.doi.org/10.1016/j.enconman.2014.07.006>.
- Harding, G., Courtney, C. & Russo, V. 2017. When geography matters. A location-adjusted blue water footprint of commercial beef in South Africa. *Journal of Cleaner Production*, 151: 494–508. <http://dx.doi.org/10.1016/j.jclepro.2017.03.076>.
- Haseeb, A.S.M.A., Fazal, M.A., Jahirul, M.I. & Masjuki, H.H. 2011. Compatibility of automotive materials in biodiesel: A review. *Fuel*, 90(3): 922–931. <http://dx.doi.org/10.1016/j.fuel.2010.10.042>.
- Huang, C.A., Yang, S.W., Chen, C.Z. & Hsu, F.-Y. 2017. Electrochemical behavior of IrO₂-Ta₂

- O 5 /Ti anodes prepared with different surface pretreatments of Ti substrate. *Surface and Coatings Technology*, 320: 270–278.
<http://linkinghub.elsevier.com/retrieve/pii/S0257897217300051>.
- Huaping, Z.H.U., Zongbin, W.U., Yuanxiong, C., Ping, Z., Shijie, D. & Xiaohua, L.I.U. 2006. Preparation of Biodiesel Catalyzed by Solid Super Base of Calcium Oxide and Its Refining Process. , 27(5): 391–396.
- Ilemobade, A.A., Adewumi, J.R. & Van Zyl, J.E. 2009. Framework for assessing the viability of implementing dual water reticulation systems in South Africa. *Water SA*, 35(2): 216–227.
- Israilides, C., Vlyssides, A., Mourafeti, V. & Karvouni, G. 1997. Olive oil wastewater treatment with the use of an electrolysis system. *Bioresource Technology*, 61(2): 163–170.
<http://www.sciencedirect.com/science/article/pii/S0960852497000230>.
- Ito, T., Sakurai, Y., Kakuta, Y., Sugano, M. & Hirano, K. 2012. Biodiesel production from waste animal fats using pyrolysis method. *Fuel Processing Technology*, 94(1): 47–52.
<http://dx.doi.org/10.1016/j.fuproc.2011.10.004>.
- Jacobson, K., Gopinath, R., Meher, L.C. & Dalai, A.K. 2008. Solid acid catalyzed biodiesel production from waste cooking oil. *Applied Catalysis B: Environmental*, 85(1–2): 86–91.
- Jaruwat, P., Kongjao, S. & Hunsom, M. 2010. Management of biodiesel wastewater by the combined processes of chemical recovery and electrochemical treatment. *Energy Conversion and Management*, 51(3): 531–537.
<http://dx.doi.org/10.1016/j.enconman.2009.10.018>.
- Kamm, B., Gruber, P.R. & Kamm, M. 2012. Biorefineries – Industrial Processes and Products. *Encyclopedia of Industrial Chemistry*. 659–683.
- Khandegar, V. & Saroha, A.K. 2013. Electrocoagulation for the treatment of textile industry effluent - A review. *Journal of Environmental Management*, 128: 949–963.
<http://dx.doi.org/10.1016/j.jenvman.2013.06.043>.
- Kilislioglu, A. & Bilgin, B. 2003. Thermodynamic and kinetic investigations of uranium adsorption on amberlite IR-118H resin. *Applied Radiation and Isotopes*, 58(2): 155–160.
- Kim, H.R., Jang, J.W. & Park, J.W. 2016. Carboxymethyl chitosan-modified magnetic-cored dendrimer as an amphoteric adsorbent. *Journal of Hazardous Materials*, 317: 108–116.

<http://dx.doi.org/10.1016/j.jhazmat.2016.06.025>.

Kouzu, M. & Hidaka, J.S. 2013. Purification to remove leached CaO catalyst from biodiesel with the help of cation-exchange resin. *Fuel*, 105: 318–324.

<http://dx.doi.org/10.1016/j.fuel.2012.06.019>.

Kumjadpai, S., Ngamlerdpokin, K., Chatanon, P., Lertsathitphongs, P. & Hunsom, M. 2011. Management of fatty acid methyl ester (fame) wastewater by a combined two stage chemical recovery and coagulation process. *Canadian Journal of Chemical Engineering*, 89(2): 369–376.

Kyzas, G.Z. & Bikiaris, D.N. 2015. Recent modifications of chitosan for adsorption applications: A critical and systematic review. *Marine Drugs*, 13(1): 312–337.

Laus, R., Costa, T.G., Szpoganicz, B. & Fávere, V.T. 2010. Adsorption and desorption of Cu(II), Cd(II) and Pb(II) ions using chitosan crosslinked with epichlorohydrin-triphosphate as the adsorbent. *Journal of Hazardous Materials*, 183(1–3): 233–241.

Leadbeater, N.E. & Stencel, L.M. 2006. Fast, easy preparation of biodiesel using microwave heating. *Energy and Fuels*, 20(5): 2281–2283.

Li, J., Wu, J., Sun, H., Cheng, F. & Liu, Y. 2016. Advanced treatment of biologically treated coking wastewater by membrane distillation coupled with pre-coagulation. *Desalination*, 380: 43–51. <http://www.sciencedirect.com/science/article/pii/S0011916415301223> 7 December 2015.

Li, Y., Bland, G.D. & Yan, W. 2016. Enhanced arsenite removal through surface-catalyzed oxidative coagulation treatment. *Chemosphere*, 150: 650–658.
<http://linkinghub.elsevier.com/retrieve/pii/S0045653516301576>.

Liu, Y. 2006. Some consideration on the Langmuir isotherm equation. *Colloids and Surfaces A: Physicochemical and Engineering Aspects*, 274(1–3): 34–36.

Liu, Y.-H., Lin, C.-Y., Huang, J.-H. & Yen, S.-C. 2016. Particle removal performance and its kinetic behavior during oxide-CMP wastewater treatment by electrocoagulation. *Journal of the Taiwan Institute of Chemical Engineers*, 60: 520–524.
<http://linkinghub.elsevier.com/retrieve/pii/S1876107015005295>.

Lobo, F.L., Wang, H., Huggins, T., Rosenblum, J., Linden, K.G. & Ren, Z.J. 2016. Low-energy

Hydraulic Fracturing Wastewater Treatment via AC Powered Electrocoagulation with Biochar. *Journal of Hazardous Materials*, 309: 180–184.
<http://www.sciencedirect.com/science/article/pii/S0304389416301327>.

- Ltaïef, A.H., D'Angelo, A., Ammar, S., Gadri, A., Galia, A. & Scialdone, O. 2017. Electrochemical treatment of aqueous solutions of catechol by various electrochemical advanced oxidation processes: Effect of the process and of operating parameters. *Journal of Electroanalytical Chemistry*, 796(February): 1–8. <http://dx.doi.org/10.1016/j.jelechem.2017.04.033>.
- Ma, F. & Hanna, M. a. 1999. Biodiesel production: a review1Journal Series #12109, Agricultural Research Division, Institute of Agriculture and Natural Resources, University of Nebraska–Lincoln.1. *Bioresource Technology*, 70(1): 1–15.
- Martínez-Huitle, C.A., De Battisti, A., Ferro, S., Reyna, S., Cerro-López, M. & Quiro, M.A. 2008. Removal of the Pesticide Methamidophos from Aqueous Solutions by Electrooxidation using Pb/PbO₂, Ti/SnO₂, and Si/BDD Electrodes. *Environmental Science & Technology*, 42(18): 6929–6935. <http://pubs.acs.org/doi/abs/10.1021/es8008419>.
- Martínez-Huitle, C.A. & Ferro, S. 2006. Electrochemical oxidation of organic pollutants for the wastewater treatment: direct and indirect processes. *Chem. Soc. Rev.*, 35(12): 1324–1340. <http://xlink.rsc.org/?DOI=B517632H>.
- Masum, B.M., Masjuki, H.H., Kalam, M.A., Rizwanul Fattah, I.M., M Palash, S. & Abedin, M.J. 2013. Effect of ethanol-gasoline blend on NO_x emission in SI engine. *Renewable and Sustainable Energy Reviews*, 24: 209–222. <http://dx.doi.org/10.1016/j.rser.2013.03.046>.
- Mckenzie, R., Sigalaba, Z. & Wegelin, W. 2012. *The State of Non-Revenue Water in South Africa (2012)*.
- Meher, L.C., Kulkarni, M.G., Dalai, A.K. & Naik, S.N. 2006. Transesterification of karanja (*Pongamia pinnata*) oil by solid basic catalysts. In *European Journal of Lipid Science and Technology*. 389–397.
- Mohammad, A.M., Salah Eldin, T.A., Hassan, M.A. & El-Anadouli, B.E. 2017. Efficient treatment of lead-containing wastewater by hydroxyapatite/chitosan nanostructures. *Arabian Journal of Chemistry*, 10(5): 683–690. <http://dx.doi.org/10.1016/j.arabjc.2014.12.016>.
- Mootabadi, H., Salamatinia, B., Bhatia, S. & Abdullah, A.Z. 2010. Ultrasonic-assisted biodiesel production process from palm oil using alkaline earth metal oxides as the heterogeneous

- catalysts. *Fuel*, 89(8): 1818–1825. <http://dx.doi.org/10.1016/j.fuel.2009.12.023>.
- Moreira, F.C., Boaventura, R.A.R., Brillas, E. & Vilar, V.J.P. 2017. Electrochemical advanced oxidation processes: A review on their application to synthetic and real wastewaters. *Applied Catalysis B: Environmental*, 202: 217–261. <http://dx.doi.org/10.1016/j.apcatb.2016.08.037>.
- Muxika, A., Etxabide, A., Uranga, J., Guerrero, P. & de la Caba, K. 2017. Chitosan as a bioactive polymer: Processing, properties and applications. *International Journal of Biological Macromolecules*, 105: 1358–1368. <https://doi.org/10.1016/j.ijbiomac.2017.07.087>.
- Ngamlerdpokin, K., Kumjadpai, S., Chatanon, P., Tungmanee, U., Chuenchuanom, S., Jaruwat, P., Lertsathitphongs, P. & Hunsom, M. 2011. Remediation of biodiesel wastewater by chemical- and electro-coagulation: A comparative study. *Journal of Environmental Management*, 92(10): 2454–2460. <http://dx.doi.org/10.1016/j.jenvman.2011.05.006>.
- Nkhonjera, G.K. 2017. Understanding the impact of climate change on the dwindling water resources of South Africa, focusing mainly on Olifants River basin: A review. *Environmental Science and Policy*, 71: 19–29. <http://dx.doi.org/10.1016/j.envsci.2017.02.004>.
- OZCAN, A., OZCAN, A., TUNALI, S., AKAR, T. & KIRAN, I. 2005. Determination of the equilibrium, kinetic and thermodynamic parameters of adsorption of copper(II) ions onto seeds of. *Journal of Hazardous Materials*, 124(1–3): 200–208. <http://linkinghub.elsevier.com/retrieve/pii/S0304389405002220>.
- Özcan, A.S., Erdem, B. & Özcan, A. 2004. Adsorption of Acid Blue 193 from aqueous solutions onto Na – bentonite and DTMA – bentonite. , 280: 44–54.
- Palomino Romero, J.A., Cardoso Junior, F.S.S., Figueiredo, R.T., Silva, D.P. & Cavalcanti, E.B. 2013. Treatment of Biodiesel Wastewater by Combined Electroflotation and Electrooxidation Processes. *Separation Science and Technology (Philadelphia)*, 48(13): 2073–2079. <http://www.tandfonline.com/doi/abs/10.1080/01496395.2013.779712> 17 January 2018.
- Panizza, M. & Cerisola, G. 2009. Direct And Mediated Anodic Oxidation of Organic Pollutants. *Chemical Reviews*, 109(12): 6541–6569.
- Panizza, M., Michaud, P.A., Cerisola, G. & Comninellis, C. 2001. Anodic oxidation of 2-naphthol

- at boron-doped diamond electrodes. *Journal of Electroanalytical Chemistry*, 507(1–2): 206–214. <http://linkinghub.elsevier.com/retrieve/pii/S0022072801003989>.
- Pitakpoolsil, W. & Hunsom, M. 2013. Adsorption of pollutants from biodiesel wastewater using chitosan flakes. *Journal of the Taiwan Institute of Chemical Engineers*, 44(6): 963–971. <http://dx.doi.org/10.1016/j.jtice.2013.02.009>.
- Pitakpoolsil, W. & Hunsom, M. 2014. Treatment of biodiesel wastewater by adsorption with commercial chitosan flakes: Parameter optimization and process kinetics. *Journal of Environmental Management*, 133: 284–292. <http://dx.doi.org/10.1016/j.jenvman.2013.12.019>.
- Rajkumar, D., Kim, J.G. & Palanivelu, K. 2005. Indirect electrochemical oxidation of phenol in the presence of chloride for wastewater treatment. *Chemical Engineering and Technology*, 28(1): 98–105.
- Rajkumar, D. & Palanivelu, K. 2004. Electrochemical treatment of industrial wastewater. *Journal of Hazardous Materials*, 113(1–3): 123–129.
- Rashed, M.N. 2013. Adsorption Technique for the Removal of Organic Pollutants from Water and Wastewater. *Organic Pollutants - Monitoring, Risk and Treatment*: 167–194.
- Rattanapan, C., Sawain, A., Suksaroj, T. & Suksaroj, C. 2011. Enhanced efficiency of dissolved air flotation for biodiesel wastewater treatment by acidification and coagulation processes. *Desalination*, 280(1–3): 370–377. <http://dx.doi.org/10.1016/j.desal.2011.07.018>.
- Renault, F., Sancey, B., Badot, P.M. & Crini, G. 2009. Chitosan for coagulation/flocculation processes - An eco-friendly approach. *European Polymer Journal*, 45(5): 1337–1348. <http://dx.doi.org/10.1016/j.eurpolymj.2008.12.027>.
- Riccardo A. A. Muzzarelli. 1983. Chitin and Its Derivatives: New Trends of Applied Research. *Carbohydrate Polymers*, 3: 53–75.
- Rodriguez Boluarte, I.A., Andersen, M., Pramanik, B.K., Chang, C.-Y., Bagshaw, S., Farago, L., Jegatheesan, V. & Shu, L. 2016. Reuse of car wash wastewater by chemical coagulation and membrane bioreactor treatment processes. *International Biodeterioration & Biodegradation*: 1–5. <http://linkinghub.elsevier.com/retrieve/pii/S0964830516300178>.
- Ruhsing Pan, J., Huang, C., Chen, S. & Chung, Y.C. 1999. Evaluation of a modified chitosan

- biopolymer for coagulation of colloidal particles. *Colloids and Surfaces A: Physicochemical and Engineering Aspects*, 147(3): 359–364.
- Sakkayawong, N., Thiravetyan, P. & Nakbanpote, W. 2005. Adsorption mechanism of synthetic reactive dye wastewater by chitosan. *Journal of Colloid and Interface Science*, 286(1): 36–42.
- Santos, M.R.G., Goulart, M.O.F., Tonholo, J. & Zanta, C.L.P.S. 2006. The application of electrochemical technology to the remediation of oily wastewater. *Chemosphere*, 64(3): 393–399.
- Saraswathi, R. & Saseetharan, M.K. 2012. Simultaneous optimization of multiple performance characteristics in coagulation-flocculation process for Indian paper industry wastewater. *Water Science and Technology*, 66(6): 1231–1238.
- Scialdone, O., Galia, A. & Randazzo, S. 2011. Oxidation of carboxylic acids in water at IrO₂-Ta₂O₅ and boron doped diamond anodes. *Chemical Engineering Journal*, 174(1): 266–274. <http://dx.doi.org/10.1016/j.cej.2011.09.016>.
- Scialdone, O., Randazzo, S., Galia, A. & Filardo, G. 2009. Electrochimica Acta Electrochemical oxidation of organics at metal oxide electrodes : The incineration of oxalic acid at IrO₂ – Ta₂O₅ (DSA-O₂) anode. , 54: 1210–1217.
- Se-Kwon Kim. 2011. *Chitin, Chitosan, Oligosaccharides and Their Derivatives: Biological Activities and Applications*.
- Shajahan, A., Shankar, S., Sathiyaseelan, A., Narayan, K.S., Narayanan, V., Kaviyaran, V. & Ignacimuthu, S. 2017. Comparative studies of chitosan and its nanoparticles for the adsorption efficiency of various dyes. *International Journal of Biological Macromolecules*, 104: 1449–1458. <http://dx.doi.org/10.1016/j.ijbiomac.2017.05.128>.
- Sharma, N.K. & Philip, L. 2016. Combined biological and photocatalytic treatment of real coke oven wastewater. *Chemical Engineering Journal*, 295: 20–28. <http://www.sciencedirect.com/science/article/pii/S1385894716302613> 2 April 2016.
- Shibasaki-Kitakawa, N., Kanagawa, K., Nakashima, K. & Yonemoto, T. 2013. Simultaneous production of high quality biodiesel and glycerin from Jatropha oil using ion-exchange resins as catalysts and adsorbent. *Bioresource Technology*, 142: 732–736. <http://dx.doi.org/10.1016/j.biortech.2013.05.111>.

- Shiklomanov, I. 1993. World fresh water resources. *Water in crisis a guide to the world's fresh water resources*: 13–24.
- Siebrits, R. & Fundikwa, B. 2017. *Market Intelligence Report*.
- Siles, J.A., Gutiérrez, M.C., Martín, M.A. & Martín, A. 2011. Physical-chemical and biomethanization treatments of wastewater from biodiesel manufacturing. *Bioresource technology*, 102(10): 6348–51.
<http://www.sciencedirect.com/science/article/pii/S0960852411003129> 2 April 2016.
- Siles, J.A., Martín, M.A., Chica, A.F. & Martín, A. 2010. Anaerobic co-digestion of glycerol and wastewater derived from biodiesel manufacturing. *Bioresource Technology*, 101(16): 6315–6321. <http://dx.doi.org/10.1016/j.biortech.2010.03.042>.
- Silitonga, A.S., Masjuki, H.H., Mahlia, T.M.I., Ong, H.C., Chong, W.T. & Boosroh, M.H. 2013. Overview properties of biodiesel diesel blends from edible and non-edible feedstock. *Renewable and Sustainable Energy Reviews*, 22: 346–360.
- Simasatitkul, L., Gani, R. & Arpornwichanop, A. 2012. Optimal Design of Biodiesel Production Process from Waste Cooking Palm Oil. *Procedia Engineering*, 42(August): 1292–1301.
<http://linkinghub.elsevier.com/retrieve/pii/S1877705812029281>.
- Soares, S.F., Rodrigues, M.I., Trindade, T. & Daniel-da-Silva, A.L. 2017. Chitosan-silica hybrid nanosorbents for oil removal from water. *Colloids and Surfaces A: Physicochemical and Engineering Aspects*, 532(April): 305–313.
- Sokker, H.H., El-Sawy, N.M., Hassan, M.A. & El-Anadouli, B.E. 2011. Adsorption of crude oil from aqueous solution by hydrogel of chitosan based polyacrylamide prepared by radiation induced graft polymerization. *Journal of Hazardous Materials*, 190(1–3): 359–365.
<http://dx.doi.org/10.1016/j.jhazmat.2011.03.055>.
- von Sperling, M. 2008. *Basic principles of wastewater treatment*. London: IWA Publishing.
<http://www.cro3.org/cgi/doi/10.5860/CHOICE.45-2632>.
- Stavarache, C., Vinatoru, M., Nishimura, R. & Maeda, Y. 2003. Conversion of Vegetable Oil to Biodiesel Using Ultrasonic Irradiation. *Chemistry Letters*, 32(8): 716–717.
<http://www.journal.csj.jp/doi/10.1246/cl.2003.716>.
- Stojković, I.J., Stamenković, O.S., Povrenović, D.S. & Veljković, V.B. 2014. Purification

- technologies for crude biodiesel obtained by alkali-catalyzed transesterification. *Renewable and Sustainable Energy Reviews*, 32: 1–15.
- Stromer, B.S., Woodbury, B. & Williams, C.F. 2018. Tylosin sorption to diatomaceous earth described by Langmuir isotherm and Freundlich isotherm models. *Chemosphere*, 193: 912–920. <https://doi.org/10.1016/j.chemosphere.2017.11.083>.
- Subedi, B. & Kannan, K. 2015. Occurrence and fate of select psychoactive pharmaceuticals and antihypertensives in two wastewater treatment plants in New York State, USA. *Science of the Total Environment*, 514: 273–280. <http://dx.doi.org/10.1016/j.scitotenv.2015.01.098>.
- Suehara, K., Kawamoto, Y., Fujii, E., Kohda, J., Nakano, Y. & Yano, T. 2005a. Biological treatment of wastewater discharged from biodiesel fuel production plant with alkali-catalyzed transesterification. *Journal of bioscience and bioengineering*, 100(4): 437–442.
- Suehara, K., Kawamoto, Y., Fujii, E., Kohda, J., Nakano, Y. & Yano, T. 2005b. Biological treatment of wastewater discharged from biodiesel fuel production plant with alkali-catalyzed transesterification. *Journal of bioscience and bioengineering*, 100(4): 437–42. <http://www.ncbi.nlm.nih.gov/pubmed/16310734> 1 April 2016.
- Sundus, F., Fazal, M.A. & Masjuki, H.H. 2017. Tribology with biodiesel : A study on enhancing biodiesel stability and its fuel properties. *Renewable and Sustainable Energy Reviews*, 70(November 2016): 399–412. <http://dx.doi.org/10.1016/j.rser.2016.11.217>.
- Tan, K.T., Gui, M.M., Lee, K.T. & Mohamed, A.R. 2010. An optimized study of methanol and ethanol in supercritical alcohol technology for biodiesel production. *Journal of Supercritical Fluids*, 53(1–3): 82–87. <http://dx.doi.org/10.1016/j.supflu.2009.12.017>.
- Tchobanoglous, G., Burton, F. & Stensel, D. 2003. Metcalf & Eddy, Inc. Wastewater Engineering - Treatment and Reuse. : 1846.
- Thirugnanasambandham, K., Sivakumar, V., Prakash Maran, J. & Kandasamy, S. 2014. Chitosan based grey wastewater treatment-A statistical design approach. *Carbohydrate Polymers*, 99: 593–600. <http://dx.doi.org/10.1016/j.carbpol.2013.08.058>.
- Thopil, G.A. & Pouris, A. 2016. A 20 year forecast of water usage in electricity generation for South Africa amidst water scarce conditions. *Renewable and Sustainable Energy Reviews*, 62: 1106–1121. <http://dx.doi.org/10.1016/j.rser.2016.05.003>.

- Vázquez, I., Rodríguez-Iglesias, J., Marañón, E., Castrillón, L. & Álvarez, M. 2007. Removal of residual phenols from coke wastewater by adsorption. *Journal of Hazardous Materials*, 147(1–2): 395–400.
- Veljković, V.B., Stamenković, O.S. & Tasić, M.B. 2014. The wastewater treatment in the biodiesel production with alkali-catalyzed transesterification. *Renewable and Sustainable Energy Reviews*, 32: 40–60.
- Verlee, A., Mincke, S. & Stevens, C. V. 2017. Recent developments in antibacterial and antifungal chitosan and its derivatives. *Carbohydrate Polymers*, 164: 268–283.
<http://dx.doi.org/10.1016/j.carbpol.2017.02.001>.
- Vlyssides, A.G. & Israilides, C.J. 1997. Detoxification of tannery waste liquors with an electrolysis system. *Environmental Pollution*, 97(1–2): 147–152.
- Vogel, C. & Zyl, K. Van. 2016. Climate Change Adaptation Strategies – An Upstream-downstream Perspective. : 195–211. <http://link.springer.com/10.1007/978-3-319-40773-9>.
- Wang, Y., Feng, S., Bai, X., Zhao, J. & Xia, S. 2016. Scum sludge as a potential feedstock for biodiesel production from wastewater treatment plants. *Waste Management*, 47: 91–97.
<http://dx.doi.org/10.1016/j.wasman.2015.06.036>.
- Wang, Y., Ou, S., Liu, P., Xue, F. & Tang, S. 2006. Comparison of two different processes to synthesize biodiesel by waste cooking oil. *Journal of Molecular Catalysis A: Chemical*, 252(1–2): 107–112.
- Water Resources Group. 2009. Charting Our Water Future. *Water*, June(3): 1–32.
http://www.mckinsey.com/App_Media/Reports/Water/Charting_Our_Water_Future_Full_Report_001.pdf%5Cnhttp://scholar.google.com/scholar?hl=en&btnG=Search&q=intitle:Charting+Our+Water+Future#1%5Cnhttp://www.mckinsey.com/App_Media/Reports/Water/Charting_Our_Wate.
- Wong, K. 2006. Preparation and characterization of carbon molecular sieve produced from palm shell. <http://eprints.utm.my/5506/>.
- Worch, E. 2012. *Adsorption Technology in Water Treatment*.
- Wu, F.C., Tseng, R.L. & Juang, R.S. 2009. Initial behavior of intraparticle diffusion model used in the description of adsorption kinetics. *Chemical Engineering Journal*, 153(1–3): 1–8.

- Wu, W., Huang, Z.-H. & Lim, T.-T. 2014a. Recent development of mixed metal oxide anodes for electrochemical oxidation of organic pollutants in water. *Applied Catalysis A: General*, 480: 58–78. <http://linkinghub.elsevier.com/retrieve/pii/S0926860X14002890>.
- Wu, W., Huang, Z.-H. & Lim, T.-T. 2014b. Recent development of mixed metal oxide anodes for electrochemical oxidation of organic pollutants in water. *Applied Catalysis A: General*, 480(0): 58–78. http://www.sciencedirect.com/science/article/pii/S0926860X14002890%5Cnhttp://ac.els-cdn.com/S0926860X14002890/1-s2.0-S0926860X14002890-main.pdf?_tid=98ab5f78-6c77-11e5-ac42-0000aacb35e&acdnat=1444169842_7b3967ec2391e46d86ba8398339d2b5e.
- WWF-SA. 2016. *Water: facts and futures*. www.wwf.org.za.
- Xiang, Y., Xiang, Y. & Wang, L. 2017. Microwave radiation improves biodiesel yields from waste cooking oil in the presence of modified coal fly ash. *Journal of Taibah University for Science*, 11(6): 1019–1029. <http://linkinghub.elsevier.com/retrieve/pii/S1658365517300687>.
- Xu, X., Cheng, Y., Zhang, T., Ji, F. & Xu, X. 2016. Treatment of pharmaceutical wastewater using interior micro-electrolysis/Fenton oxidation-coagulation and biological degradation. *Chemosphere*, 152: 23–30. <http://www.sciencedirect.com/science/article/pii/S0045653516302624> 8 March 2016.
- Yaakob, Z., Mohammad, M., Alherbawi, M., Alam, Z. & Sopian, K. 2013. Overview of the production of biodiesel from Waste cooking oil. *Renewable and Sustainable Energy Reviews*, 18: 184–193. <http://dx.doi.org/10.1016/j.rser.2012.10.016>.
- Yan, Z., Zhao, Y., Zhang, Z., Li, G., Li, H., Wang, J., Feng, Z., Tang, M., Yuan, X., Zhang, R. & Du, Y. 2015. A study on the performance of IrO₂-Ta₂O₅ coated anodes with surface treated Ti substrates. *Electrochimica Acta*, 157: 345–350. <http://dx.doi.org/10.1016/j.electacta.2015.01.005>.
- Yang, R., Li, H., Huang, M., Li, A. & Yang, H. 2016. Chitosan-based flocculants and their applications in water treatment *. *Water Research*, 95(51378250): 59–89. <http://dx.doi.org/10.1016/j.watres.2016.02.068>.
- Zhai, L., Bai, Z., Zhu, Y., Wang, B. & Luo, W. 2017. Fabrication of chitosan microspheres for efficient adsorption of methyl orange. *Chinese Journal of Chemical Engineering*.

<http://linkinghub.elsevier.com/retrieve/pii/S1004954117302045>.

- Zhang, M.H., Zhao, Q.L., Bai, X. & Ye, Z.F. 2010. Adsorption of organic pollutants from coking wastewater by activated coke. *Colloids and Surfaces A: Physicochemical and Engineering Aspects*, 362(1–3): 140–146. <http://dx.doi.org/10.1016/j.colsurfa.2010.04.007>.
- Zhou, M., Särkkä, H. & Sillanpää, M. 2011. A comparative experimental study on methyl orange degradation by electrochemical oxidation on BDD and MMO electrodes. *Separation and Purification Technology*, 78(3): 290–297. <http://dx.doi.org/10.1016/j.seppur.2011.02.013>.
- Zongo, I., Maiga, A.H., Wéthé, J., Valentin, G., Leclerc, J.P., Paternotte, G. & Lapique, F. 2009. Electrocoagulation for the treatment of textile wastewaters with Al or Fe electrodes: Compared variations of COD levels, turbidity and absorbance. *Journal of Hazardous Materials*, 169(1–3): 70–76.
- Zou, J., Peng, X., Li, M., Xiong, Y., Wang, B., Dong, F. & Wang, B. 2017. Electrochemical oxidation of COD from real textile wastewaters: Kinetic study and energy consumption. *Chemosphere*, 171: 332–338. <http://dx.doi.org/10.1016/j.chemosphere.2016.12.065>.

APPENDICES

Appendix A

City of Cape Town: Wastewater and Industrial Effluent By law, 2013

Section A: General		Not less than	Not to exceed
1	Temperature at point of entry	0	40
2	Electrical conductivity at 25°C		500
3	pH Value at 25°C	5.5	12
4	Chemical Oxygen Demand		5000

Section B: Chemical substances other than heavy metals - maximum concentrations		
1	Settleable solids (60 minutes)	50 ml/l
2	Suspended solids	1000 mg/l
3	Total dissolved solids at 105 °C	4000 mg/l
4	Chloride as Cl	1500 mg/l
5	Total sulphates as SO ₄	1500 mg/l
6	Total phosphates as P	25 mg/l
7	Total cyanides as CN	20 mg/l
8	Total Sulphides as S	50 mg/l
9	Phenol Index	50 mg/l
10	Total sugars and starches as glucose	1500 mg/l
11	Oils, greases, waxes and fat	400 mg/l
12	Sodium as Na	1000 mg/l

Section C: Metals and inorganic content - maximum concentrations Group 1		
1	Total Iron as Fe	50 mg/l
2	Total chromium as Cr	10 mg/l
3	Total copper as Cu	20 mg/l
4	Total zinc as Zn	30 mg/l
Total collective concentration of all metals in Group 1 shall not exceed 50 mg/l		

Section C: Metals and inorganic content - maximum concentrations Group 2		
5	Total arsenic as As	5 mg/l
6	Total boron as B	5 mg/l
7	Total lead as Pb	5 mg/l
8	Total selenium as Se	5 mg/l
9	Total mercury as Hg	5 mg/l
10	Total titanium as Ti	5 mg/l
11	Total cadmium as Cd	5 mg/l
12	Total nickel as Ni	5 mg/l

Reference: (City of Cape Town, 2013)

Appendix B

Data from initial electrochemical oxidation experiments: Instantaneous current efficiency.

The effect of **current density** on the instantaneous current efficiency, at the following experimental conditions.

Experimental parameters

Volume of reactor,	1L
Temperature of solution,	60°C
NaCl concentration,	0.08 M
Current Density,	1 - 4 mA/cm²
Time,	24 hrs.

Table B 1: Results from experiment A.

Experiment	Current density (mA/cm ²)	Time (hrs.)	NaCl (M)
A	1	24	0

Parameter	Units	Experiment A							
		Initial	2	4	6	8	10	12	24
Time	hrs.								
Salinity	g/l	1.3	0.9	1.1	1.1	1.0	1.1	1.1	1.1
EC	mS/cm	2.2	1.9	1.9	1.9	1.8	1.9	1.9	2.0
TDS	g/l	1.5	1.3	1.3	1.2	1.2	1.2	1.2	1.3
Turbidity	NTU	23.5	15.7	11.8	12.3	8.8	4.0	2.8	0.9
pH		2.7	1.5	1.3	1.4	1.5	1.5	1.1	1.4
COD	g/L	87.9	79.3	72.3	69.1	67.5	64.4	60.3	54.6
COD Rem	%	0	9.8	17.7	21.4	23.2	26.8	31.4	37.9
ICE	(%)	0	3.3	3.0	2.4	1.9	1.8	1.8	1.1

Table B 2: Results from experiment B.

Experiment	Current density (mA/cm ²)	Time (hrs.)	NaCl (M)
B	2	24	0

Parameter	Units	Experiment B							
		Initial	2	4	6	8	10	12	24
Time	hrs.								
Salinity	g/l	1.3	0.7	1.2	1.1	1.2	1.1	1.2	1.3
EC	mS/cm	2.2	1.2	2.0	2.0	2.1	2.0	2.1	2.4
TDS	g/l	1.5	0.9	1.3	1.3	1.4	1.3	1.4	1.5
Turbidity	NTU	23.5	10.1	8.1	2.8	4.6	3.2	1.8	0.6
pH		2.7	1.3	1.4	1.3	1.4	1.3	1.2	1.0
COD	g/L	50.0	41.1	43.2	44.1	44.1	43.8	41.7	39.3
COD Rem	%	0.0	17.7	13.5	11.9	11.8	12.3	16.6	21.5
ICE	(%)	0.0	1.7	0.6	0.4	0.3	0.2	0.3	0.2

Table B 3: Results from experiment C.

Experiment	Current density (mA/cm ²)	Time (hrs.)	NaCl (M)
C	4	24	0

Parameter	Units	Experiment C							
		Initial	2	4	6	8	10	12	24
Time	hrs.								
Salinity	g/l	1.4	1.5	1.4	1.4	1.4	1.4	1.4	1.4
EC	mS/cm	2.4	2.6	2.6	2.5	2.5	2.4	2.4	2.6
TDS	g/l	1.6	1.7	1.7	1.6	1.6	1.6	1.6	1.6
Turbidity	NTU	15.3	8.3	5.7	9.0	4.3	3.3	1.2	1.1
pH		1.9	1.4	1.4	1.4	1.6	1.4	1.4	1.4
COD	g/L	50.1	47.2	45.7	44.3	42.2	41.3	38.7	35.4
COD Rem	%	0.0	5.7	8.9	11.6	15.8	17.6	22.8	29.4
ICE	(%)	0.0	0.3	0.2	0.2	0.2	0.2	0.2	0.1

The effect of **NaCl concentration** on the instantaneous current efficiency, at the following experimental conditions.

Experimental parameters

Volume of reactor,	1L
Temperature of solution,	60°C
NaCl concentration,	0.02 – 0.1 M
Current Density,	1 mA/cm ²
Time,	24 hrs.

Table B 4: Results from experiment D.

Experiment	Current density (mA/cm ²)	Time (hrs.)	NaCl (M)
D	1	24	0.02

Parameter	Units	Experiment D							
		Initial	2	4	6	8	10	12	24
Time	hrs.								
Salinity	g/l	11.8	11.8	11.8	10.2	10.1	10.4	11.0	11.7
EC	mS/cm	18.6	18.6	18.6	16.2	16.3	16.9	17.3	18.4
TDS	g/l	12.1	12.6	11.3	10.5	10.4	10.9	11.5	12.0
Turbidity	NTU	45.4	35.4	30.2	28.4	25.2	1.3	1.0	0.9
pH		2.3	2.1	12.0	1.5	1.3	1.0	0.6	0.8
COD	g/L	48.7	47.5	44.2	42.1	43.8	35.1	34.2	31.0
COD Rem	%	0.0	2.5	9.2	13.5	10.1	27.9	29.8	36.3
ICE	(%)	0.0	5.3	9.9	9.4	15.0	11.7	10.3	6.3

Table B 5: Results from experiment E.

Experiment	Current density (mA/cm ²)	Time (hrs.)	NaCl (M)
E	1	24	0.04

Parameter	Units	Experiment E							
		Initial	2	4	6	8	10	12	24
Time	hrs.								
Salinity	g/l	13.1	10.1	9.0	8.3	8.2	8.2	8.2	9.1
EC	mS/cm	20.2	15.9	13.8	13.6	13.5	13.4	13.4	14.2
TDS	g/l	13.1	10.7	9.2	8.9	8.6	8.6	8.7	9.3
Turbidity	NTU	88.5	28.9	11.6	2.5	1.0	1.0	1.0	0.7
pH		2.6	2.3	2.0	1.5	1.3	1.3	1.4	1.4
COD	g/L	41.6	39.7	34.1	31.4	32.5	33.9	36.7	35.4
COD Rem	%	0.0	4.6	18.0	24.5	21.9	18.5	11.8	14.9
ICE	(%)	0	9.9	16.4	14.7	9.7	6.5	3.6	2.2

Table B 6: Results from experiment F.

Experiment	Current density (mA/cm ²)	Time (hrs.)	NaCl (M)
F	1	24	0.06

Parameter	Units	Experiment F							
		Initial	2	4	6	8	10	12	24
Time	hrs.								
Salinity	g/l	7.5	8.2	8.2	7.1	6.8	7.0	7.5	6.9
EC	mS/cm	14.0	13.3	9.3	11.7	11.2	11.4	11.9	11.3
TDS	g/l	9.2	8.7	7.2	7.3	7.3	7.4	7.8	7.4
Turbidity	NTU	20.6	3.2	3.1	4.1	1.2	0.6	0.8	0.5
pH		1.6	1.3	1.1	1.1	1.1	1.5	1.4	1.0
COD	g/L	47.3	43.1	43.1	44.7	41.6	41.5	39.2	40.7
COD Rem	%	0.0	8.9	8.9	5.5	12.1	12.3	17.1	14.0
ICE	(%)	0.0	18.4	9.3	3.8	6.0	4.9	5.7	2.3

Table B 7: Results from experiment G.

Experiment	Current density (mA/cm ²)	Time (hrs.)	NaCl (M)
G	1	24	0.08

Parameter	Units	Experiment G							
		Initial	2	4	6	8	10	12	24
Time	hrs.								
Salinity	g/l	4.2	4.2	4.0	3.8	4.0	3.7	3.7	3.9
EC	mS/cm	7.1	7.1	6.8	6.5	6.9	6.3	6.3	6.7
TDS	g/l	4.6	4.5	4.4	4.2	4.2	4.1	4.0	4.3
Turbidity	NTU	15.6	5.0	2.0	1.1	1.0	1.0	1.0	0.7
pH		1.6	1.4	1.0	1.5	1.5	1.5	1.3	1.4
COD	g/L	55.0	48.2	46.6	44.5	43.2	42.2	41.1	43.1
COD Rem	%	0.0	12.4	15.3	19.1	21.5	23.3	25.3	21.6
ICE	(%)	0.0	28.6	17.5	14.8	12.3	10.7	9.8	4.2

Table B 8: Results from experiment H.

Experiment	Current density (mA/cm ²)	Time (hrs.)	NaCl (M)
H	1	24	0.1

Parameter	Units	Experiment H							
		Initial	2	4	6	8	10	12	24
Time	hrs.								
Salinity	g/l	11.4	10.1	9.8	11.6	11.8	11.9	11.7	11.5
EC	mS/cm	18.0	15.7	15.8	16.8	19.1	19.8	18.2	18.4
TDS	g/l	11.6	10.3	10.2	11.4	13.1	12.1	12.0	11.7
Turbidity	NTU	94.8	28.3	10.6	6.1	2.8	1.9	1.4	3.0
pH		2.5	1.2	1.5	1.6	1.3	1.3	1.2	1.3
COD	g/L	55.3	47.1	45.9	47.1	43.1	44.1	37.2	37.1
COD Rem	%	0.0	14.8	17.0	14.8	22.1	20.3	32.7	32.9
ICE	(%)	0	26.3	14.6	5.8	4.9	4.4	6.9	5.9

Appendix C

Data from initial electrochemical oxidation experiments: Effect of current density and NaCl concentration of COD removal.

The effect of **current density** on the removal of COD, and other impurities, at the following experimental conditions.

Experimental parameters

Volume of reactor,	1L
Temperature of solution,	60°C
NaCl concentration,	0.08 M
Current Density,	0.5 - 4 mA/cm²
Time,	100 hrs.

Table C 1. 1: Results from experiment 1.1.

Experiment	Current Density	NaCl (M)
1.1	0.5	0.08

Parameter	Units	Experiment 1.1															
		0	2	4	6	8	10	12	24	26	28	30	32	34	36	48	50
Time	hrs.																
Salinity	g/l	1.5	2.0	2.2	2.3	2.4	2.3	2.1	2.2	2.4	2.5	2.5	2.4	2.5	2.6	2.5	2.7
EC	mS/cm	2.6	3.4	3.9	3.9	4.1	4.0	3.7	3.8	4.1	4.4	4.4	4.3	4.4	4.5	4.4	4.5
TDS	g/l	1.7	2.3	2.5	2.6	2.7	2.6	2.3	2.5	2.7	2.9	2.8	2.5	2.8	2.9	2.9	3.0
Turbidity	NTU	31.3	13.7	9.4	6.2	4.4	2.3	3.5	2.6	2.5	2.0	1.6	1.4	1.2	1.4	1.2	1.2
pH		1.9	1.2	1.2	1.0	1.1	1.0	1.2	1.5	1.0	1.2	1.0	1.1	1.2	1.1	1.2	1.2
COD Total	g/L	59.2	58.0	54.3	52.5	52.6	49.8	49.8	49.0	44.8	45.3	41.7	40.8	40.5	38.7	38.1	36.3
% COD Removal		0.0	2.0	8.4	11.3	11.1	16.0	15.9	17.3	24.3	23.5	29.6	31.2	31.7	34.6	35.7	38.7

Parameter	Units	Experiment 1.1														
		52	54	56	58	60	72	74	76	78	80	82	84	96	98	100
Time	hrs.															
Salinity	g/l	2.6	2.7	2.5	2.6	2.5	2.6	2.6	2.6	2.9	2.6	2.9	2.7	2.3	2.5	2.9
EC	mS/cm	4.6	4.5	4.3	4.4	4.3	4.5	5.0	4.7	4.7	4.8	5.0	4.6	4.0	4.3	5.0
TDS	g/l	2.9	2.9	3.1	2.9	2.8	2.9	3.2	3.0	3.2	3.2	3.2	3.0	2.6	2.8	3.3
Turbidity	NTU	1.0	1.8	1.1	1.0	1.1	1.4	1.3	2.2	1.6	1.8	1.4	1.3	1.3	1.0	2.4
pH		1.2	1.1	1.2	1.2	1.2	1.7	1.2	1.1	1.2	1.2	1.2	1.2	1.3	1.2	1.1
COD Total	g/L	34.4	29.3	28.2	30.3	24.3	23.2	22.7	22.6	25.6	25.7	25.7	23.4	20.7	19.9	19.7
% COD Removal		41.9	50.5	52.4	48.8	59.1	60.8	61.7	61.8	56.8	56.6	56.5	60.4	65.0	66.5	66.7

Table C 1. 2: Results from experiment 1.2

Parameter	Units	Experiment 1.2															
		0	2	4	6	8	10	12	24	26	28	30	32	34	36	48	50
Time	hrs.																
Salinity	g/l	4.2	4.3	4.0	3.8	3.9	3.7	3.8	3.8	4.0	4.2	4.1	4.1	3.2	3.8	3.7	4.0
EC	mS/cm	7.1	7.2	6.8	6.5	6.6	6.4	6.2	6.6	6.9	7.2	6.6	7.2	6.6	6.5	6.4	6.7
TDS	g/l	4.6	4.7	4.4	4.2	4.3	4.0	4.1	4.2	4.3	4.6	4.3	4.3	4.1	4.2	4.2	4.4
Turbidity	NTU	15.6	8.2	5.2	5.5	1.9	2.0	1.1	1.3	0.8	1.6	1.7	1.7	1.0	0.8	0.9	0.6
pH		1.6	1.1	1.1	1.2	1.1	1.2	1.3	1.6	1.3	1.3	1.0	0.9	1.0	1.3	1.3	1.2
COD Total	g/L	56.0	54.9	53.9	49.5	50.2	50.4	47.6	46.0	44.9	45.3	42.9	43.2	43.2	43.0	41.6	42.2
% COD Removal		0.0	1.9	3.7	11.6	10.4	10.0	14.9	17.8	19.8	19.1	23.4	22.8	22.9	23.2	25.7	24.7

Parameter	Units	Experiment 1.2														
		52	54	56	58	60	72	74	76	78	80	82	84	96	98	100
Time	hrs.															
Salinity	g/l	3.8	4.0	3.9	4.2	3.9	4.0	3.9	4.3	4.7	4.5	5.0	4.9	4.4	4.4	4.5
EC	mS/cm	6.8	6.7	6.6	6.7	6.7	6.8	6.7	7.3	7.8	7.6	8.0	7.8	7.9	7.6	7.8
TDS	g/l	4.2	4.4	4.1	4.5	4.3	4.3	4.4	4.5	5.1	5.0	5.3	5.3	5.2	5.2	5.2
Turbidity	NTU	0.8	0.6	0.8	0.7	0.7	1.4	0.7	2.0	1.8	0.9	0.7	0.7	0.7	0.5	0.5
pH		1.2	1.1	1.3	1.3	1.4	1.4	1.1	1.1	2.0	1.0	1.0	1.1	1.4	1.1	1.2
COD Total	g/L	44.5	43.3	39.3	36.6	32.3	23.3	23.0	23.1	23.0	23.1	23.5	21.8	19.0	19.8	19.3
% COD Removal		20.5	22.7	29.8	34.7	42.2	58.3	58.8	58.7	59.0	58.7	58.1	61.0	66.1	64.7	65.6

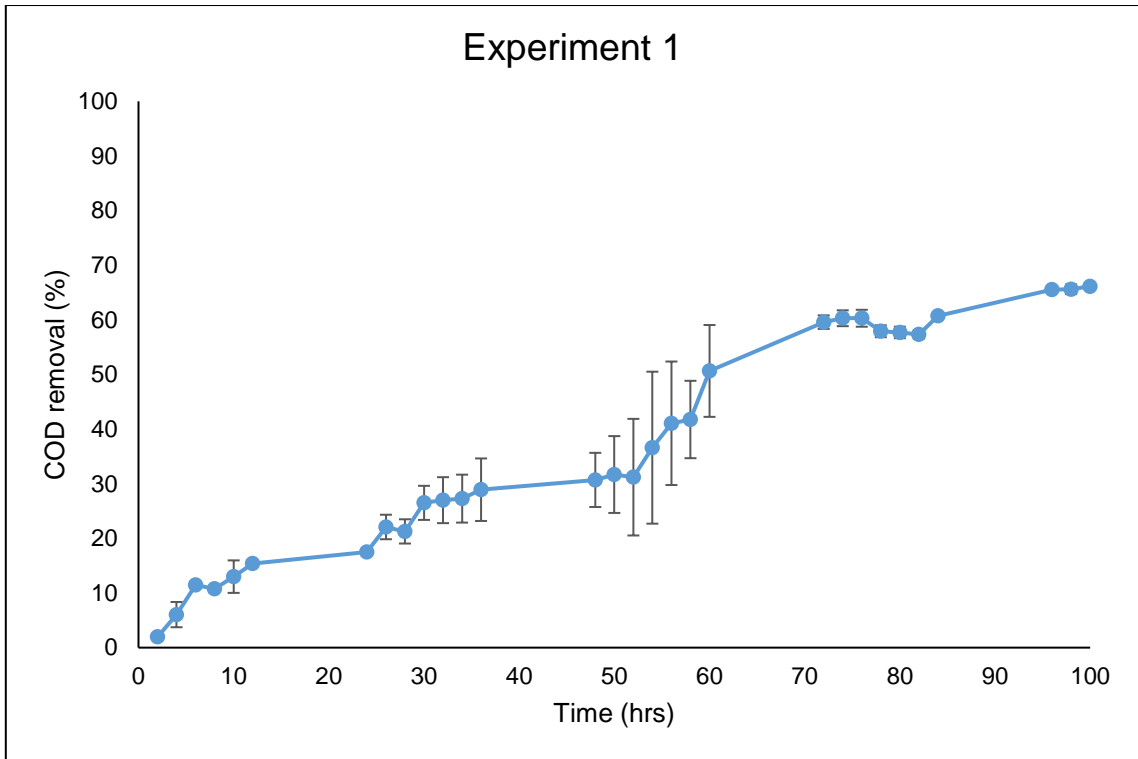


Figure C. 1: Average COD removal from experiment 1.1 and 1.2.:

Anova: Single Factor

SUMMARY

Groups	Count	Sum	Average	Variance
Experiment 1 .1 COD Removal	31	1196.94	38.6108	450.514
Experiment 1.2 COD Removal	31	1010.9	32.6098	469.921

ANOVA

Source of Variation	SS	df	MS	F	P-value	F crit
Between Groups	558.193	1	558.193	1.21289	0.27516	4.00119
Within Groups	27613.1	60	460.218			
Total	28171.3	61				

Table C 1. 3: Results from experiment 2.1

Experiment	Current Density	NaCl (M)
2.1	0.75	0.08

Parameter	Units	Experiment 2.1															
		0	2	4	6	8	10	12	24	26	28	30	32	34	36	48	50
Time	hrs.																
Salinity	g/l	6.0	4.6	4.7	4.5	4.5	4.2	4.1	4.1	4.1	4.2	4.5	4.6	4.8	4.5	4.5	4.6
EC	mS/cm	9.7	7.8	7.7	7.5	7.6	7.0	6.8	6.6	7.1	7.1	7.2	7.6	7.4	7.6	7.8	7.8
TDS	g/l	6.3	5.0	5.0	4.9	4.9	4.5	4.4	4.4	4.4	4.6	4.7	5.0	4.8	4.9	5.1	5.0
Turbidity	NTU	11.7	3.2	2.3	2.2	1.0	1.1	0.8	0.8	0.9	1.2	0.8	0.6	1.1	0.9	0.6	0.6
pH		1.0	0.5	0.4	0.6	0.7	0.7	0.6	0.6	0.6	1.3	1.2	1.0	1.1	1.3	1.3	1.4
COD Total	g/L	41.6	40.8	40.4	38.9	39.0	36.6	35.8	37.3	34.2	36.0	33.9	30.7	31.6	26.0	27.3	24.2
% COD Removal		0.0	2.0	2.8	6.5	6.2	12.0	14.0	10.2	17.7	13.5	18.4	26.2	23.9	37.6	34.3	41.8

Parameter	Units	Experiment 2.1														
		52	54	56	58	60	72	74	76	78	80	82	84	96	98	100
Time	hrs.															
Salinity	g/l	4.6	4.9	5.1	5.2	5.3	5.4	5.8	5.2	5.4	5.7	8.3	7.8	6.3	7.2	8.6
EC	mS/cm	7.7	8.2	8.2	8.8	8.3	8.2	2.2	8.8	9.1	9.5	10.8	10.4	10.4	11.1	14.5
TDS	g/l	5.0	5.3	5.3	5.6	5.2	5.6	7.1	5.8	5.8	6.4	7.7	6.9	6.8	7.5	8.3
Turbidity	NTU	0.4	0.7	0.6	0.6	0.5	0.8	0.7	0.7	0.7	0.5	1.3	1.1	0.5	1.1	0.5
pH		0.5	0.4	0.7	0.5	0.5	0.7	0.5	0.4	0.3	0.3	0.3	0.2	0.4	0.3	0.4
COD Total	g/L	23.5	25.6	25.5	25.4	22.2	22.0	21.7	21.5	20.8	21.0	19.9	16.7	14.2	13.0	12.8
% COD Removal		43.4	38.5	38.6	38.9	46.6	47.1	47.8	48.4	50.0	49.5	52.1	59.8	65.9	68.7	69.2

Table C 1. 4: Results from experiment 2.2

Parameter	Units	Experiment 2.2															
		0	2	4	6	8	10	12	24	26	28	30	32	34	36	48	50
Time	hrs.																
Salinity	g/l	5.6	5.5	5.1	5.8	5.2	5.4	6.2	5.2	4.8	5.5	6.3	6.1	6.0	5.9	8.1	10.5
EC	mS/cm	9.4	8.3	8.6	8.5	9.0	9.4	8.5	8.1	8.1	9.5	9.2	10.7	10.4	10.3	13.0	14.1
TDS	g/l	6.1	6.0	5.5	5.6	6.0	5.5	5.3	5.3	5.3	5.7	6.3	6.2	7.2	7.0	8.5	10.2
Turbidity	NTU	8.3	6.2	2.0	1.3	1.1	0.9	0.7	0.7	0.6	0.4	0.5	1.1	0.8	0.8	1.0	1.0
pH		0.7	0.7	0.6	0.2	0.2	0.3	0.2	0.3	0.5	0.3	0.5	0.5	13.1	0.2	0.2	0.5
COD Total	g/L	41.6	40.2	40.4	38.5	39.3	35.4	35.4	35.9	35.0	35.9	32.3	30.6	31.1	26.5	27.5	23.4
% COD Removal		0.0	3.7	3.2	7.7	5.7	15.2	15.2	14.0	16.1	14.0	22.4	26.6	25.3	36.5	34.2	43.8

Parameter	Units	Experiment 2.2														
		52	54	56	58	60	72	74	76	78	80	82	84	96	98	100
Time	hrs.															
Salinity	g/l	10.2	12.9	13.1	12.7	12.6	14.8	14.0	13.3	16.7	16.5	15.3	15.3	14.9	13.8	13.6
EC	mS/cm	16.0	18.7	22.2	21.3	20.1	21.7	23.0	21.9	21.9	26.5	25.0	24.3	25.1	24.2	23.8
TDS	g/l	10.5	12.5	12.6	14.9	13.6	14.3	13.4	15.3	15.1	15.9	14.5	14.4	14.5	16.4	15.9
Turbidity	NTU	0.8	0.7	0.9	0.9	0.8	0.9	0.7	0.5	0.9	0.8	0.6	0.6	0.6	0.8	0.7
pH		0.6	0.2	0.6	0.5	0.5	0.3	0.3	0.3	0.3	0.3	0.3	0.3	0.3	0.2	0.3
COD Total	g/L	24.2	25.3	25.1	25.2	22.0	22.0	21.1	21.3	20.2	20.7	18.8	17.7	14.9	13.4	13.3
% COD Removal		42.1	39.3	39.8	39.6	47.2	47.4	49.5	48.8	51.5	50.3	55.0	57.5	64.4	67.8	68.1

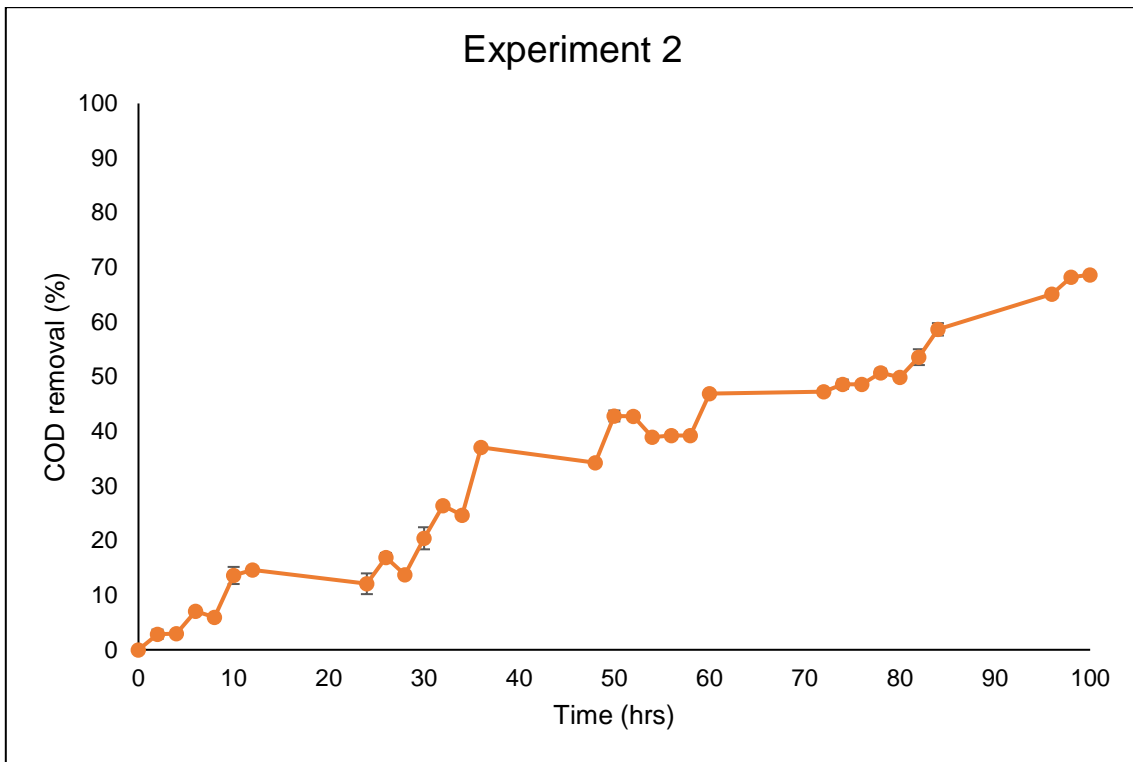


Figure C. 2: Average COD removal from experiment 2.1 and 2.2.

Anova: Single Factor

SUMMARY

Groups	Count	Sum	Average	Variance
Experiment 2.1 COD Removal	31	1031.35	33.2693	436.815
Experiment 2.2 COD Removal	31	1051.72	33.9263	416.009

ANOVA

Source of Variation	SS	df	MS	F	P-value	F crit
Between Groups	6.68979	1	6.68979	0.01569	0.90074	4.00119
Within Groups	25584.7	60	426.412			
Total	25591.4	61				

Table C 1. 5: Results from experiment 3.1.

Experiment	Current Density	NaCl (M)
3	1	0.08

Parameter	Units	Experiment 3.1															
		0	2	4	6	8	10	12	24	26	28	30	32	34	36	48	50
Time	hrs.																
Salinity	g/l	1.5	1.9	2.0	2.0	2.1	2.2	1.9	2.1	2.3	2.3	2.4	2.3	2.3	2.3	2.4	2.5
EC	mS/cm	2.6	3.3	3.4	3.5	3.6	3.8	3.3	3.7	4.0	4.1	4.1	4.0	4.1	3.9	4.2	4.2
TDS	g/l	1.7	1.3	2.3	2.3	2.3	2.5	2.2	2.4	2.6	2.7	2.7	2.6	2.7	2.6	2.8	2.8
Turbidity	NTU	31.3	5.6	3.8	3.0	2.4	2.5	3.0	1.7	2.1	1.9	1.7	1.7	1.6	1.8	1.7	1.6
pH		2.0	1.3	1.1	1.1	1.1	1.1	1.0	1.2	1.0	1.4	1.3	1.2	1.2	1.1	1.1	1.1
COD Total	g/L	55	53.1	53.1	49.7	43.1	42.2	41.5	43	46.3	40.5	40.3	40.2	32.8	31	34.3	28
% COD Removal		0	3.4	3.4	9.7	21.7	23.3	24.5	21.8	15.8	26.3	26.7	26.9	40.4	43.6	37.6	49.1

Parameter	Units	Experiment 3.1														
		52	54	56	58	60	72	74	76	78	80	82	84	96	98	100
Time	hrs.															
Salinity	g/l	2.3	2.5	2.4	2.5	2.5	2.4	2.5	2.3	2.7	2.4	2.3	2.6	2.2	2.3	2.4
EC	mS/cm	4.0	4.2	4.1	4.3	4.3	4.1	4.3	4.1	4.7	4.2	3.9	4.5	3.8	4.0	4.2
TDS	g/l	2.6	2.8	2.7	2.8	2.8	2.7	2.8	2.6	3.0	2.7	2.6	2.9	2.5	2.6	2.7
Turbidity	NTU	1.5	1.7	1.3	1.7	1.4	1.4	1.6	1.5	2.0	1.4	1.7	1.6	1.5	1.5	1.9
pH		1.1	1.1	1.1	1.1	1.1	1.2	1.1	1.1	1.3	1.1	1.0	1.1	1.1	1.1	1.1
COD Total	g/L	25.9	16.6	17.1	16.4	17.2	14.1	11.9	10.9	11.3	11.3	11.6	9.9	8.6	8.3	7.8
% COD Removal		53.0	69.9	69.0	70.2	68.7	74.3	78.3	80.2	79.4	79.5	78.9	82.0	84.3	85.0	85.8

Table C 1. 6: Results from experiment 3.2.

Parameter	Units	Experiment 3.2															
		0	2	4	6	8	10	12	24	26	28	30	32	34	36	48	50
Time	hrs.																
Salinity	g/l	4.2	4.2	4.0	3.8	4.0	3.7	3.7	3.9	3.9	4.0	4.0	3.9	3.8	4.2	4.1	4.0
EC	mS/cm	7.1	7.1	6.8	6.5	6.9	6.3	6.3	6.7	6.6	6.9	6.8	6.6	6.5	7.1	6.7	6.7
TDS	g/l	4.6	4.5	4.4	4.2	4.2	4.1	4.0	4.3	4.2	4.4	4.4	4.5	4.3	4.4	4.5	4.4
Turbidity	NTU	15.6	5.0	2.0	1.1	1.0	1.0	1.0	0.7	0.5	0.6	0.6	0.8	0.8	0.6	0.7	0.6
pH		1.6	1.4	1.0	1.5	1.5	1.5	1.3	1.4	1.3	1.4	1.4	1.1	1.1	1.2	1.3	1.2
COD Total	g/L	55	43.23	40.15	39.16	43.4	42.2	40.5	43.2	39.1	38.6	38.8	39.2	38.2	39.4	26.2	22.7
% COD Removal		0	21.4	27	28.8	21.1	23.2	26.32	21.5	28.8	29.9	29.4	28.8	30.5	28.3	52.4	58.7

Parameter	Units	Experiment 3.2															
		52	54	56	58	60	72	74	76	78	80	82	84	96	98	100	
Time	hrs.																
Salinity	g/l	3.9	4.3	4.0	4.1	4.1	4.1	4.3	3.8	5.0	5.0	5.6	5.6	5.6	5.7	5.7	
EC	mS/cm	6.6	6.7	6.8	6.8	6.8	6.8	7.4	6.4	8.3	8.2	8.8	8.4	8.5	8.4	8.4	
TDS	g/l	4.4	4.4	4.4	4.5	4.4	4.5	4.8	4.2	5.4	5.4	5.7	5.4	5.4	5.7	5.7	
Turbidity	NTU	0.7	0.4	0.6	0.7	0.6	0.5	0.6	0.6	0.6	0.5	0.8	0.8	0.8	0.5	0.5	
pH		1.2	1.2	1.2	1.2	1.3	1.4	1.3	1.3	1.2	1.2	1.3	1.0	1.2	1.0	0.9	
COD Total	g/L	23.1	21.9	19.3	16.9	15.8	11.9	11.7	12.0	11.3	11.2	11.2	10.0	8.8	8.4	7.7	
% COD Removal		57.9	60.1	64.9	69.3	71.3	78.4	78.7	78.2	79.4	79.7	79.7	81.9	84.0	84.7	85.9	

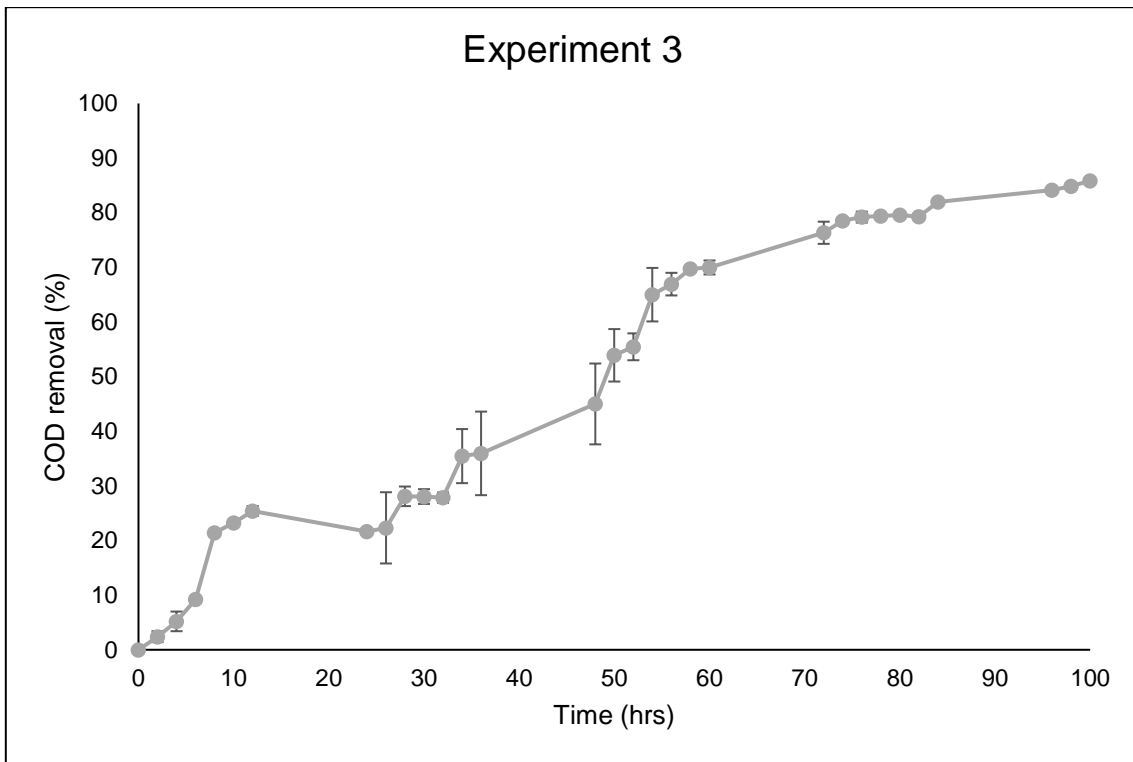


Figure C. 3: Average COD removal from experiment 3.1 and 3.2.

Anova: Single Factor

SUMMARY

Groups	Count	Sum	Average	Variance
Experiment 3.1 COD Removal	31	1530.18	49.3606	830.424
Experiment 3.2 COD Removal	31	1512.7	48.7968	852.708

ANOVA

Source of Variation	SS	df	MS	F	P-value	F crit
Between Groups	4.92823	1	4.92823	0.00586	0.93926	4.00119
Within Groups	50493.9	60	841.566			
Total	50498.9	61				

Table C 1. 7: Results from experiment 4.1.

Experiment	Current Density	NaCl (M)
4	1.25	0.08

Parameter	Units	Experiment 4.1															
		0	2	4	6	8	10	12	24	26	28	30	32	34	36	48	50
Time	hrs.																
Salinity	g/l	11.8	9.8	9.6	10.7	10.2	10.9	8.5	10.0	10.3	12.0	11.4	12.9	11.9	11.8	14.2	15.5
EC	mS/cm	18.4	15.9	15.5	15.6	16.8	18.0	13.7	16.1	17.0	17.1	18.7	18.0	19.7	18.3	20.4	23.9
TDS	g/l	12.0	10.2	9.9	10.5	11.3	10.7	8.9	10.6	10.3	11.6	11.1	12.3	13.6	13.0	13.8	15.6
Turbidity	NTU	7.4	2.5	2.5	0.9	0.8	0.7	0.8	1.2	0.6	4.8	0.8	0.9	0.8	0.8	0.8	0.7
pH		1.1	0.4	0.4	0.1	0.3	0.2	0.3	0.2	0.4	0.3	0.1	0.3	0.2	0.2	0.4	0.3
COD Total	g/L	50.1	40.9	49.6	40.9	38.3	45.5	51.2	41.9	34.7	34.4	30.5	29.8	28.9	31.2	23.4	25.5
% COD Removal		0.0	18.4	1.0	18.2	23.4	9.0	-2.2	16.4	30.8	31.2	39.0	40.4	42.3	37.6	53.3	49.0

Parameter	Units	Experiment 4.1														
		52	54	56	58	60	72	74	76	78	80	82	84	96	98	100
Time	hrs.															
Salinity	g/l	15.3	15.5	15.3	15.4	15.4	14.9	14.7	15.4	18.7	18.2	17.9	17.9	19.1	20.1	18.8
EC	mS/cm	23.5	23.8	23.7	22.9	23.9	22.3	26.0	25.7	25.4	29.0	28.1	28.0	27.9	27.3	28.2
TDS	g/l	15.4	15.5	15.4	15.4	15.4	14.7	14.6	17.6	17.6	17.3	19.1	19.2	20.1	20.3	18.3
Turbidity	NTU	0.6	0.7	0.7	0.6	0.6	0.9	0.5	0.9	0.7	0.6	0.7	0.6	0.6	0.6	1.2
pH		0.2	0.4	0.3	0.3	0.3	0.2	0.3	0.3	0.2	0.2	0.2	0.2	0.3	0.3	0.2
COD Total	g/L	29.2	21.8	25.7	28.4	25.2	17.3	18.1	16.4	14.5	14.4	14.2	9.8	9.5	9.4	9.0
% COD Removal		41.8	56.5	48.6	43.2	49.6	65.5	63.8	67.3	71.0	71.2	71.5	80.3	81.1	81.2	82.1

Table C 1. 8: Results from experiment 4.2.

Parameter	Units	Experiment 4.2															
		0	2	4	6	8	10	12	24	26	28	30	32	34	36	48	50
Time	hrs.																
Salinity	g/l	10.8	10.1	9.6	9.5	10.1	9.7	9.1	8.8	8.3	9.8	9.7	10.5	10.5	9.9	10.2	11.1
EC	mS/cm	17.1	15.5	15.7	15.7	15.1	16.1	15.0	13.2	13.3	16.2	16.2	15.4	17.4	15.8	15.4	18.4
TDS	g/l	11.1	10.2	9.6	10.6	10.2	9.8	10.1	8.7	8.7	9.9	10.2	10.4	10.5	10.9	10.4	11.1
Turbidity	NTU	113.3	33.2	3.3	1.1	0.9	0.8	1.5	2.7	0.8	3.6	0.7	0.9	3.8	1.0	1.8	4.0
pH		1.4	0.6	0.6	0.8	0.6	0.7	0.7	0.6	0.5	0.6	0.6	0.4	0.8	0.5	0.6	0.6
COD Total	g/L	49.2	46.6	42.5	45.0	41.3	41.4	40.8	31.5	36.1	35.0	35.2	35.1	32.6	32.5	29.4	29.0
% COD Removal		0.0	5.1	13.6	8.5	16.1	15.9	17.1	35.9	26.5	28.7	28.4	28.6	33.7	33.9	40.3	41.1

Parameter	Units	Experiment 4.2														
		52	54	56	58	60	72	74	76	78	80	82	84	96	98	100
Time	hrs.															
Salinity	g/l	11.6	11.4	12.5	11.8	12.8	13.7	13.9	14.2	14.7	14.3	13.3	14.9	15.0	13.3	14.3
EC	mS/cm	18.8	18.5	18.1	17.6	18.8	20.9	21.8	22.2	21.6	22.3	20.9	22.0	23.2	23.3	24.1
TDS	g/l	11.5	12.6	12.2	11.7	12.6	13.7	13.9	15.1	14.2	14.2	14.5	14.6	14.9	15.3	14.1
Turbidity	NTU	0.9	0.9	0.9	0.9	0.7	0.8	0.5	0.7	0.8	1.1	0.8	1.0	1.0	0.6	0.7
pH		0.6	0.6	0.6	0.5	0.3	0.7	0.5	0.6	0.5	0.5	0.5	0.3	0.6	0.6	0.6
COD Total	g/L	28.8	28.9	29.9	27.0	27.4	22.9	23.5	20.2	16.9	19.2	17.3	15.1	9.9	8.8	8.6
% COD Removal		41.4	41.2	39.1	45.1	44.2	53.4	52.2	58.8	65.7	61.0	64.9	69.4	79.9	82.1	82.4

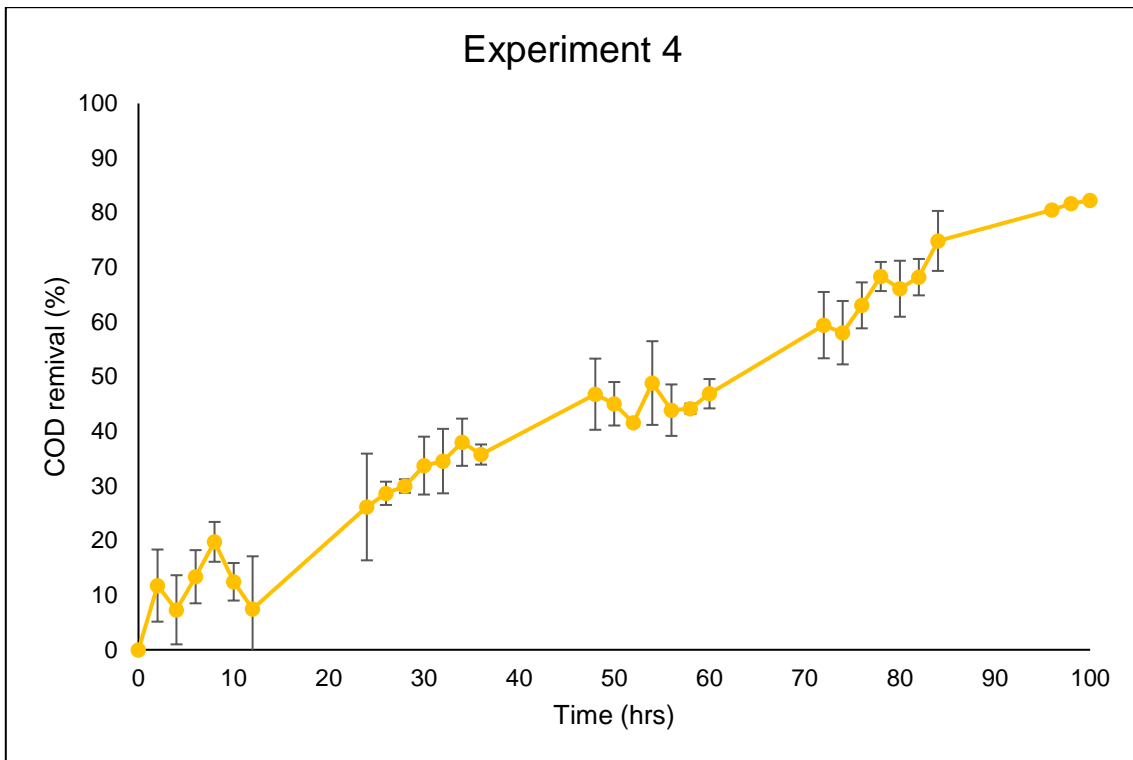


Figure C. 4: Average COD removal from experiment 4.1 and 4.2.

Anova: Single Factor

SUMMARY

Groups	Count	Sum	Average	Variance
Experiment 4.1 COD Removal	31	1382.42	44.5941	651.41
Experiment 4.2 COD Removal	31	1254.21	40.4583	510.515

ANOVA

Source of Variation	SS	df	MS	F	P-value	F crit
Between Groups	265.133	1	265.133	0.45637	0.50192	4.00119
Within Groups	34857.7	60	580.962			
Total	35122.9	61				

Table C 1. 9: Results from experiment 5.1.

Experiment	Current Density	NaCl (M)
5	1.75	0.08

Parameter	Units	Experiment 5.1															
		0.0	2.0	4.0	6.0	8.0	10.0	12.0	24.0	26.0	28.0	30.0	32.0	34.0	36.0	48.0	50.0
Time	hrs.																
Salinity	g/l	12.1	9.5	9.2	9.6	10.6	10.5	10.1	8.9	10.3	12.1	11.6	12.9	13.3	11.9	11.8	11.6
EC	mS/cm	19.0	15.3	15.8	15.5	16.0	17.2	16.1	14.3	17.0	19.7	18.7	20.1	19.5	19.2	19.1	18.1
TDS	g/l	12.4	10.1	9.9	9.8	10.6	11.4	10.5	9.3	11.3	11.9	12.6	12.6	13.1	12.0	11.9	11.8
Turbidity	NTU	51.7	7.7	1.1	1.2	1.2	1.3	1.3	1.1	2.3	1.1	1.2	1.3	0.7	1.9	1.7	0.9
pH		1.2	0.9	0.6	0.7	0.4	0.5	0.4	0.7	0.6	0.7	0.7	0.5	0.9	0.7	0.5	0.5
COD Total	g/L	49.3	47.3	44.2	40.0	39.2	37.1	36.5	35.8	36.1	35.9	38.9	39.6	32.6	32.2	26.4	29.2
% COD Removal		0.0	4.0	10.3	18.8	20.5	24.7	26.0	27.5	26.8	27.2	21.0	19.6	33.8	34.7	46.4	40.8

Parameter	Units	Experiment 5.1														
		52	54	56	58	60	72	74	76	78	80	82	84	96	98	100
Time	hrs.															
Salinity	g/l	13.2	13.4	12.4	12.9	11.0	10.5	13.4	12.1	11.5	14.6	15.2	12.6	12.6	13.8	14.1
EC	mS/cm	20.1	19.4	20.1	20.7	17.9	16.6	20.6	18.7	18.0	22.6	22.9	19.9	20.2	21.3	22.0
TDS	g/l	13.3	13.1	13.3	12.6	11.6	11.5	13.5	12.2	11.7	15.0	15.7	12.4	12.9	13.9	14.6
Turbidity	NTU	1.5	1.1	1.1	0.9	0.9	0.7	2.9	0.7	1.7	1.1	1.2	1.5	1.0	0.9	1.3
pH		0.5	0.5	0.6	0.5	0.6	0.8	0.6	1.1	0.5	0.5	0.5	0.5	1.0	0.9	0.7
COD Total	g/L	28.2	26.8	26.0	24.3	23.4	21.3	21.2	17.0	17.7	16.6	15.9	15.3	10.0	10.2	10.0
% COD Removal		42.7	45.6	47.3	50.7	52.5	56.7	56.9	65.5	64.1	66.4	67.7	68.9	79.7	79.4	79.7

Table C 1. 10: Results from experiment 5.2.

Parameter	Units	Experiment 5.2															
		0	2	4	6	8	10	12	24	26	28	30	32	34	36	48	50
Time	hrs.																
Salinity	g/l	12.1	9.3	8.8	8.7	10.5	8.7	8.5	8.9	12.4	12.2	13.5	12.9	21.8	12.9	12.5	11.5
EC	mS/cm	19.0	14.5	13.7	14.5	17.3	13.9	13.8	14.5	18.0	19.8	19.6	20.1	20.3	20.5	20.1	18.2
TDS	g/l	12.4	9.6	9.1	9.6	10.5	9.8	8.9	9.3	12.1	13.4	13.2	14.2	13.8	13.8	12.6	12.0
Turbidity	NTU	51.7	4.0	4.1	2.6	2.3	2.0	1.3	0.9	1.1	1.3	0.7	1.2	1.5	1.3	1.1	1.5
pH		1.2	0.5	0.3	0.5	0.5	0.6	0.4	0.6	0.6	0.7	0.7	0.6	0.6	0.6	0.6	0.6
COD Total	g/L	39.1	38.9	33.2	33.7	33.6	34.1	33.8	31.2	32.0	31.0	30.3	31.4	31.4	31.9	23.0	23.2
% COD Removal		0.0	0.4	15.1	13.8	14.1	12.7	13.5	20.0	18.0	20.6	22.4	19.7	19.7	18.3	41.1	40.7

Parameter	Units	Experiment 5.2														
		52	54	56	58	60	72	74	76	78	80	82	84	96	98	100
Time	hrs.															
Salinity	g/l	12.08	13.51	13.66	12.64	12.6	11.32	14.36	14.34	14.14	15.2	13.81	13.75	13.5	14.1	13.8
EC	mS/cm	22.4	21.8	20.2	19.47	19.42	17.31	22.3	22.2	21.7	23.6	21.2	21.3	21.5	22.5	21.8
TDS	g/l	12.59	13.55	13.41	12.73	12.72	10.89	14.11	14.24	14.17	15.55	13.81	13.75	13.82	14.12	14.2
Turbidity	NTU	0.92	0.92	0.99	0.94	0.88	0.78	0.74	0.6	0.67	0.74	0.69	0.64	0.68	0.7	0.97
pH		0.67	0.56	0.65	0.51	0.55	0.48	0.72	0.72	0.63	0.58	0.55	0.59	0.65	0.69	0.85
COD Total	g/L	21.6	21.6	22.1	21.5	20.6	20.8	16.8	15.5	13.9	15.0	13.1	16.0	8.3	8.4	8.3
% COD Removal		44.6	44.8	43.4	45.1	47.3	46.8	57.0	60.3	64.4	61.5	66.5	59.2	78.7	78.6	78.7

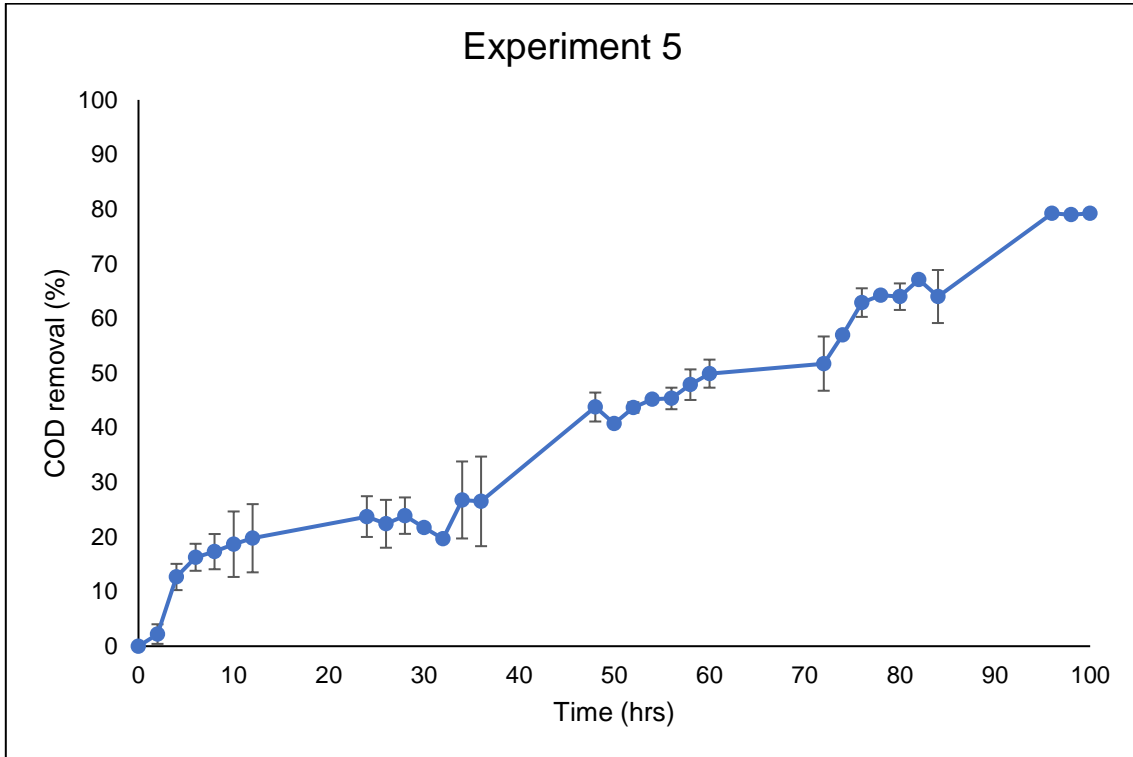


Figure C. 5: Average COD removal from experiment 5.1 and 5.2.

Anova: Single Factor

SUMMARY

Groups	Count	Sum	Average	Variance
Experiment 5.1 COD Removal	31	1305.85	42.1241	514.494
Experiment 5.2 COD Removal	31	1167.04	37.6465	559.528

ANOVA

Source of Variation	SS	df	MS	F	P-value	F crit
Between Groups	310.76	1	310.76	0.57868	0.44981	4.00119
Within Groups	32220.7	60	537.011			
Total	32531.4	61				

Table C 1. 11: Results from experiment 6.1.

Experiment	Current Density	NaCl (M)
6	2	0.08

Parameter	Units	Experiment 6.1															
		0	2	4	6	8	10	12	24	26	28	30	32	34	36	48	50
Time	hrs.																
Salinity	g/l	11.2	9.0	11.5	12.5	13.2	13.5	12.5	9.6	10.3	12.5	13.6	13.9	13.5	14.2	12.6	12.5
EC	mS/cm	17.6	14.7	18.5	18.8	20.2	21.1	19.7	14.8	17.4	18.8	21.6	21.1	21.7	21.1	22.0	12.7
TDS	g/l	11.5	9.5	11.5	12.5	12.8	13.4	12.8	9.7	11.4	12.4	13.2	13.9	14.6	13.8	14.3	13.2
Turbidity	NTU	24.4	4.8	1.0	0.8	0.6	0.3	0.5	1.2	0.9	4.2	0.8	0.9	0.7	0.8	1.0	0.8
pH		1.1	0.9	1.0	1.1	0.9	0.8	0.9	0.7	0.8	1.1	0.9	0.9	0.8	0.8	0.8	0.8
COD Total	g/L	54.9	46.1	43.8	45.8	42.6	41.1	35.8	37.0	35.6	33.3	34.3	35.1	30.7	32.9	26.3	29.2
% COD Removal		0.0	16.0	20.2	16.5	22.4	25.2	34.8	32.7	35.1	39.4	37.6	36.0	44.1	40.1	52.1	46.8

Parameter	Units	Experiment 6.1														
		52	54	56	58	60	72	74	76	78	80	82	84	96	98	100
Time	hrs.															
Salinity	g/l	14.1	13.6	13.9	14.4	12.5	13.2	12.7	14.5	14.5	13.9	15.2	15.4	16.5	19.3	18.7
EC	mS/cm	21.4	21.3	21.9	22.5	19.7	19.5	19.5	22.0	21.0	23.5	22.9	23.8	22.6	26.9	26.8
TDS	g/l	14.1	14.6	14.0	14.8	13.1	12.8	12.7	14.4	14.7	14.6	15.5	15.5	14.6	16.9	18.2
Turbidity	NTU	1.2	1.0	0.7	0.8	0.7	0.7	0.9	1.5	0.9	0.7	0.7	0.8	0.7	0.7	1.0
pH		0.6	0.9	0.8	0.8	0.8	0.8	0.8	1.2	1.0	0.8	0.8	0.7	0.8	0.7	0.8
COD Total	g/L	26.8	27.0	25.1	22.9	18.5	19.0	18.0	17.6	17.4	18.7	15.5	16.1	11.7	11.8	10.4
% COD Removal		51.2	50.8	54.3	58.3	66.3	65.4	67.2	67.9	68.2	65.9	71.7	70.6	78.8	78.6	81.1

Table C 1. 12: Results from experiment 6.2.

Parameter	Units	Experiment 6.2															
		0	2	4	6	8	10	12	24	26	28	30	32	34	36	48	50
Time	hrs.																
Salinity	g/l	3.6	3.9	3.7	3.5	3.6	3.9	3.6	3.7	3.9	3.9	3.9	4.0	4.1	4.1	4.4	4.3
EC	mS/cm	6.3	6.6	6.3	6.1	6.0	6.0	6.2	6.4	6.5	6.6	6.7	6.8	7.0	7.0	7.2	7.3
TDS	g/l	4.1	3.9	4.1	3.9	3.9	3.9	4.1	4.1	4.2	4.3	4.3	4.4	4.5	4.7	4.8	4.8
Turbidity	NTU	25.8	9.7	8.8	2.3	1.5	1.0	1.3	1.0	0.9	0.9	0.9	0.9	1.0	1.0	0.9	0.9
pH		2.4	1.6	1.6	1.1	1.2	1.3	1.4	1.2	1.2	1.5	1.4	1.4	1.4	1.4	1.4	1.4
COD Total	g/L	54.7	52.4	43.4	43.6	44.8	42.9	50.2	37.1	35.2	40.6	41.7	38.7	43.8	33.7	35.9	27.6
% COD Removal		0.0	4.1	20.6	20.3	18.1	21.5	8.2	32.1	35.6	25.8	23.6	29.2	19.9	38.4	34.3	49.6

Parameter	Units	Experiment 6.2														
		52	54	56	58	60	72	74	76	78	80	82	84	96	98	100
Time	hrs.															
Salinity	g/l	4.4	4.5	4.3	4.6	4.6	4.4	12.7	14.4	14.0	14.8	15.1	15.7	14.6	18.0	18.7
EC	mS/cm	7.3	7.6	7.3	7.6	7.8	7.4	19.5	21.9	21.9	23.1	22.8	23.1	22.7	27.3	27.7
TDS	g/l	4.8	4.9	4.7	5.0	5.1	4.8	12.6	14.4	14.4	14.7	15.1	15.4	14.9	17.6	18.1
Turbidity	NTU	1.0	0.9	0.5	1.2	1.1	1.1	0.8	1.4	0.9	0.7	0.8	0.7	0.8	0.8	1.0
pH		1.4	1.4	1.5	1.3	1.3	1.3	0.8	1.1	0.9	0.8	0.8	0.7	0.8	0.6	0.8
COD Total	g/L	31.2	26.5	24.5	24.1	23.4	21.2	18.1	17.5	17.8	18.9	15.3	16.3	11.6	11.8	10.2
% COD Removal		42.9	51.5	55.1	55.8	57.2	61.2	67.0	68.0	67.5	65.4	72.0	70.1	78.7	78.5	81.3

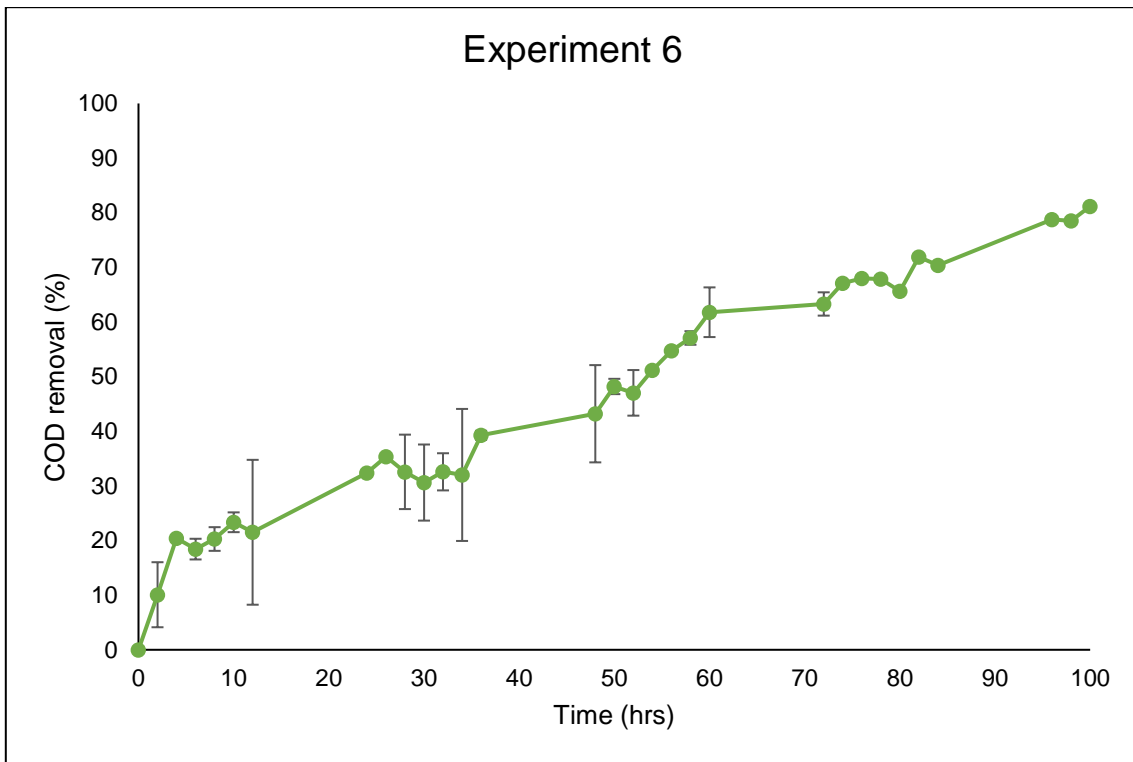


Figure C. 6: Average COD removal from experiment 6.1 and 6.2.

Anova: Single Factor

SUMMARY

Groups	Count	Sum	Average	Variance
Experiment 6.1 COD Removal	31	1495.39	48.2384	453.782
Experiment 6.2 COD Removal	31	1353.78	43.6704	571.989

ANOVA

Source of Variation	SS	df	MS	F	P-value	F crit
Between Groups	323.433	1	323.433	0.63061	0.43026	4.00119
Within Groups	30773.2	60	512.886			
Total	31096.6	61				

Table C 1. 13: Results from experiment 7.1.

Experiment	Current Density	NaCl (M)
7	4	0.08

Parameter	Units	Experiment 7.1															
		0	2	4	6	8	10	12	24	26	28	30	32	34	36	48	50
Time	hrs.																
Salinity	g/l	11.1	10.7	10.6	11.5	12.2	10.7	11.2	9.9	11.3	11.8	11.8	12.4	13.1	12.7	13.1	12.3
EC	mS/cm	17.6	17.6	17.3	18.5	18.5	16.8	18.2	16.5	17.0	18.1	18.9	20.2	19.7	20.1	19.3	19.6
TDS	g/l	11.5	10.8	11.6	11.6	12.2	11.4	11.7	10.2	11.2	11.9	12.6	12.4	12.4	13.0	13.0	13.3
Turbidity	NTU	24.4	2.4	1.7	0.8	0.7	0.6	0.6	1.0	0.9	0.6	1.2	1.3	0.8	0.9	0.9	0.7
pH		1.0	0.7	0.8	0.9	0.9	1.0	0.9	0.9	0.9	1.1	0.8	1.0	0.8	1.0	1.0	0.7
COD Total	g/L	56.6	47.0	54.2	51.5	45.2	48.0	47.4	39.9	40.4	39.4	38.2	37.2	35.9	39.5	27.3	29.9
% COD Removal		0.0	17.0	4.2	8.9	20.1	15.2	16.2	29.4	28.6	30.4	32.6	34.2	36.5	30.1	51.8	47.2

Parameter	Units	Experiment 7.1														
		52	54	56	58	60	72	74	76	78	80	82	84	96	98	100
Time	hrs.															
Salinity	g/l	13.0	13.6	13.1	12.4	11.9	11.7	13.1	12.9	14.0	13.4	14.3	14.3	12.1	11.9	11.6
EC	mS/cm	20.5	20.4	20.6	19.2	17.9	18.1	20.5	20.1	21.3	21.1	22.3	22.3	19.2	18.9	18.8
TDS	g/l	12.7	13.3	13.2	11.7	12.2	11.8	13.4	13.0	14.0	14.1	14.3	14.3	12.4	12.1	12.2
Turbidity	NTU	1.2	1.4	1.1	1.1	1.0	0.8	0.9	0.9	1.0	0.7	1.1	1.1	1.0	1.2	1.0
pH		0.9	0.8	0.8	0.9	0.9	0.8	0.6	0.9	0.9	0.7	0.7	0.8	0.8	1.1	1.8
COD Total	g/L	26.0	23.4	23.2	16.0	15.3	15.7	14.5	12.9	11.2	11.5	9.7	8.4	10.2	11.1	10.9
% COD Removal		54.1	58.6	59.1	71.7	72.9	72.2	74.3	77.3	80.3	79.7	82.8	85.2	82.0	80.5	80.7

Table C 1. 14: Results from experiment 7.2.

Parameter	Units	Experiment 7.2															
		0	2	4	6	8	10	12	24	26	28	30	32	34	36	48	50
Time	hrs.																
Salinity	g/l	3.6	3.4	3.5	3.4	3.4	3.5	3.7	3.7	3.7	3.8	3.8	3.9	4.0	4.0	4.1	4.1
EC	mS/cm	6.3	5.5	5.9	5.8	5.8	6.0	6.1	6.3	6.3	6.4	6.5	6.6	6.8	6.7	6.9	6.8
TDS	g/l	4.1	3.9	3.8	3.8	3.8	3.9	4.0	4.1	4.1	4.2	4.6	4.3	4.4	4.4	4.5	4.5
Turbidity	NTU	25.8	9.0	8.8	4.0	1.5	0.9	1.1	0.9	1.0	0.8	0.8	0.8	0.9	0.9	0.9	0.7
pH		2.4	1.1	1.0	1.1	1.7	1.2	1.3	1.1	1.1	1.2	1.5	1.2	1.1	1.1	1.4	1.2
COD Total	g/L	54.3	53.5	52.3	50.4	45.1	44.6	43.3	43.2	43.6	41.9	40.3	38.0	37.3	32.4	27.8	26.5
% COD Removal		0.0	1.5	3.7	7.2	16.9	17.8	20.3	20.5	19.8	22.9	25.8	30.1	31.2	40.3	48.7	51.2

Parameter	Units	Experiment 7.2														
		52	54	56	58	60	72	74	76	78	80	82	84	96	98	100
Time	hrs.															
Salinity	g/l	4.3	4.3	4.2	4.32	4.39	4.4	4.38	12.85	14.04	13.44	14.34	14.33	12.09	11.89	11.62
EC	mS/cm	7.1	7.0	7.08	7.32	7.34	7.35	7.89	8.1	9.21	8.76	9.34	9.52	10.2	9.75	8.95
TDS	g/l	4.6	4.6	4.61	4.68	4.78	4.8	4.38	4.51	4.52	3.86	4.97	5.12	5.62	4.68	5.1
Turbidity	NTU	0.9	1.3	1.18	1.1	0.69	0.87	0.83	0.95	1.05	0.75	1.2	1.5	0.87	1.52	1.24
pH		1.3	1.5	1.25	1.31	1.22	1.32	1.25	1.36	1.42	1.43	1.52	1.62	1.7	1.21	1.68
COD Total	g/L	26.8	27.1	25.19	23.6	25.36	24.82	14.52	13.31	11.28	12.6	10.84	11.65	10.29	11.17	10.84
% COD Removal		50.6	50.2	53.6	56.53	53.29	54.29	73.25	75.48	79.23	76.8	80.04	78.54	81.05	79.43	80.04

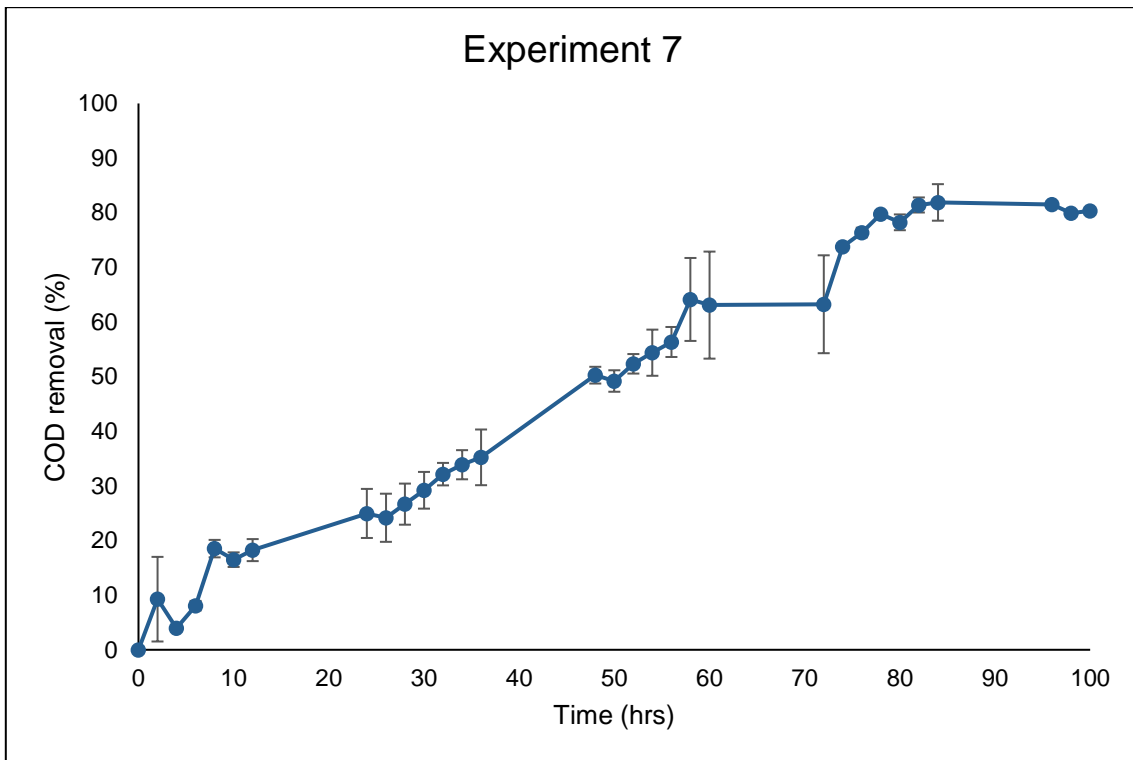


Figure C. 7: Average COD removal from experiment 7.1 and 7.2.

Anova: Single Factor

SUMMARY

Groups	Count	Sum	Average	Variance
Experiment 7.1 COD Removal	31	1513.9	48.8354	766.377
Experiment 7.2 COD Removal	31	1380.24	44.524	738.498

ANOVA

Source of Variation	SS	df	MS	F	P-value	F crit
Between Groups	288.118	1	288.118	0.38291	0.53839	4.00119
Within Groups	45146.2	60	752.437			
Total	45434.4	61				

The effect of **NaCl** on the removal of COD, and other impurities, at the following experimental conditions.

Experimental parameters

Volume of reactor,	1L
Temperature of solution,	60°C
NaCl concentration,	0 – 0.1 M
Current Density,	1 mA/cm ²
Time,	100 hrs.

Table C 1. 15: Results from experiment 8.1.

Experiment	Current Density	NaCl (M)
8	1	0

Parameter	Units	Experiment 8.1														
		0	2	4	6	8	10	12	24	26	28	30	32	34	36	48
Time	hrs.															
Salinity	g/l	11.9	9.2	8.1	7.4	7.6	6.4	6.9	13.1	8.3	12.1	12.5	12.1	12.0	11.9	12.3
EC	mS/cm	18.7	15.2	12.5	12.4	12.5	11.2	10.4	20.2	12.4	18.9	19.7	18.8	18.8	19.2	19.1
TDS	g/l	12.2	9.2	8.3	8.1	7.8	6.9	6.5	13.4	8.2	12.2	12.7	12.3	12.1	12.0	12.2
Turbidity	NTU	511.6	95.4	29.5	11.5	6.6	5.4	5.2	2.7	2.5	1.5	1.5	0.5	1.0	0.9	1.5
pH		2.1	1.2	1.0	1.0	1.1	1.9	1.5	1.5	1.5	1.7	1.6	1.3	1.7	1.5	1.7
COD Total	g/L	51.4	50.9	47.7	46.1	41.9	44.2	45.4	49.1	43.2	40.5	40.9	40.5	40.8	44.8	39.0
% COD Removal		0.0	1.0	7.2	10.4	18.6	14.1	11.7	4.5	15.9	21.2	20.5	21.3	20.7	12.9	24.2

Parameter	Units	Experiment 8.1														
		52	54	56	58	60	72	74	76	78	80	82	84	96	98	100
Time	hrs.															
Salinity	g/l	12.3	12.4	12.0	12.1	12.4	12.2	12.5	13.0	13.3	13.2	12.9	13.2	12.9	13.1	13.2
EC	mS/cm	19.4	19.6	18.8	19.1	19.1	18.9	18.3	20.4	13.3	19.2	18.7	20.2	18.7	18.8	19.2
TDS	g/l	12.6	12.6	12.3	12.4	12.3	12.2	12.3	1.9	20.5	18.9	13.3	12.2	13.3	12.8	13.2
Turbidity	NTU	0.8	3.2	0.8	0.8	0.8	0.9	1.4	0.8	0.8	0.9	0.7	0.8	1.0	1.0	0.8
pH		1.2	1.7	1.4	1.5	1.5	1.3	1.4	13.2	1.4	1.4	1.4	1.3	1.3	1.3	1.1
COD Total	g/L	37.2	36.0	37.2	36.1	34.2	33.1	32.5	28.4	28.5	28.2	26.3	23.7	24.8	28.9	30.0
% COD Removal		27.7	30.1	27.7	29.7	33.5	35.7	36.8	44.7	44.5	45.2	48.8	53.9	51.8	43.7	41.7

Table C 1. 16: Results from experiment 8.2.

Parameter	Units	Experiment 8.2															
		0	2	4	6	8	10	12	24	26	28	30	32	34	36	48	50
Time	hrs.																
Salinity	g/l	11.9	7.2	6.8	6.8	6.6	5.9	5.7	12.6	12.1	11.7	11.6	11.6	11.7	11.6	10.5	12.0
EC	mS/cm	18.7	12.2	11.3	10.9	11.1	10.9	10.3	19.7	18.9	18.2	18.4	18.4	18.2	18.2	16.8	18.9
TDS	g/l	12.2	8.2	7.1	7.2	7.2	7.1	6.9	12.6	12.4	11.9	12.0	11.9	11.8	12.6	11.0	12.6
Turbidity	NTU	511.6	92.5	19.4	10.7	7.3	13.1	8.3	16.7	3.4	1.7	1.0	1.0	1.6	1.4	1.2	0.9
pH		2.0	2.0	1.5	1.6	1.6	1.4	1.5	1.2	1.3	1.6	1.3	1.6	0.5	1.2	1.2	1.4
COD Total	g/L	51.2	50.5	50.8	48.3	46.1	46.6	46.1	42.3	43.2	41.0	41.7	40.4	40.5	40.3	41.9	42.1
% COD Removal		0.0	1.2	0.6	5.5	9.9	8.8	9.8	17.3	15.5	19.8	18.4	21.0	20.9	21.3	18.2	17.6

Parameter	Units	Experiment 8.2														
		52	54	56	58	60	72	74	76	78	80	82	84	96	98	100
Time	hrs.															
Salinity	g/l	11.9	11.9	11.8	11.6	11.5	11.	12.7	12.	12.8	13.0	12.9	13.4	12.8	12.7	13.3
EC	mS/cm	18.6	18.9	18.5	18.4	18.3	18.2	19.9	19.4	19.9	20.0	19.8	20.1	19.	18.7	20.1
TDS	g/l	12.1	12.3	12.0	12.0	12.1	11.5	12.9	12.6	12.5	13.3	12.9	13.4	14.1	12.5	13.3
Turbidity	NTU	0.	0.7	0.5	0.5	0.6	1.4	0.4	0.7	0.82	0.9	0.7	0.8	0.9	0.9	1.1
pH		1.56	1.1	0.9	1.2	1.3	1.1	1.2	1.4	1.2	1.4	1.3	1.4	1.3	1.3	1.2
COD Total	g/L	39.3	37.7	36.7	36.9	35.0	33.2	33.2	30.8	28.1	28.7	30.5	30.7	28.2	23.2	22.7
% COD Removal		23.1	26.2	28.3	27.8	31.5	35.2	35.1	39.8	45.1	44.0	40.3	39.9	44.8	54.7	55.7

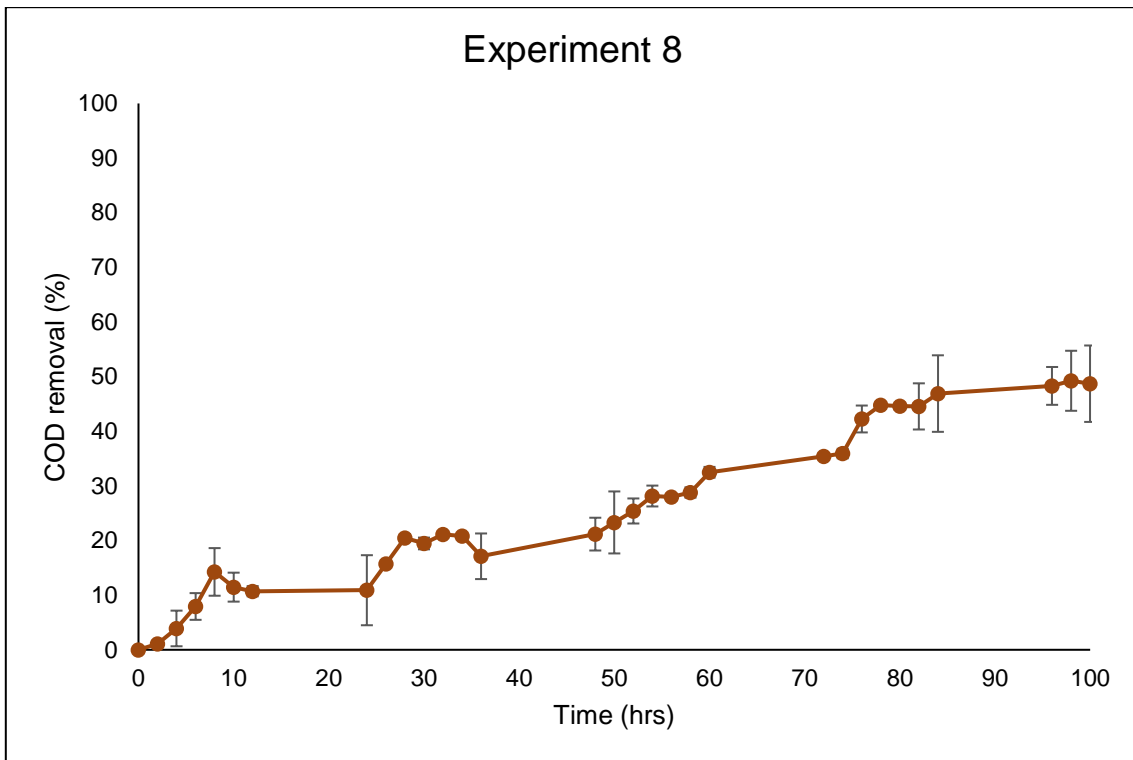


Figure C. 8: Average COD removal from experiment 8.1 and 8.2.

Anova: Single Factor

SUMMARY

Groups	Count	Sum	Average	Variance
Experiment 8.1 COD Removal	31	828.663	26.7311	234.133
Experiment 8.2 COD Removal	31	777.204	25.0711	239.481

ANOVA

Source of Variation	SS	df	MS	F	P-value	F crit
Between Groups	42.7098	1	42.7098	0.18036	0.67259	4.00119
Within Groups	14208.4	60	236.807			
Total	14251.1	61				

Table C 1. 17: Results from experiment 9.1.

Experiment	Current Density	NaCl (M)
9	1	0.02

Parameter	Units	Experiment 9.1															
		0	2	4	6	8	10	12	24	26	28	30	32	34	36	48	50
Time	hrs.																
Salinity	g/l	11.8	11.8	11.8	10.8	10.2	10.9	10.9	10.9	11.0	11.2	11.9	12.3	11.9	12.0	12.0	12.2
EC	mS/cm	18.6	19.2	18.4	17.4	16.1	17.7	17.7	17.6	17.4	18.3	19.0	18.8	18.7	19.0	18.8	19.2
TDS	g/l	12.1	11.7	11.4	10.7	10.5	11.1	11.1	11.1	11.0	12.2	12.0	12.4	12.4	12.5	12.4	12.4
Turbidity	NTU	45.4	40.1	30.2	28.0	23.5	2.6	1.4	1.1	1.0	0.9	1.6	1.1	1.3	1.1	1.3	1.6
pH		2.3	2.1	1.8	1.7	0.8	0.7	0.7	0.4	0.5	1.5	1.6	1.6	1.8	1.4	1.3	1.4
COD Total	g/L	55.0	53.1	48.6	44.4	32.6	42.0	40.1	36.0	29.0	27.0	26.3	31.3	29.9	35.2	27.5	30.1
% COD Removal		0.0	3.5	11.6	19.2	40.7	23.6	27.1	34.6	47.2	50.9	52.2	43.1	45.6	36.0	50.0	45.2

Parameter	Units	Experiment 9.1														
		52	54	56	58	60	72	74	76	78	80	82	84	96	98	100
Time	hrs.															
Salinity	g/l	13.2	13.9	13.3	13.5	13.5	13.4	13.5	14.7	14.8	15.0	14.6	14.6	13.9	14.0	14.9
EC	mS/cm	20.2	21.3	20.7	21.3	21.2	20.9	20.2	22.7	22.5	23.1	22.5	21.3	22.1	22.0	22.5
TDS	g/l	13.2	14.0	13.6	13.5	13.5	13.9	14.0	14.7	14.7	15.1	14.7	14.8	15.2	15.3	14.5
Turbidity	NTU	1.2	0.9	0.8	0.7	0.6	0.7	0.5	1.0	0.7	0.9	0.8	0.9	0.7	0.8	0.7
pH		1.9	2.0	1.7	1.4	1.3	1.4	1.3	1.3	1.7	1.6	1.7	1.5	1.5	1.5	1.8
COD Total	g/L	25.9	24.3	25.5	22.3	21.9	20.1	21.6	19.4	18.0	18.4	18.2	20.5	19.6	19.0	18.7
% COD Removal		52.9	55.9	53.6	59.5	60.2	63.5	60.8	64.8	67.3	66.5	66.9	62.7	64.3	65.5	66.0

Table C 1. 18: Results from experiment 9.2.

Parameter	Units	Experiment 9.2															
		0	2	4	6	8	10	12	24	26	28	30	32	34	36	48	50
Time	hrs.																
Salinity	g/l	11.8	11.8	11.8	10.2	10.1	10.4	11.0	11.7	12.4	12.5	12.2	12.5	12.5	12.9	12.6	13.5
EC	mS/cm	18.6	18.6	18.6	16.2	16.3	16.9	17.3	18.4	19.7	19.1	19.3	19.7	20.1	19.9	19.4	21.1
TDS	g/l	12.1	12.6	11.3	10.5	10.4	10.9	11.5	12.0	12.5	12.6	12.6	12.6	12.7	12.8	12.7	13.8
Turbidity	NTU	45.4	35.4	30.2	28.4	25.2	1.3	1.0	0.9	0.9	1.0	0.6	0.8	0.9	1.0	0.8	0.7
pH		2.3	2.1	12.0	1.5	1.3	1.0	0.6	0.8	0.6	0.3	1.5	1.2	1.2	1.3	1.2	1.5
COD Total	g/L	42.8	42.2	39.7	39.8	36.5	27.9	28.2	25.8	24.4	23.0	27.3	25.3	24.3	23.2	23.9	14.9
% COD Removal		0.0	1.4	7.2	6.9	14.6	34.7	34.2	39.7	43.1	46.1	36.1	40.8	43.2	45.9	44.2	65.3

Parameter	Units	Experiment 9.2														
		52	54	56	58	60	72	74	76	78	80	82	84	96	98	100
Time	hrs.															
Salinity	g/l	13.8	14.2	14.2	14.1	14.2	14.4	14.9	15.8	15.1	14.8	14.8	14.9	15.0	15.3	14.9
EC	mS/cm	21.7	22.2	22.0	21.8	19.9	19.9	23.1	24.5	23.2	22.7	22.1	22.8	22.9	23.6	22.9
TDS	g/l	14.1	14.2	14.3	14.3	14.2	14.4	15.0	16.1	15.1	14.8	15.1	15.2	15.0	15.2	15.0
Turbidity	NTU	0.9	0.5	0.8	0.7	0.8	0.9	0.8	0.9	0.7	0.6	0.6	0.7	0.6	0.7	0.4
pH		1.1	1.1	1.0	1.3	1.3	1.3	1.0	1.4	1.4	1.3	1.4	1.4	1.3	1.1	1.3
COD Total	g/L	14.1	14.3	16.1	18.3	21.6	22.2	20.4	17.1	16.2	16.2	15.8	15.1	15.1	14.4	14.2
% COD Removal		67.1	66.5	62.3	57.2	49.6	48.1	52.3	60.0	62.1	62.2	63.1	64.8	64.8	66.5	66.8

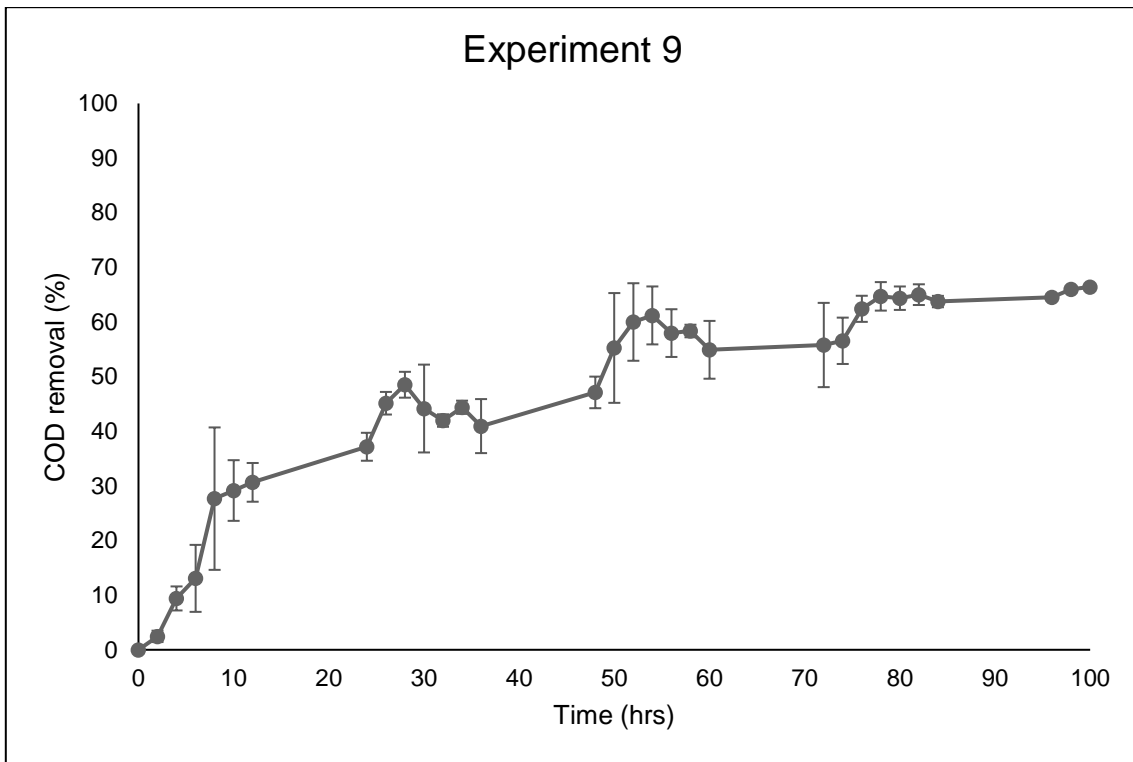


Figure C. 9: Average COD removal from experiment 9.1 and 9.2.

Anova: Single Factor

SUMMARY

Groups	Count	Sum	Average	Variance
Experiment 9.1 COD Removal	31	1460.88	47.1252	372.044
Experiment 9.2 COD Removal	31	1416.94	45.7078	427.459

ANOVA

Source of Variation	SS	df	MS	F	P-value	F crit
Between Groups	31.1395	1	31.1395	0.0779	0.78113	4.00119
Within Groups	23985.1	60	399.751			
Total	24016.2	61				

Table C 1. 19: Results from experiment 10.1

Experiment	Current Density	NaCl (M)
10	1	0.04

Parameter	Units	Experiment 10.1															
		0	2	4	6	8	10	12	24	26	28	30	32	34	36	48	50
Time	hrs.																
Salinity	g/l	13.1	10.7	9.1	8.5	8.6	8.2	8.3	8.3	8.6	8.6	8.5	8.4	8.6	8.4	8.4	7.4
EC	mS/cm	20.2	16.8	14.7	14.1	13.3	13.6	13.5	14.2	12.5	12.5	2.5	12.5	12.4	12.4	13.3	12.1
TDS	g/l	13.1	10.9	9.6	8.8	8.8	8.9	8.8	8.9	8.3	8.3	8.3	8.3	8.2	8.2	8.2	7.8
Turbidity	NTU	88.4	57.9	15.1	2.0	1.1	0.8	0.7	0.7	0.9	0.9	0.9	0.7	0.8	0.6	0.8	0.7
pH		2.6	1.5	1.4	1.4	1.5	1.5	1.4	1.5	1.5	1.4	1.4	1.6	1.4	1.3	1.3	1.5
COD Total	g/L	42.2	41.3	37.5	31.7	30.0	28.3	33.8	33.7	35.3	36.6	37.2	35.3	34.2	33.6	31.2	29.6
% COD Removal		0.0	2.2	11.2	24.8	28.9	32.9	19.9	20.1	16.4	13.2	11.7	16.4	18.9	20.3	25.9	29.9

Parameter	Units	Experiment 10.1														
		52	54	56	58	60	72	74	76	78	80	82	84	96	98	100
Time	hrs.															
Salinity	g/l	7.4	7.4	7.4	7.5	7.4	7.5	7.5	8.8	10.3	11.1	9.0	9.1	9.2	9.2	9.5
EC	mS/cm	12.1	12.1	12.1	12.2	12.2	12.2	12.4	14.5	16.9	16.5	14.7	14.8	14.9	14.9	15.2
TDS	g/l	7.9	7.9	7.9	8.2	8.2	8.5	8.6	9.7	10.7	11.2	9.9	10.1	11.3	11.3	12.1
Turbidity	NTU	0.7	0.6	0.6	0.7	0.6	0.6	0.7	0.4	1.1	1.0	1.2	1.1	0.9	0.5	0.6
pH		0.4	1.5	1.5	1.4	1.5	1.4	1.4	1.6	1.6	1.4	1.7	1.6	1.6	1.5	1.5
COD Total	g/L	32.6	30.6	30.5	29.9	34.1	22.9	18.8	16.5	15.4	13.6	14.2	14.1	14.7	13.8	14.1
% COD Removal		22.8	27.4	27.8	29.2	19.2	45.6	55.5	60.9	63.5	67.8	66.4	66.6	65.1	67.3	66.6

Table C 1. 20: Results from experiment 10.2

Parameter	Units	Experiment 10.2															
		0	2	4	6	8	10	12	24	26	28	30	32	34	36	48	50
Time	hrs.																
Salinity	g/l	13.1	10.1	9.0	8.3	8.2	8.2	8.2	9.1	8.2	8.0	7.5	7.5	7.5	7.4	7.6	7.6
EC	mS/cm	20.2	15.9	13.8	13.6	13.5	13.4	13.4	14.2	13.6	17.6	12.4	12.4	12.4	11.6	12.3	12.7
TDS	g/l	13.1	10.7	9.2	8.9	8.6	8.6	8.7	9.3	8.2	8.0	8.0	7.8	7.3	8.0	8.2	8.2
Turbidity	NTU	88.5	28.9	11.6	2.5	1.0	1.0	1.0	0.7	0.9	0.8	0.9	0.9	0.7	0.6	1.0	0.9
pH		2.6	2.3	2.0	1.5	1.3	1.3	1.4	1.4	1.9	1.7	1.9	1.9	2.0	1.7	1.4	1.5
COD Total	g/L	41.4	37.6	30.5	30.7	35.0	39.7	39.5	37.1	38.1	39.3	39.8	36.0	32.8	34.3	30.9	38.2
% COD Removal		0.0	9.2	26.3	25.7	15.4	4.0	4.4	10.4	7.8	5.1	3.7	12.9	20.7	17.0	25.3	7.7

Parameter	Units	Experiment 10.2														
		52	54	56	58	60	72	74	76	78	80	82	84	96	98	100
Time	hrs.															
Salinity	g/l	7.7	7.7	7.7	7.8	7.8	7.9	8.8	8.9	9.7	9.0	8.6	9.2	9.1	10.1	11.2
EC	mS/cm	12.7	12.7	12.7	12.9	13.0	12.8	14.3	14.0	15.8	15.6	13.5	13.5	14.2	14.4	14.7
TDS	g/l	8.2	8.2	8.3	8.3	8.4	8.4	9.1	9.2	10.8	9.1	8.9	8.9	9.2	9.2	10.3
Turbidity	NTU	0.8	0.9	0.7	0.9	0.8	0.7	0.7	0.6	0.8	0.8	0.5	0.6	0.6	0.6	0.6
pH		1.5	1.5	1.5	1.5	0.4	1.5	1.9	2.0	1.4	1.5	2.2	2.1	2.0	1.2	1.4
COD Total	g/L	33.2	34.3	35.4	36.6	33.8	19.9	19.9	22.2	19.7	17.9	16.9	17.4	14.0	14.0	13.6
% COD Removal		19.8	17.0	14.4	11.6	18.2	52.0	51.9	46.3	52.4	56.6	59.2	58.0	66.1	66.2	67.2

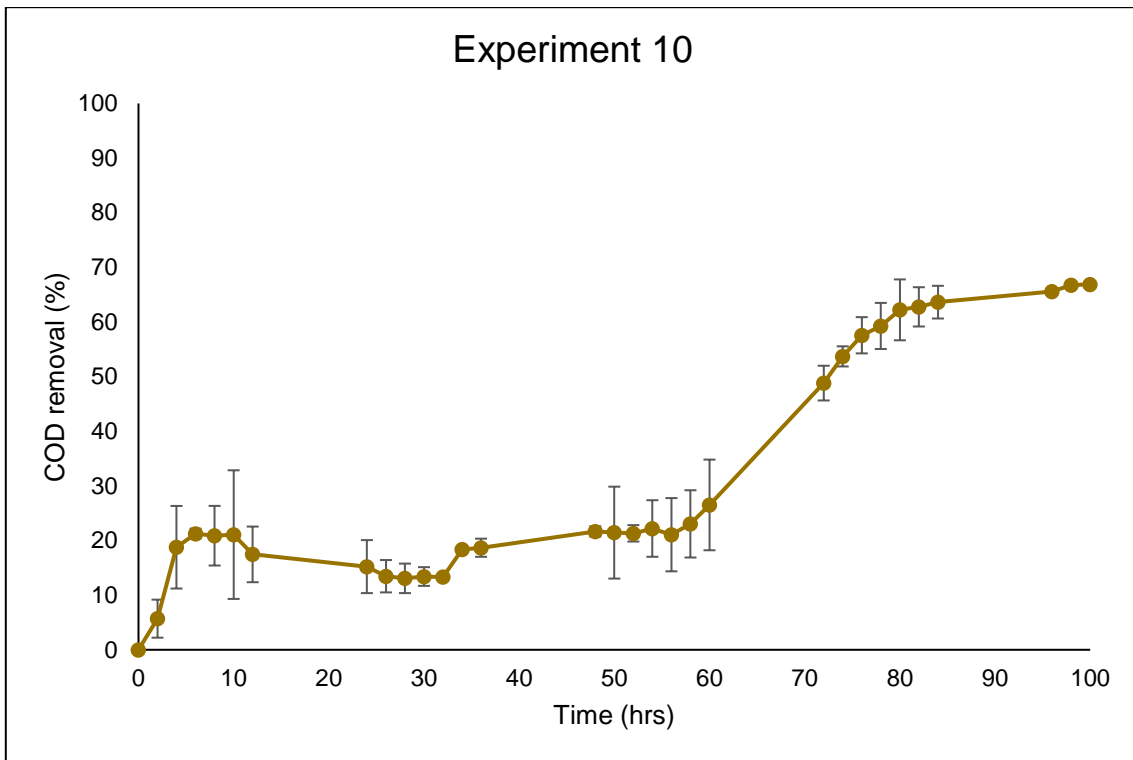


Figure C. 10: Average COD removal from experiment 10.1 and 10.2.

Anova: Single Factor

SUMMARY

Groups	Count	Sum	Average	Variance
Experiment 10.1 COD Removal	31	1044.4	33.6914	475.448
Experiment 10.2 COD Removal	31	852.39	27.4966	501.125

ANOVA

Source of Variation	SS	df	MS	F	P-value	F crit
Between Groups	594.82	1	594.824	1.21819	0.2741	4.0011
Within Groups	29297.	60	488.287		2	9
Total	29892	61				

Table C 1. 21: Results from experiment 11.1

Experiment	Current Density	NaCl (M)
11	1	0.06

Parameter	Units	Experiment 11.1															
		0	2	4	6	8	10	12	24	26	28	30	32	34	36	48	50
Time	hrs.																
Salinity	g/l	7.5	11.4	7.6	7.3	7.4	6.8	7.4	6.9	8.2	8.0	8.6	9.9	9.6	9.7	8.8	8.9
EC	mS/cm	14.0	18.0	12.3	12.3	11.9	11.3	12.3	11.3	12.3	12.8	14.3	14.6	15.6	15.5	14.9	14.1
TDS	g/l	9.2	11.7	8.0	7.7	7.8	7.3	7.9	7.4	9.0	8.3	9.8	9.8	10.2	10.4	11.3	9.3
Turbidity	NTU	20.6	4.2	4.0	4.5	4.0	4.3	3.3	2.6	1.6	0.8	0.7	1.1	0.8	0.8	0.8	1.0
pH		1.6	1.1	0.7	1.6	1.5	1.2	0.8	1.6	1.2	1.3	0.4	1.5	1.1	1.4	1.4	1.4
COD Total	g/L	48.7	43.8	42.7	47.6	40.9	40.9	36.6	40.5	39.4	36.6	37.9	35.1	36.0	35.1	35.6	32.0
% COD Removal		0.0	9.9	12.3	2.1	16.0	15.9	24.7	16.8	19.0	24.7	22.1	27.9	26.0	27.9	26.9	34.4

Parameter	Units	Experiment 11.1														
		52	54	56	58	60	72	74	76	78	80	82	84	96	98	100
Time	hrs.															
Salinity	g/l	9.6	10.4	11.7	10.9	10.1	10.2	10.1	11.5	10.2	12.0	12.8	12.0	12.3	10.8	11.1
EC	mS/cm	16.1	17.5	17.2	17.9	16.3	15.2	15.5	16.8	16.6	19.7	19.0	19.2	18.9	17.2	17.2
TDS	g/l	10.9	10.4	11.6	12.2	10.4	10.3	10.4	11.3	11.1	11.8	12.6	13.1	12.0	11.2	11.3
Turbidity	NTU	0.6	0.8	0.9	0.6	0.9	1.0	1.1	0.6	0.8	0.6	0.5	0.6	0.7	1.0	0.8
pH		1.4	0.4	1.4	1.3	1.1	1.1	1.2	1.4	1.3	1.5	1.4	1.4	1.3	1.2	1.2
COD Total	g/L	33.0	30.4	29.3	28.5	25.2	24.1	23.6	21.3	20.5	19.4	17.2	15.1	12.2	12.1	10.6
% COD Removal		32.2	37.5	39.9	41.4	48.2	50.5	51.6	56.2	57.9	60.2	64.7	69.0	74.9	75.1	78.3

Table C 1. 22: Results from experiment 11.2.

Parameter	Units	Experiment 11.2															
		0	2	4	6	8	10	12	24	26	28	30	32	34	36	48	50
Time	hrs.																
Salinity	g/l	7.5	8.2	8.2	7.1	6.8	7.0	7.5	6.9	7.5	8.4	9.1	9.5	9.6	9.7	10.1	8.9
EC	mS/cm	14.0	13.3	9.3	11.7	11.2	11.4	11.9	11.3	12.4	14.0	13.8	15.9	16.2	16.1	15.9	14.8
TDS	g/l	9.2	8.7	7.2	7.3	7.3	7.4	7.8	7.4	8.2	8.5	9.2	9.6	9.5	9.9	8.7	9.1
Turbidity	NTU	20.6	3.2	3.1	4.1	1.2	0.6	0.8	0.5	0.8	0.9	0.9	0.9	0.7	0.9	0.9	1.9
pH		1.6	1.3	1.1	1.1	1.1	1.5	1.4	1.0	1.1	1.2	1.1	1.2	1.2	1.4	1.0	1.5
COD Total	g/L	46.0	42.0	43.1	41.6	42.3	42.1	41.8	41.0	38.1	35.0	36.0	34.2	33.6	34.3	33.2	30.6
% COD Removal		0.0	8.6	6.2	9.6	8.0	8.5	9.1	10.9	17.2	23.9	21.7	25.6	26.9	25.5	27.8	33.4

Parameter	Units	Experiment 11.2														
		52	54	56	58	60	72	74	76	78	80	82	84	96	98	100
Time	hrs.															
Salinity	g/l	10.3	10.0	10.8	11.4	11.1	12.1	9.6	11.0	11.2	11.2	11.9	12.1	12.2	10.9	11.1
EC	mS/cm	15.3	16.4	17.9	17.0	17.3	16.6	15.3	18.1	16.5	18.4	19.5	19.4	18.9	17.1	17.0
TDS	g/l	10.2	11.2	19.7	11.3	12.1	11.6	10.6	10.9	11.1	12.4	11.9	12.1	11.9	11.1	11.1
Turbidity	NTU	1.1	0.4	0.7	0.6	1.2	0.8	0.6	4.6	0.7	0.9	0.8	0.6	0.8	0.7	0.7
pH		1.3	1.5	1.5	1.1	13.2	1.2	1.3	1.0	1.0	0.8	1.4	1.4	1.4	1.4	1.4
COD Total	g/L	31.6	29.1	28.5	27.9	25.7	21.8	20.7	20.1	19.6	18.1	15.0	15.3	12.2	11.8	9.9
% COD Removal		31.3	36.8	38.0	39.2	44.1	52.6	55.0	56.3	57.4	60.6	67.3	66.7	73.4	74.4	78.5

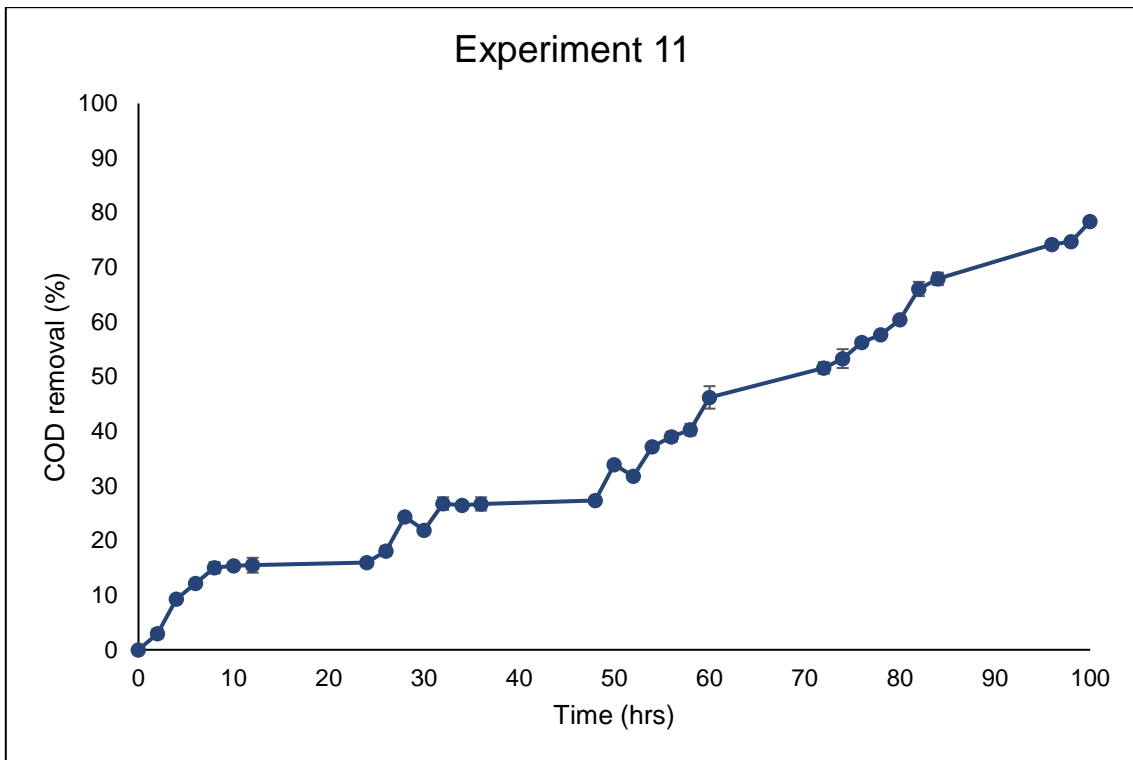


Figure C. 11: Average COD removal from experiment 11.1 and 11.2.

Anova: Single Factor

SUMMARY

Groups	Count	Sum	Average	Variance
Experiment 11.1 COD Removal	31	1136.1	36.6488	501.257
Experiment 11.2 COD Removal	31	1116.9	36.0303	513.13

ANOVA

Source of Variation	SS	df	MS	F	P-value	F crit
Between Groups	5.9304	1	5.93045	0.01169	0.9142	4.0011
Within Groups	30431.	60	507.194		5	9
Total	30437.	61				

Table C 1. 23: Results from experiment 12.1

Experiment	Current Density	NaCl (M)
12	1	0.1

Parameter	Units	Experiment 12.1															
		0	2	4	6	8	10	12	24	26	28	30	32	34	36	48	50
Time	hrs.																
Salinity	g/l	11.4	10.0	10.3	10.7	19.9	13.4	12.0	11.0	11.3	11.5	13.7	14.9	14.0	14.3	14.2	14.4
EC	mS/cm	18.0	16.1	16.5	17.4	12.0	19.3	19.1	18.6	18.3	18.5	22.1	21.2	23.7	23.4	23.0	22.7
TDS	g/l	11.6	10.5	10.7	11.7	4.4	13.0	12.6	11.5	11.5	12.6	13.0	14.3	16.3	16.4	16.6	16.6
Turbidity	NTU	94.8	20.4	9.2	5.8	1.2	7.1	6.9	4.2	1.3	2.1	1.0	0.9	0.9	0.9	0.8	0.8
pH		2.5	1.3	1.3	1.2	1.3	1.4	1.2	1.5	1.2	1.1	1.3	1.4	1.3	1.3	1.4	1.3
COD	mg/L	5425	4490	4345	4320	3605	3835	2995	3625	4365	4080	4020	3815	3480	3340	3050	2785
COD Total	g/L	59.7	49.4	47.8	47.5	39.7	42.2	32.9	39.9	48.0	44.9	44.2	42.0	38.3	36.7	33.6	30.6
% COD Removal		0.0	17.2	19.9	20.4	33.5	29.3	44.8	33.2	19.5	24.8	25.9	29.7	35.9	38.4	43.8	48.7

Parameter	Units	Experiment 12.1														
		52	54	56	58	60	72	74	76	78	80	82	84	96	98	100
Time	hrs.															
Salinity	g/l	14.2	15.3	14.4	15.2	15.1	14.8	16.9	11.1	14.0	14.3	15.1	13.9	12.6	12.5	12.7
EC	mS/cm	23.1	21.1	20.7	22.3	22.2	21.3	19.8	17.9	20.3	23.0	25.1	22.1	20.7	20.4	20.7
TDS	g/l	17.2	15.9	17.1	16.8	17.0	18.0	15.2	11.4	13.6	15.8	14.5	13.7	13.7	13.6	14.1
Turbidity	NTU	0.8	0.6	0.8	1.1	0.7	0.7	0.9	1.8	0.8	3.0	2.3	2.7	1.0	1.0	4.6
pH		1.3	1.4	1.0	1.3	1.3	1.4	1.4	0.9	1.2	0.9	1.0	0.5	0.7	0.7	0.9
COD	mg/L	2685	2435	2015	1920	1728	1627	1533	1556	1203	1012	899	880	895	900	860
COD Total	g/L	29.5	26.8	22.2	21.1	19.0	17.9	16.9	17.1	13.2	11.1	9.9	9.7	9.8	9.9	9.5
% COD Removal		50.5	55.1	62.9	64.6	68.1	70.0	71.7	71.3	77.8	81.3	83.4	83.8	83.5	83.4	84.1

Table C 1. 24: Results from experiment 12.2

Parameter	Units	Experiment 12.2															
		hrs.	0	2	4	6	8	10	12	24	26	28	30	32	34	36	48
Salinity	g/l	11.4	10.1	9.8	11.6	11.8	11.9	11.7	11.5	11.6	13.3	13.6	15.0	15.6	15.4	15.3	14.2
EC	mS/cm	18.0	15.7	15.8	16.8	19.1	19.8	18.2	18.4	18.4	19.5	22.2	25.0	22.2	22.1	21.7	21.6
TDS	g/l	11.6	10.3	10.2	11.4	13.1	12.1	12.0	11.7	11.8	13.0	15.0	14.5	15.0	15.0	15.0	14.6
Turbidity	NTU	94.8	28.3	10.6	6.1	2.8	1.9	1.4	3.0	1.5	1.3	1.4	1.9	1.2	1.1	1.0	1.1
pH		2.5	1.2	1.5	1.6	1.3	1.3	1.2	1.3	1.3	1.6	1.5	1.5	1.5	1.5	1.4	1.5
COD Total	g/L	50.9	44.6	43.9	46.7	46.2	45.7	40.9	34.0	39.8	39.0	38.4	35.8	34.3	32.5	28.5	25.9
% COD Removal		0.0	12.3	13.7	8.2	9.2	10.3	19.6	33.1	21.7	23.4	24.6	29.7	32.5	36.2	44.0	49.0

Parameter	Units	Experiment 12.2														
		hrs.	52	54	56	58	60	72	74	76	78	80	82	84	96	98
Salinity	g/l	14.9	15.1	16.2	15.3	16.2	17.2	11.4	12.2	13.9	15.5	14.5	14.4	13.5	13.4	14.1
EC	mS/cm	22.3	21.7	22.1	22.0	21.3	20.3	20.1	20.4	22.8	22.0	23.4	22.9	22.1	21.9	20.1
TDS	g/l	15.1	15.3	14.4	13.9	15.0	15.0	15.1	13.5	13.6	14.7	16.2	16.9	13.5	13.3	13.5
Turbidity	NTU	1.0	1.0	1.2	0.7	0.7	0.9	1.2	1.4	0.8	0.9	1.1	1.2	0.9	0.8	0.7
pH		1.5	1.5	1.4	1.6	1.2	1.3	1.4	0.8	1.1	1.0	0.9	1.0	0.7	0.7	0.9
COD Total	g/L	24.7	22.5	20.0	18.6	17.2	14.6	14.0	13.8	11.5	9.5	8.7	8.4	8.2	8.2	8.2
% COD Removal		51.5	55.7	60.6	63.4	66.1	71.3	72.6	72.9	77.4	81.3	82.9	83.5	83.8	83.8	84.0

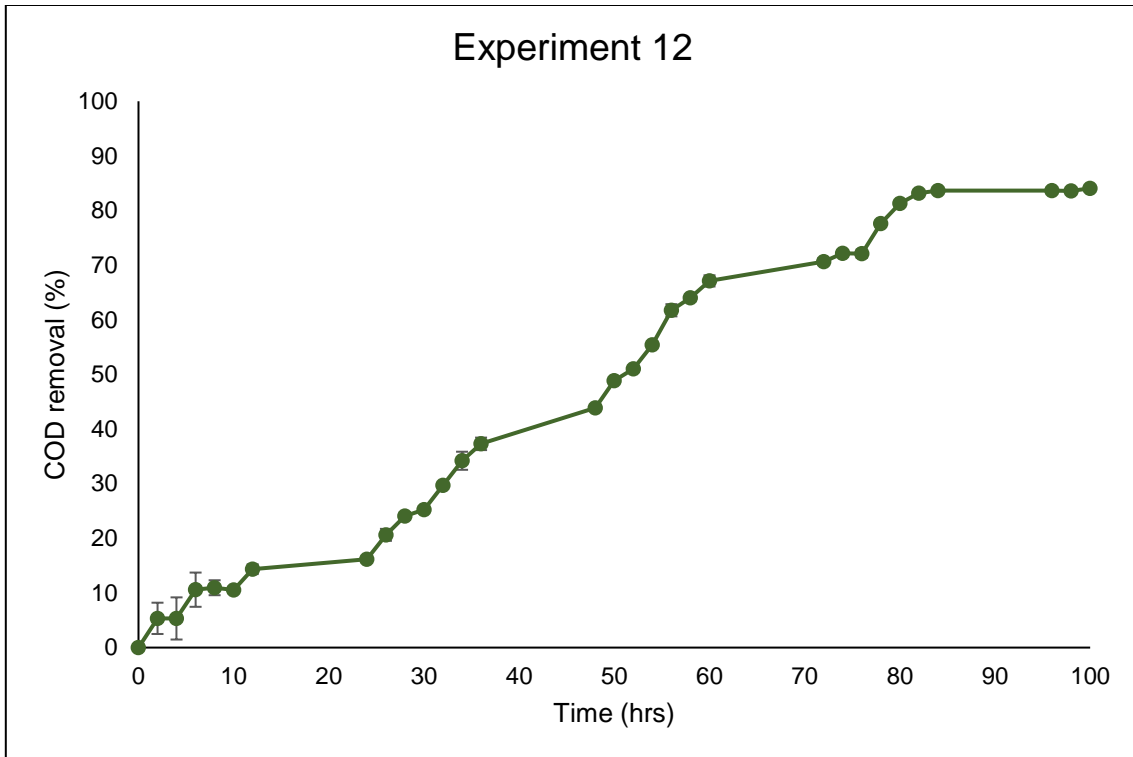


Figure C. 12: Average COD removal from experiment 12.1 and 12.2.

Anova: Single Factor

SUMMARY

Groups	Count	Sum	Average	Variance
Experiment 12.1 COD Removal	31	1420.31	45.8166	880.266
Experiment 12.2 COD Removal	31	1436.82	46.3491	824.95

ANOVA

Source of Variation	SS	df	MS	F	P-value	F crit
Between Groups	4.39553	1	4.39553	0.00516	0.943	4.00119
Within Groups	51156.5	60	852.608			
Total	51160.9	61				

Appendix D

Data from the adsorption experiments: Effect of chitosan dosage and pH on the removal of COD.

The effect of chitosan dosage on the removal of COD, at the following experimental conditions.

Experimental parameters

Volume of reactor,	1L
Temperature of solution,	ambient
Stirring speed,	350 rpm
Chitosan dosage,	2.5 – 4.5 g/L
pH,	2

Experiment	pH	Chitosan dosage
1.1	2	2.5 g/L

Time (hours)	COD (mg/L)	% Removal
Initial	4510	0.0
1	4435	1.7
2	4025	10.8
3	3890	13.7

Experiment	pH	Chitosan dosage
1.2	2	2.5 g/L

Time (hours)	COD (mg/L)	% Removal
Initial	3890	
1	3720	17.5
2	3705	17.8
3	3340	25.9

Experiment	pH	Chitosan dosage
1.3	2	2.5 g/L

Time (hours)	COD (mg/L)	% Removal
Initial	3340	
1	3190	29.3
2	2975	34.0
3	2850	36.8

Table D. 1: Adsorption data from experiment 1.

Experiment	pH	Chitosan dosage
2.1	2	3.5 g/L

Time (hours)	COD (mg/L)	% Removal
Initial	5805	0.0
1	5345	7.9
2	4620	20.4
3	4485	22.7

Experiment	pH	Chitosan dosage
2.2	2	3.5 g/L

Time (hours)	COD (mg/L)	% Removal
Initial	4485	
1	3970	31.6
2	3845	33.8
3	3665	36.9

Experiment	pH	Chitosan dosage
2.3	2	3.5 g/L

Time (hours)	COD (mg/L)	% Removal
Initial	3665	
1	3470	40.2
2	3415	41.2
3	3150	45.7

Table D. 2: Adsorption data from experiment 2.

Experiment	pH	Chitosan dosage
3.1	2	4.5 g/L

Time (hours)	COD (mg/L)	% Removal
Initial	3895	0.0
1	3680	5.5
2	3250	16.6
3	3225	17.2

Experiment	pH	Chitosan dosage
3.2	2	4.5 g/L

Time (hours)	COD (mg/L)	% Removal
Initial	3225	
1	2935	24.6
2	2905	25.4
3	2515	35.4

Experiment	pH	Chitosan dosage
3.3	2	4.5 g/L

Time (hours)	COD (mg/L)	% Removal
Initial	2515	
1	2265	41.8
2	1850	52.5
3	1745	55.2

Table D. 3: Adsorption data from experiment 3.

The effect of chitosan dosage on the removal of COD, at the following experimental conditions.

Experimental parameters

Volume of reactor,	1L
Temperature of solution,	ambient
Stirring speed,	350 rpm
Chitosan dosage,	2.5 – 4.5 g/L
pH,	4

Experiment	pH	Chitosan dosage
4.1	4	2.5 g/L

Time (hours)	COD (mg/L)	% Removal
Initial	4445	0.0
1	4345	2.3
2	4080	8.9
3	3855	15.3

Experiment	pH	Chitosan dosage
4.2	2	2.5 g/L

Time (hours)	COD (mg/L)	% Removal
Initial	3855	
1	3650	17.9
2	3590	19.2
3	3560	19.9

Experiment	pH	Chitosan dosage
4.3	2	2.5 g/L

Time (hours)	COD (mg/L)	% Removal
Initial	3560	
1	3550	20.1
2	3510	21.0
3	3505	21.1

Table D. 4: Adsorption data from experiment 4.

Experiment	pH	Chitosan dosage
5.1	4	3.5 g/L

Time (hours)	COD (mg/L)	% Removal
Initial	4150	0.0
1	3820	8.0
2	3615	12.9
3	3455	16.7

Experiment	pH	Chitosan dosage
5.2	4	3.5 g/L

Time (hours)	COD (mg/L)	% Removal
Initial	3455	
1	3290	20.7
2	3275	21.1
3	3120	24.8

Experiment	pH	Chitosan dosage
5.3	4	3.5 g/L

Time (hours)	COD (mg/L)	% Removal
Initial	3120	
1	3030	27.0
2	2985	28.1
3	2975	28.3

Table D. 5: Adsorption data from experiment 5

Experiment	pH	Chitosan dosage
6.1	4	4.5 g/L

Time (hours)	COD (mg/L)	% Removal
Initial	4595	0.0
1	3825	16.8
2	3690	19.7
3	3580	22.1

Experiment	pH	Chitosan dosage
6.2	4	4.5 g/L

Time (hours)	COD (mg/L)	% Removal
Initial	3580	
1	3515	23.5
2	3530	23.2
3	3380	26.4

Experiment	pH	Chitosan dosage
6.3	4	4.5 g/L

Time (hours)	COD (mg/L)	% Removal
Initial	3380	
1	2910	36.7
2	2785	39.4
3	2760	39.9

Table D. 6: Adsorption data from experiment 6

The effect of chitosan dosage on the removal of COD, at the following experimental conditions.

Experimental parameters

Volume of reactor,	1L
Temperature of solution,	ambient
Stirring speed,	350 rpm
Chitosan dosage,	2.5 – 4.5 g/L
pH,	6

Experiment	pH	Chitosan dosage
7.1	6	2.5 g/L

Time (hours)	COD (mg/L)	% Removal
Initial	3780	0.0
1	3660	3.2
2	3670	2.9
3	3565	5.7

Experiment	pH	Chitosan dosage
7.2	4	2.5 g/L

Time (hours)	COD (mg/L)	% Removal
Initial	3565	
1	3495	7.5
2	3605	4.6
3	3580	5.3

Experiment	pH	Chitosan dosage
7.3	6	2.5 g/L

Time (hours)	COD (mg/L)	% Removal
Initial	3850	
1	3510	7.1
2	3465	8.3
3	3325	12.0

Table D. 7: Adsorption data from experiment 7.

Experiment	pH	Chitosan dosage
8.1	6	3.5 g/L

Time (hours)	COD (mg/L)	% Removal
Initial	3990	0.0
1	3885	2.6
2	3860	3.3
3	3705	7.1

Experiment	pH	Chitosan dosage
8.2	6	3.5 g/L

Time (hours)	COD (mg/L)	% Removal
Initial	3705	
1	3565	10.7
2	3445	13.7
3	3275	17.9

Experiment	pH	Chitosan dosage
8.3	6	3.5 g/L

Time (hours)	COD (mg/L)	% Removal
Initial	3445	
1	3300	17.3
2	3305	17.2
3	3275	17.9

Table D. 8: Adsorption data from experiment 8

Experiment	pH	Chitosan dosage
9.1	6	4.5 g/L

Time (hours)	COD (mg/L)	% Removal
Initial	4280	0.0
1	4120	3.7
2	4015	6.2
3	3805	11.1

Experiment	pH	Chitosan dosage
9.2	6	4.5 g/L

Time (hours)	COD (mg/L)	% Removal
Initial	3310	
1	3195	25.4
2	3055	28.6
3	2990	30.1

Experiment	pH	Chitosan dosage
9.3	6	4.5 g/L

Time (hours)	COD (mg/L)	% Removal
Initial	2925	
1	2885	32.6
2	2785	34.9
3	2755	35.6

Table D. 9: Adsorption data from experiment 9

Adsorption data from Langmuir isotherm.

Experiment 1 – 3

Experimental parameters

Volume of reactor,	1L
Temperature of solution,	ambient
Stirring speed,	350 rpm
Chitosan dosage,	2.5 – 4.5 g/L
pH,	2

Langmuir (pH 2) (2.5 g/L)			
	COD (mg/L)	q_e (mg/g)	ce/q_e
C_0	4510		
C_e	3890	248.0	15.68548
C_0	3890		
C_e	3340	220.0	15.18182
C_0	3340		
C_e	2850	196.0	14.54082

Langmuir (pH 2) (2.5 g/L)		
$y=0.0011x+11.451$		
slope	$=1/q_m$	
0.0011	$=1/Q_m$	
Q_m	909.1	mg/g
Intercept	$=1/Q_m * K_L$	
11.451	$=1/Q_m * K_L$	
K_L	9.61E-05	
R_L	0.697721	Favorable

Table D. 10: Langmuir Isotherm Data Experiment 1.

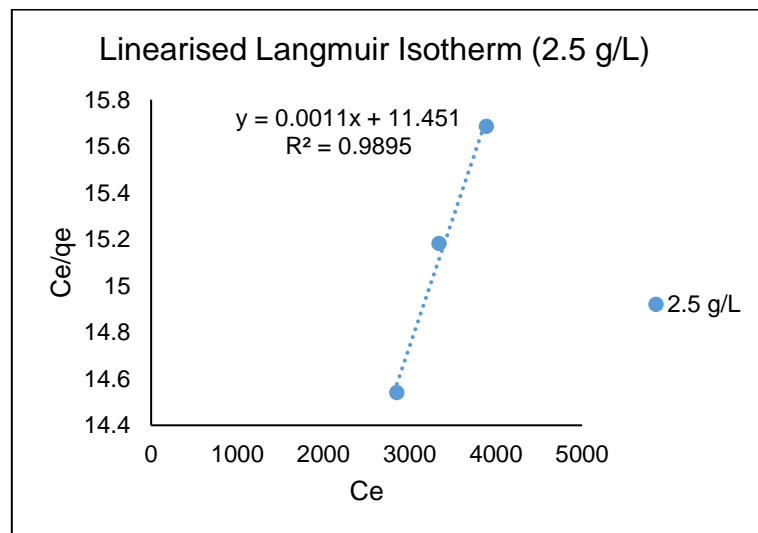


Figure D. 1: Linearized Langmuir Isotherm (2.5 g/L)

Langmuir (pH 2) (3.5 g/L)			
	COD (mg/L)	q_e (mg/g)	ce/q_e
C_0	5805		
C_e	4485	377.1	11.892
C_0	4485		
C_e	3665	234.3	15.6433
C_0	3665		
C_e	3150	147.1	21.4078

Langmuir 3.5		
$y = -0.0069x + 42.278$		
slope	$= 1/q_0$	
0.0069	$= 1/q_0$	
Q_0	144.9	mg/g
Intercept	$= 1/Q_0 * K_I$	
42.278	$= 1/Q_0 * K_I$	
K_I	0.0001632	
R_L	0.5135	Favorable

Table D. 11: Langmuir Isotherm Data Experiment 2

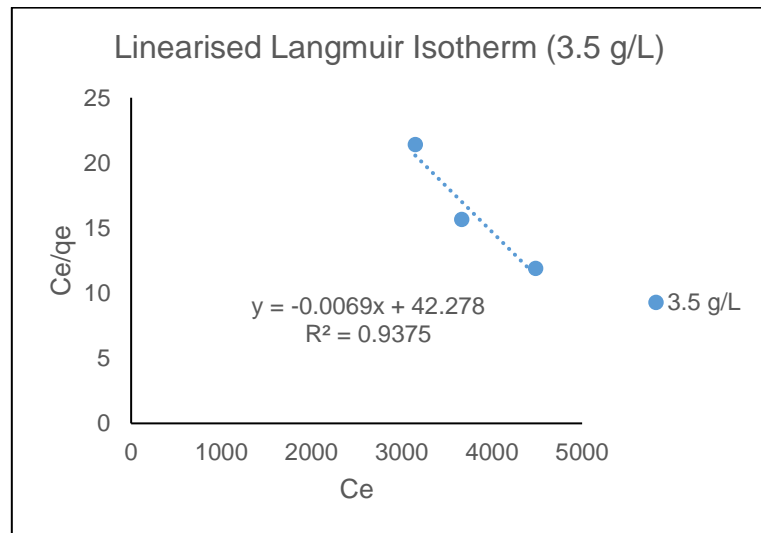


Figure D. 2: Linearized Langmuir Isotherm (3.5 g/L).

Langmuir (pH 2) (4.5 g/L)			
	COD (mg/L)	q_e (mg/g)	ce/q_e
C_0	3895		
C_e	3225	148.9	21.6604
C_0	3225		
C_e	2515	157.8	15.9401
C_0	2515		
C_e	1745	171.1	10.1981

Langmuir 3.5		
$y=0.0077x-3.3805$		
slope	$=1/q_0$	
0.0077	$=1/q_0$	
Q_0	129.9	mg/g
Intercept	$=1/Q_0 \cdot K_I$	
3.3805	$=1/Q_0 \cdot K_I$	
K_I	0.0022777	
R_L	0.101	Favorable

Table D. 12: Langmuir Isotherm Data Experiment 3.

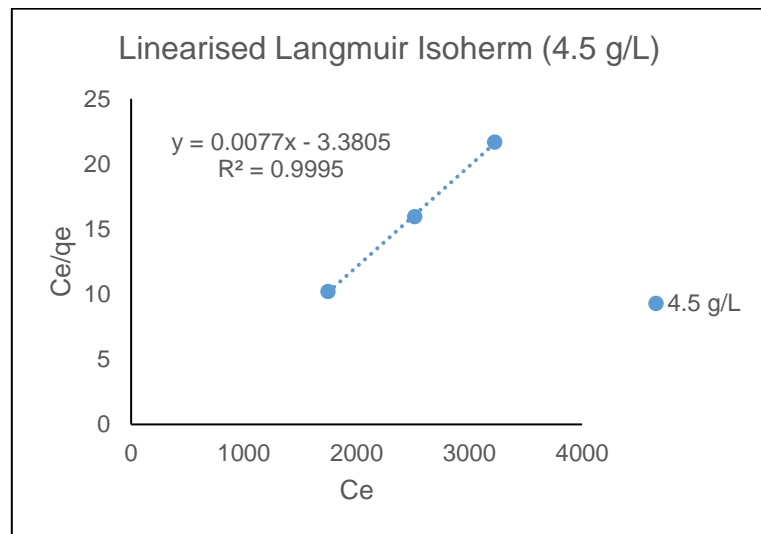


Figure D. 3: Linearized Langmuir Isotherm (4.5 g/L).

Adsorption data from Freundlich isotherm.

Experiment 1 – 3

Experimental parameters

Volume of reactor,	1L
Temperature of solution,	ambient
Stirring speed,	350 rpm
Chitosan dosage,	2.5 – 4.5 g/L
pH,	2

Freundlich (pH 2) (2.5 g/L)				
	COD (mg/L)	q _e (mg/g)	Log(q _e)	Log (c _e)
C ₀	4510			
C _e	3890	248.0	2.39445	3.58995
C ₀	3890			
C _e	3340	220.0	2.34242	3.52375
C ₀	3340			
C _e	2850	196.0	2.29226	3.45484

Freundlich (pH 2) (2.5 g/L)	
y=0.7562x+0.321	
slope	=1/n
0.7562	=1/n
n	1.3224
Intercept	=Ln(K)
0.321	=Ln(K)
K	1.37851

Table D. 13: Freundlich Isotherm Data Experiment 1.

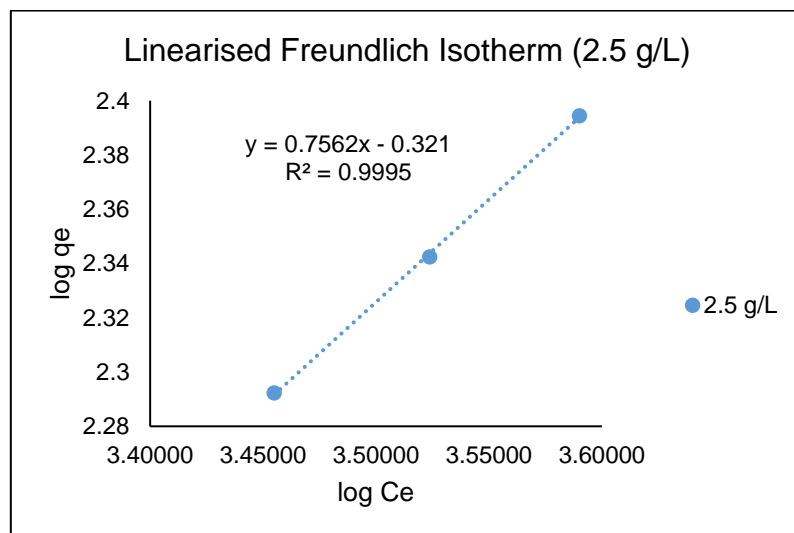


Figure D. 4: Linearized Freundlich Isotherm (2.5 g/L).

Freundlich (pH 2) (3.5 g/L)				
	COD (mg/L)	q _e (mg/g)	Log(q _e)	Log (c _e)
C ₀	5805			
C _e	4485	377.1	2.57651	3.65176
C ₀	4485			
C _e	3665	234.3	2.36975	3.56407
C ₀	3665			
C _e	3150	147.1	2.16774	3.49831

Freundlich (pH 2) (3.5 g/L)	
y=2.6473x-7.0831	
slope	=1/n
2.6473	=1/n
n	0.37774
Intercept	=Ln(K)
7.0831	=Ln(K)
K	1191.66

Table D. 14: Freundlich Isotherm Data Experiment 2.

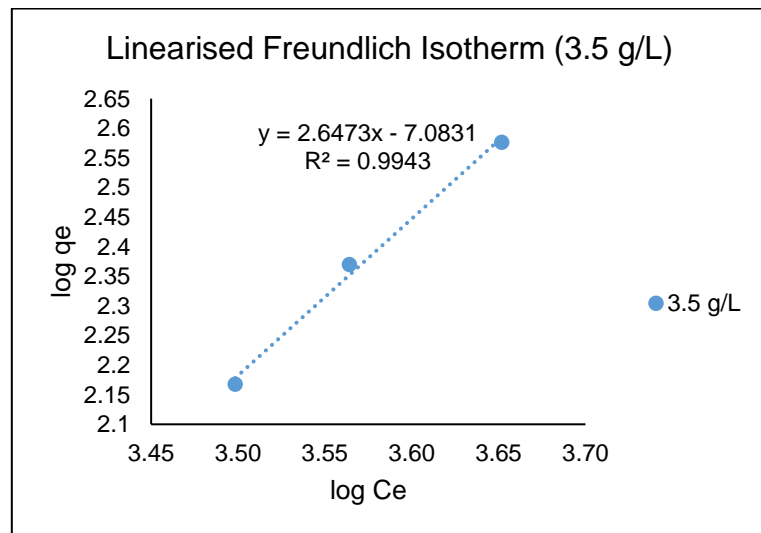


Figure D. 5: Linearized Freundlich Isotherm (3.5 g/L)

Freundlich (pH 2) (4.5 g/L)				
	COD (mg/L)	q _e (mg/g)	Log(q _e)	Log (c _e)
C ₀	3895			
C _e	3225	148.9	2.17286	3.50853
C ₀	3225			
C _e	2515	157.8	2.19805	3.40054
C ₀	2515			
C _e	1745	171.1	2.23328	3.24180

Freundlich (pH 2) (4.5 g/L)	
y=0.2262x+2.9666	
slope	=1/n
0.2262	=1/n
n	4.4209
Intercept	=Ln(K)
2.9666	=Ln(K)
K	19.426

Table D. 15: Freundlich Isotherm Data Experiment 3.

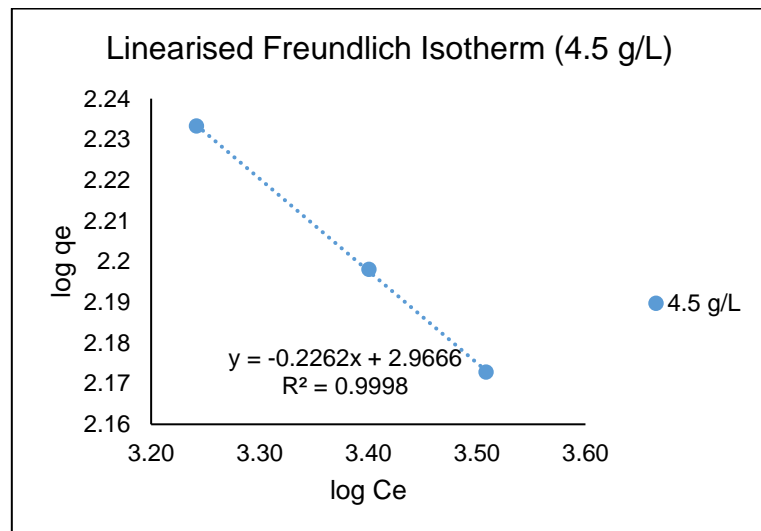


Figure D. 6: Linearized Freundlich Isotherm (4.5 g/L).

Adsorption data from Dubinin-Raduschkevich isotherm.

Experiment 1 – 3

Experimental parameters

Volume of reactor,	1L
Temperature of solution,	ambient
Stirring speed,	350 rpm
Chitosan dosage,	2.5 – 4.5 g/L
pH,	2

Dubinin-Raduschkevich (pH 2) (2.5 g/L)			
	COD (mg/L)	q_e (mg/g)	ϵ
C_0	4510		
C_e	3890	248.0	0.63715
C_0	3890		
C_e	3340	220.0	0.74205
C_0	3340		
C_e	2850	196.0	0.86961

Dubinin-Raduschkevich (pH 2) (4.5 g/L)	
$y = -0.6644x + 5.7744$	
slope	$= \ln(q_s)$
0.6644	$= \ln(q_s)$
q_s	1.94
Intercept	$= k \cdot e^2$
5.7744	$= k \cdot e^2$
K	14.22
E	0.187

Table D. 16: Dubinin-Raduschkevich Isotherm Data Experiment 1

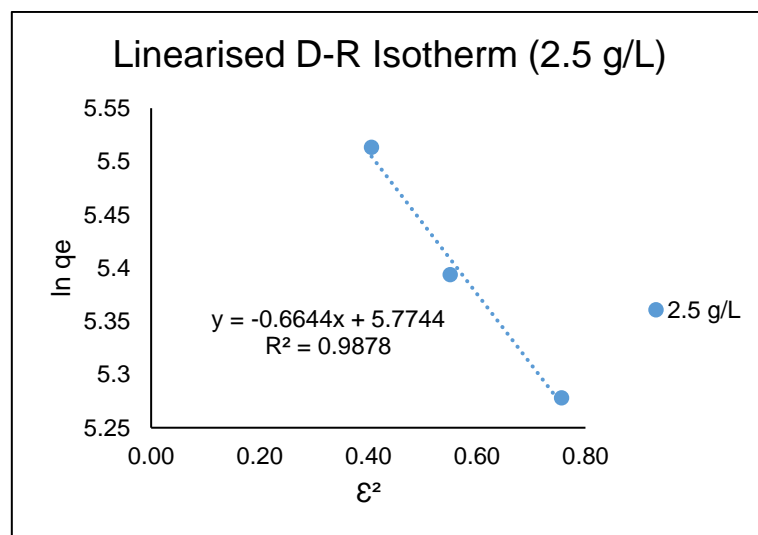


Figure D. 7: Linearize Dubinin-Raduschkevich isotherm (2.5 g/L).

Dubinin-Raduschkevich (pH 2) (3.5 g/L)			
	COD (mg/L)	q_e (mg/g)	ϵ
C_0	5805		
C_e	4485	377.1	0.55263
C_0	4485		
C_e	3665	234.3	0.67626
C_0	3665		
C_e	3150	147.1	0.7868

Dubinin-Raduschkevich (pH 2) (4.5 g/L)	
$y = -2.9994x + 6.8417$	
slope	$= \ln(q_s)$
2.9994	$= \ln(q_s)$
q_s	20.073
Intercept	$= k \cdot e^2$
6.8417	$= k \cdot e^2$
K	22.4
E	0.149

Table D. 17: Dubinin-Raduschkevich Isotherm Data Experiment 2.

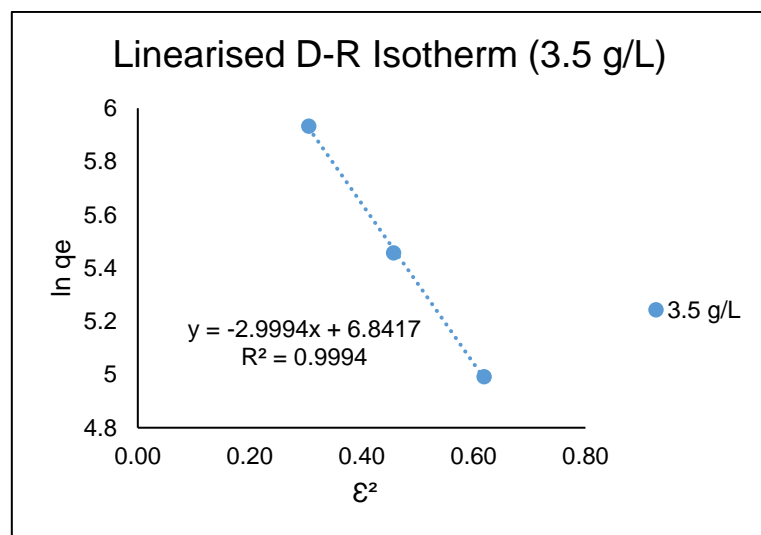


Figure D. 8: Linearize Dubinin-Raduschkevich isotherm (3.5 g/L).

Dubinin-Raduschkevich (pH 2) (4.5 g/L)			
	COD (mg/L)	q_e (mg/g)	ϵ
C_0	3895		
C_e	3225	148.9	0.76851
C_0	3225		
C_e	2515	157.8	0.98542
C_0	2515		
C_e	1745	171.1	1.42012

Dubinin-Raduschkevich (pH 2) (4.5 g/L)	
$y=0.0933x+4.9576$	
slope	$=\ln(q_s)$
4.9576	$=\ln(q_s)$
q_s	1.09
Intercept	$=k \cdot e^2$
6.8417	$=k \cdot e^2$
K	11.58
E	0.2078

Table D. 18: Dubinin-Raduschkevich Isotherm Data Experiment 3.

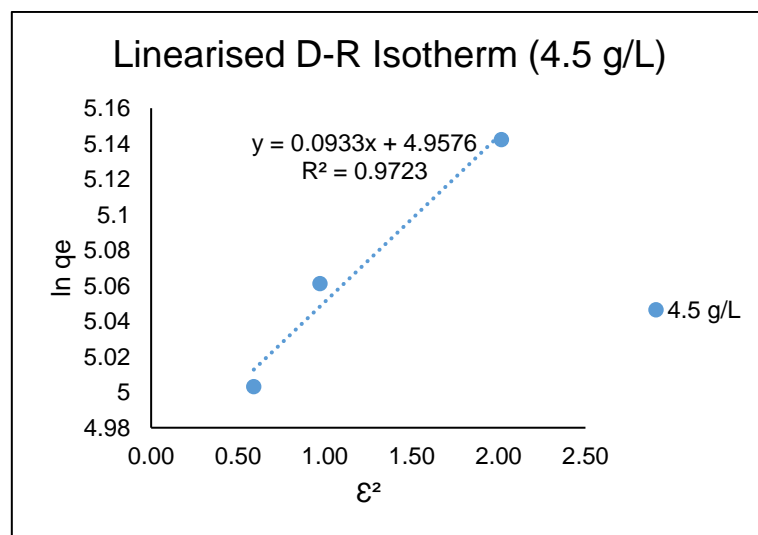


Figure D. 9: Linearize Dubinin-Raduschkevich isotherm (4.5 g/L).

Appendix E

Sample calculations for all major calculations performed

1. Oil recovery from acidification

- pH of 2

A 500ml sample of raw biodiesel was acidified to a final pH of 2. After 24 hours the oil was separated from the aqueous phase through slow decantation. The oil that remained was measured in a small glass measuring cylinder.

- 9 ml oil was removed from 500ml acidified wastewater.
- The amount of removed oil was calculated as ml oil / 100ml wastewater
- $9 \text{ ml} / 5 = 1.8 \text{ ml oil} / 100 \text{ ml wastewater}$
- %COD Removal was calculated:

$$\% \text{COD Removal} = \frac{(\text{COD}_t) - (\text{COD}_{t+\Delta t})}{(\text{COD}_t)} \times 100$$

$$\% \text{COD Removal} = \frac{(10485) - (8870)}{(10485)} \times 100$$

$$\% \text{COD Removal} = 15$$

Results for the acidification of biodiesel wastewater at various pH levels are presented in Figure 4.1.

2. Current Density

- 1.25 mA/cm²

After the current density was selected, the required current density was calculated as follows:

$$\text{Current Density} = \frac{\text{Current (mA)}}{\text{Anode Surface Area (cm}^2\text{)}}$$

$$1.25 \text{ mA/cm}^2 = \frac{\text{Current (mA)}}{(10\text{cm} \times 10\text{cm}) \times 4}$$

$$\text{Current (mA)} = 1.25 \text{ mA/cm}^2 \times 400 \text{ cm}^2$$

$$\text{Current (mA)} = 500 \text{ mA} = 0.5 \text{ Ampere}$$

Experiment	Current Density (mA/cm ²)
1	0.5
2	0.75
3	1
4	1.25
5	1.75
6	2
7	4

3. Sodium Chloride Concentration

The NaCl concentration (M) was calculated as follows:

$$\text{Molarity (M)} = \frac{\text{moles of solute}}{\text{volume of solution}}$$

$$0.08\text{M} = \frac{\text{moles of solute}}{1 \text{ L}}$$

$$\text{moles of solute} = 0.08 \text{ moles NaCl}$$

3.1. Mass of NaCl to be added

$$n \text{ (moles)} = \frac{\text{Mass (g)}}{M \text{ (g/mol)}}$$

$$0.08 \text{ mol} = \frac{\text{Mass (g)}}{58.44 \text{ g/mol}}$$

$$\text{Mass (g)} = 0.08 \text{ mol} \times 58.44 \text{ g/mol}$$

$$\text{Mass (g)} = 4.67 \text{ gram NaCl}$$

4. Instantaneous Current Efficiency (%ICE)

The ICE% for a current density of 1.25mA/cm² was calculated at time = 4 hours as follows:

Experiment 4							
Time (hours)	0	2	4	6	8	10	12
COD (g/L)	545.71	481.27	506.08	472.50	437.71	477.95	505.47
ICE (%)	0	20	6.64	7	8	4	2

$$\text{ICE (\%)} = \frac{[\text{COD}]_t - [\text{COD}]_{t+\Delta t}}{8I\Delta t} FL \times 100$$

Where:

$[\text{COD}]_t$ Chemical Oxygen Demand at time t (g/L)

$[\text{COD}]_{t+\Delta t}$ Chemical Oxygen Demand at time t + Δt (g/L)

t Electrolysis time (seconds)

I Current Intensity (A)

F Faraday constant (96485 C/mol)

L Volume of wastewater in the electrochemical reactor (m³)

$[\text{COD}]_t = 545.7 \text{ g/L}$

$[\text{COD}]_{t+\Delta t} = 506.08 \text{ g/L}$

t = 14400 seconds

I = 0.5 Amp

F = Faraday constant (96485 C/mol)

L = 0.5 m³

$$\text{ICE (\%)} = \frac{[545.7]_{t=0} - [506.08]_{t=4}}{8(0.5)(14400)} (96485)(0.001) \times 100$$

$$\text{ICE (\%)} = 6.64$$

5. Adsorption capacity

The equilibrium adsorption capacity as well as the adsorption capacity at any given time was calculated using equation 2.1.

$$Q_e = \frac{(C_0 - C_e)V}{m}$$

$$Q_e = \frac{(4510 - 3890)0.2}{0.5}$$

$$Q_e = 248 \text{ mg/g}$$

6. Langmuir Isotherm

Equation 2.2 was used for the Langmuir Isotherm:

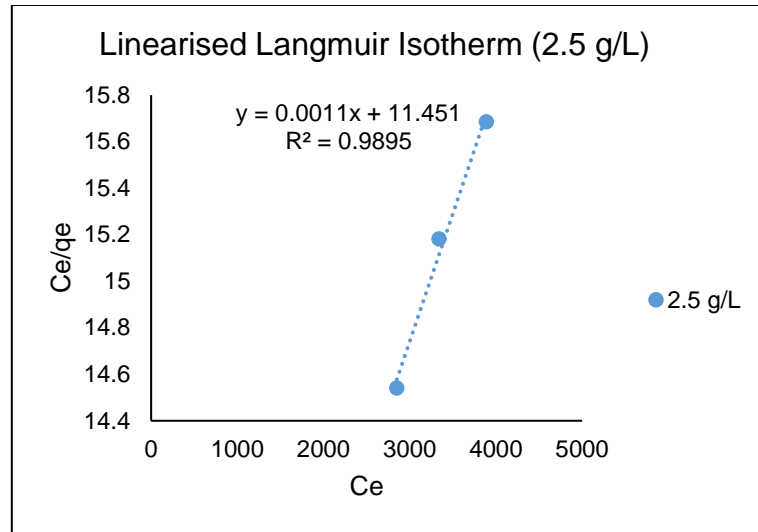
$$q_e = \frac{q_m K_L C_e}{1 + K_L C_e}$$

K_L and q_m was determined from a linearized form of Equation 2.2. as shown in Equation 2.3

$$\frac{C_e}{q_e} = \frac{1}{q_m} C_e + \frac{1}{K_L q_m}$$

Where the slope of the equation is $\frac{1}{q_m}$ and the intercept is $\frac{1}{K_L q_m}$.

The equation of the linearized plot of the Langmuir isotherm was then used to calculate the variables:



$$y = 0.0011x + 11.451$$

$$\therefore 0.0011 = \frac{1}{q_m}$$

$$\therefore q_m = 909.1 \text{ mg/g}$$

$$\therefore 11.451 = \frac{1}{K_L q_m}$$

$$\therefore K_L = 9.61 \times 10^{-5}$$

R_L was calculated using equation 2.4.

$$R_L = \frac{1}{1 + K_L C_0}$$

$$R_L = \frac{1}{(1 + 9.61 \times 10^{-5}) 4510}$$

$$R_L = 0.6977721$$

7. Freundlich Isotherm.

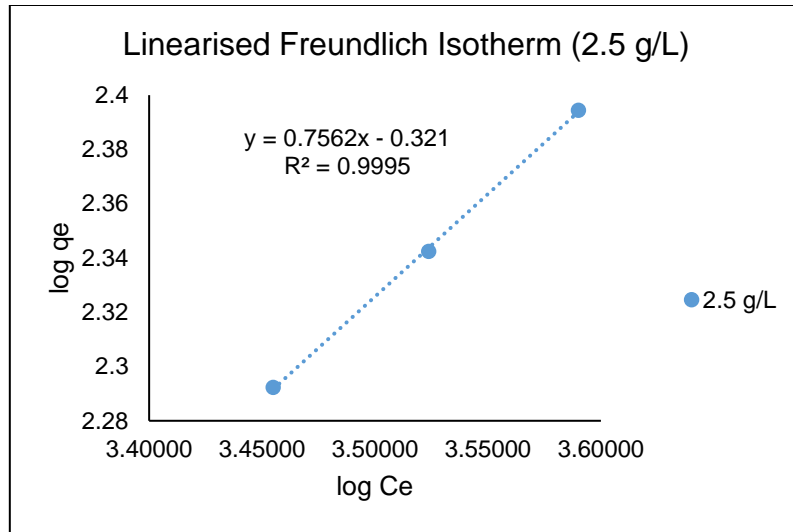
Equation 2.5 was used to fit data to the Freundlich Isotherm.

$$Q_e = K_F C_e^{1/n}$$

The linear form of the Freundlich isotherm, Equation 2.6, was used to plot $\log q_e$ versus C_e (Figure 4.26). This allowed for the determination of the constant K_f and exponent $1/n$.

$$\log q_e = \log K_F + \frac{1}{n} \log C_e$$

The equation of the linearized plot of the Freundlich isotherm has a slope $\frac{1}{n}$ and an intercept $(\ln K)$.



$$y = 0.7562x - 0.231$$

$$\therefore 0.7562 = \frac{1}{n}$$

$$\therefore n = 1.322$$

$$\therefore 0.321 = \ln(K)$$

$$\therefore K = 19.426$$

8. Dubinin-Raduschkevich isotherm

Equation 2.7 was used to fit data to the Dubinin-Raduschkevich isotherm.

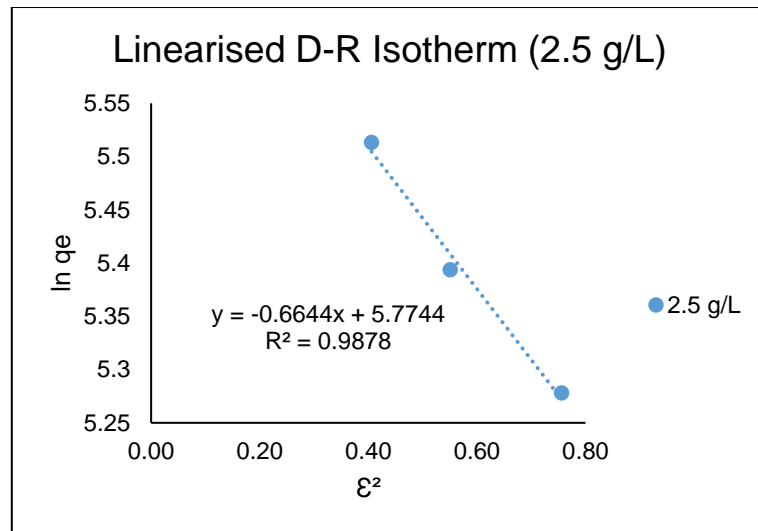
$$q_e = q_m \exp(-k\varepsilon^2)$$

The Polanyi potential (ε) (J/mol) was calculated with Equation 2.8.

$$\varepsilon = RT \ln \left(1 + \frac{1}{C_e} \right)$$

The linear form of Equation 2.8 allows for the values of q_m and K to be deduced by plotting $\ln(q_e)$ versus ε^2

$$\ln q_e = \ln q_m - k\varepsilon^2$$



The straight-line equation from the plot of $\ln q_e$ vs. ϵ^2 has a slope of q_m and an intercept $k\epsilon^2$

$$y = -0.6644x + 5.7744$$

$$\therefore 0.6644 = \ln(q_m)$$

$$\therefore q_m = 1.94$$

$$\therefore 5.7744 = k\epsilon^2$$

$$\therefore k = \frac{5.7744}{(0.6371)^2}$$

$$\therefore k = 14.224$$

The mean energy of adsorption (E) can be calculated from Equation 2.10.

$$E = (-2K)^{-1/2}$$

$$\therefore E = (-2 * 14.224)^{-1/2}$$

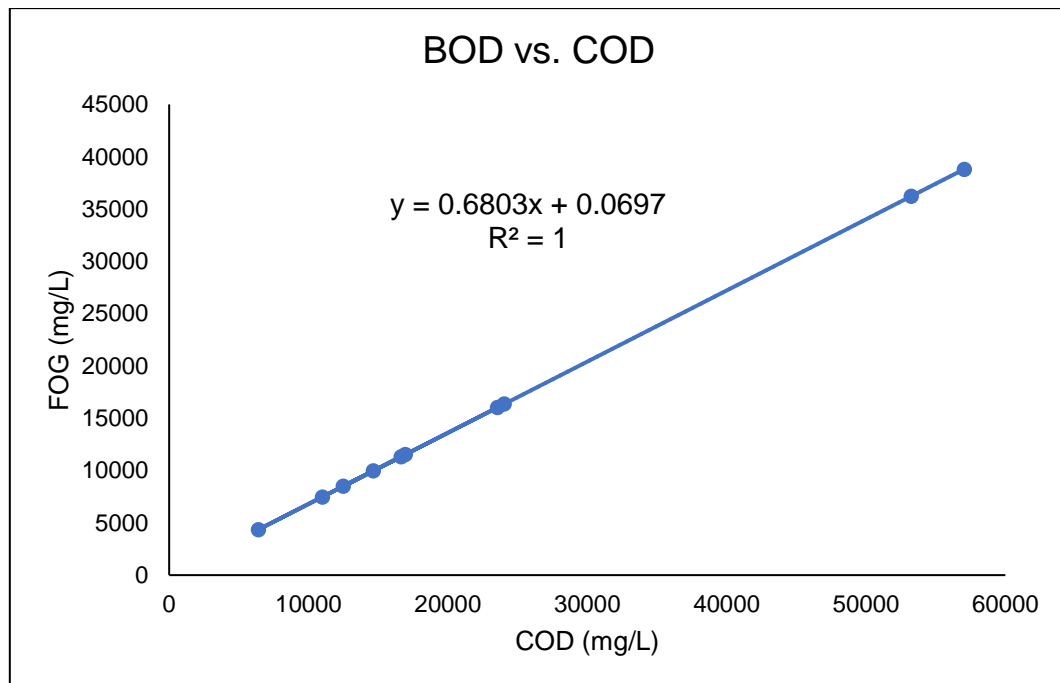
$$\therefore E = 0.1875$$

9. BOD and FOG correlations

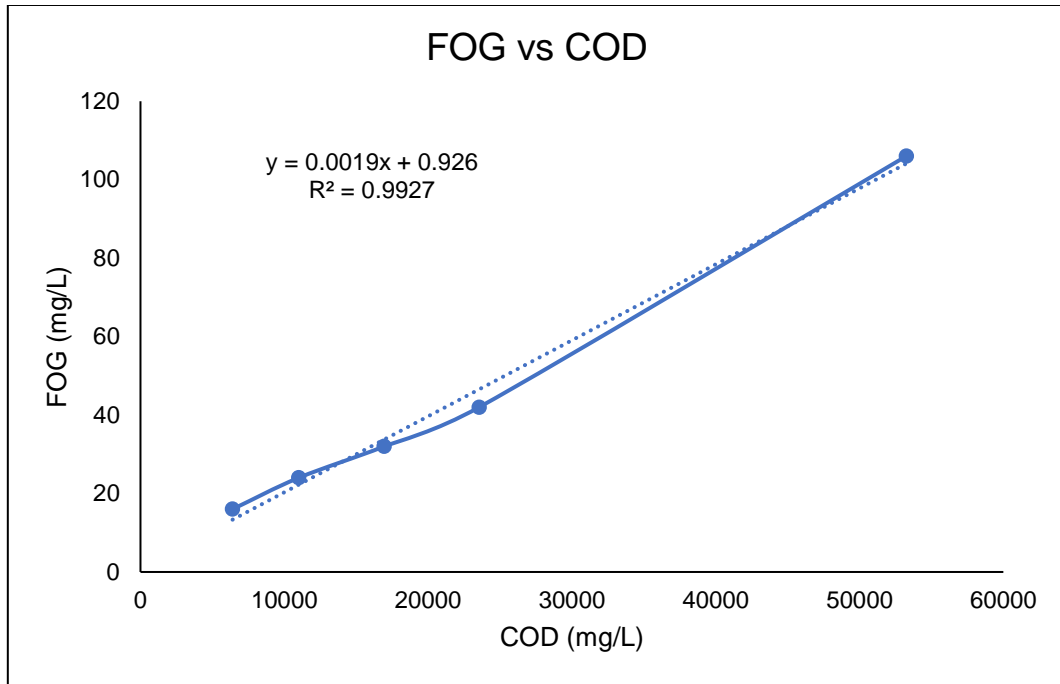
Various samples at different stages of the treatment process were analysed for COD, BOD and FOG concentrations by an accredited laboratory.

The results obtained from the analysis was used to create a correlation for BOD vs. COD and for FOG vs. COD in order to estimate BOD and FOG values at all instances during the treatment process.

The correlation for BOD vs. COD is shown below which has the equation: $y = 0.6803x + 0.0697$ and a R^2 value of 1.



Similarly, the plot of FOG vs. COD is shown below, it has the equation: $y = 0.0019x + 0.926$ with a R^2 value of 0.9927.



Appendix F

Sample preparation and analytical procedures.

Procedure followed for determination of COD.

All procedures were followed as prescribed by Merck.

1. Definition

During all experiments the COD was measured in time intervals as indicated in the relevant text. The COD expresses the amount of oxygen originating from potassium dichromate that reacts with the oxidizable substances contained in 1L of water under the working conditions of the specified process.

2. Method

The water sample is oxidised with hot sulfuric solution of potassium dichromate, with silver sulphate as the catalyst. Chloride is masked with mercury sulphate. The concentration of unconsumed yellow $\text{Cr}_2\text{O}_7^{2-}$ ions or respectively, of green Cr^{3+} ions is then determined photometrically. The method corresponds to DIN ISO 15705 and is analogous to EPA 410.4, APHA 5220 D, and APHA D1252-06 B.

3. Measuring range and reagents

Solution A (Cat. No. 114679) and Solution B (Cat. No. 114680) with a measuring range (mg/L COD) of 500 – 10 000, was used.

4. Preparation

Samples were taken as indicated in the relevant text. Since it was known that the majority of initial samples would fall out of the range that the reagents were capable of measuring, all samples were diluted (1:10) with deionised Millipore water. Once the COD results were obtained, the value was multiplied by a factor of 11 to account for the dilution.

5. Procedure

- Pipette solution A (2.2 ml) and solution B (1.8 ml) into an empty cell (free of scratches and organic impurities).
- Suspend any bottom sediment present in the cell by swirling.
- Tightly attach the screw cap to the cell.
- Vigorously mix the contents of the cell (a vortex mixer was used for 5 seconds).
- Heat the cell at 148°C in the preheated thermos-reactor (TR 420 Thermo-reactor) for 120 minutes.
- Remove the hot cell from the thermos-reactor and allow to cool in a test-tube rack.
- Wait 10 minutes, swirl the cell, and return to the rack for complete cooling to room temperature.
- Measure in the photometer (NOVA 60)